THE EFFECT OF SUBSTRATE SURFACE CONDITIONS ON MECHANICAL PERFORMANCE OF ELECTRICALLY CONDUCTIVE ADHESIVES

WAN AHMAD BIN WAN ABDUL RAHMAN

UNIVERSITI TEKNIKAL MALAYSIA MELAKA

THE EFFECT OF SUBSTRATE SURFACE CONDITIONS ON MECHANICAL PERFORMANCE OF ELECTRICALLY CONDUCTIVE ADHESIVES

WAN AHMAD BIN WAN ABDUL RAHMAN

A report submitted
In fulfillment of the requirements for the degree of
Bachelor of Mechanical Engineering (Hons)

Faculty of Mechanical Engineering
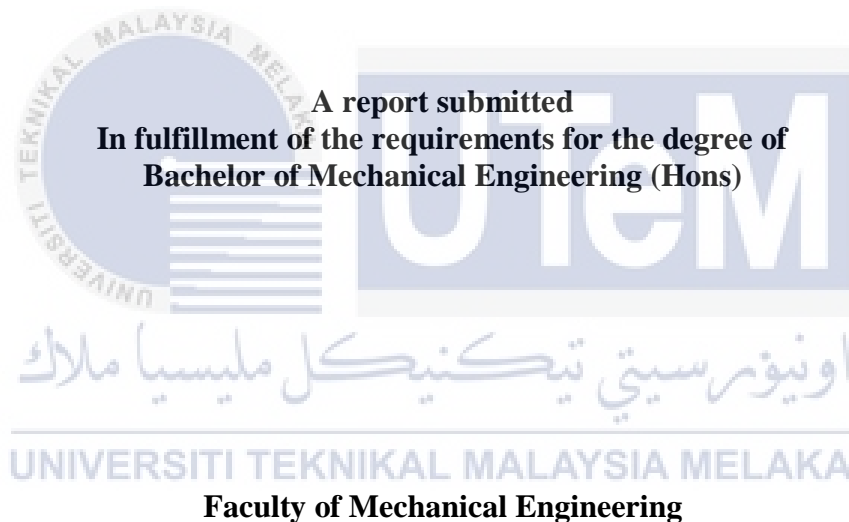
UNIVERSITI TEKNIKAL MALAYSIA MELAKA

2018

DECLARATION

I declare that this project report entitled "The Effect of Substrate Surface Conditions on Mechanical Performance of Electrically Conductive Adhesives" is the result of my own work except as cited in references.
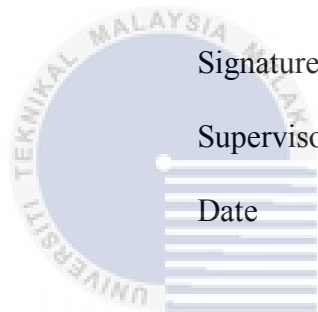
Signature : ……………………………………………………..

Name   : ……………………………………………………..

Date   : ……………………………………………………..

APPROVAL

I hereby declare that I have read this project report and in my opinion this report is sufficient in terms of scope and quality for the award of the degree of Bachelor of Mechanical Engineering (Hons).

Signature   : ……………………………………...

Supervisor's Name : ……………………………………...

Date   : ……………………………………...

DEDICATION

This report is dedicated to my beloved mother,

Maria Binti Hasan Basri

ABSTRACT

Nowadays, with increasing awareness to protect the environment, the use of lead-based solder for electronic components interconnection in printed circuit board (PCB) are gradually replaced by the lead-free electrically conducive adhesive (ECA) in microelectronic industry. As interconnect materials, the mechanical strength of ECA is another aspect to be improvised in addition to the electrical conductive performance. This research project investigates the effect of substrate surface treatment in terms of the surface roughness and surface wettability which contributed to shear strength of multi-walled carbon nanotube (MWCNT) filled ECA bonded to aluminium-aluminium substrate, and the effect of varying MWCNT filler loading on ECA mechanical and electrical properties. Surface roughness is measured using a stylus profilometer and the contact angle test is conducted to measure aluminium substrate surface wettability. The result of four-point probe test reveals that the sheet resistance of the ECA decreased with an increase in the MWCNT filler loading from 5 wt.% to 7 wt.%, due to enhanced formation of percolated linkages between MWCNT particles. Surface treated, and untreated aluminium substrate were used as substrate for single-lap shear adhesively bonded experiment. The surface treatments consist of grinding with silicone carbide (SiC) abrasive paper grit 180 and alkaline/acidic etching. The mechanical properties of ECA bonded to as-received and chemically etched aluminium substrates show an increase in shear strength with an increase MWCNT filler loading from 5 wt.% to 6 wt.% and decrease in shear strength with an increase of MWCNT filler loading from 6 wt.% to 7 wt.%. Higher shear strength is obtained when the ECA experience an adhesive-cohesive failure as compared to the adhesively failed ECA. The surface morphology study on fractured surface of ECA following lap shear test reveals high density of hollow structures/voids on the entire surface of ECA with 7 wt.% MWCNT filler loading, possibly due to agglomeration of MWCNT in the composites, which results in poorer mechanical properties. Overall, the alkaline/acidic etched aluminium substrate exhibit the highest surface roughness and the highest wettability as compared to other surface conditions which results in largest effective bond area between ECA/substrate interface, hence, highest shear strength of the ECA is obtained. Meanwhile, the grinded aluminium substrate with SiC abrasive paper grit 180 has the lowest wettability and slightly higher surface roughness than as-received aluminium substrate which yield to the lowest shear strength of the ECA. This is due to low degree of wettability of grinded aluminium substrate which yield in the low effective bond area, results in an insufficient anchoring of ECA towards the substrate surface.

ABSTRAK

Pada masa kini, peningkatan kesedaran terhadap penjagaan alam sekitar telah menyebabkan penggunaan pateri berasaskan plumbum untuk penyambungan antara komponen-komponen elektronik pada "printed circuit board" (PCB) telah digantikan secara berperingkat kepada "electrically conductive adhesive" (ECA) yang bebas plumbum dalam industri mikroelektronik. Sebagai bahan penyambung antara komponen elektronik, kekuatan mekanikal ECA perlu ditingkatkan selain daripada keupayaan mengalirkan elektrik. Projek penyelidikan ini dijalankan untuk mengkaji kesan rawatan permukaan terhadap kekasaran dan kebolehbasahan permukaan yang memberi kesan terhadap kekuatan ricih ECA komposit yang mengandungi "multi-walled carbon nanotube" (MWCNT) apabila disambungkan pada dua permukaan substrat aluminium, dan kesan perbezaan kandungan MWCNT terhadap sifat mekanikal dan elektrikal ECA. Stylus profilometer digunakan bagi mengukur kekasaran permukaan dan ujian sudut sentuhan dijalankan bagi menguji kebolehbasahan permukaan substrat aluminium. Keputusan ujian empat titik pemeriksaan menunjukkan rintangan lembaran pada ECA mencatatkan penurunan dengan peningkatan kandungan MWCNT daripada 5 wt.% kepada 7 wt.%. yang disebabkan oleh peningkatan hubungan dan sentuhan antara partikel MWCNT. Substrat aluminium yang dirawat dan tidak dirawat digunakan untuk ujian tegangan ricih pada dua permukaan aluminium yang dilekatkan. Rawatan permukaan terdiri daripada dua teknik iaitu mencanai dengan menggunakan kertas pengikis "silicon carbide" (SiC) grit 180 dan hakisan alkali/asid pada permukaan substrat aluminium. Kekuatan ricih ECA yang disambungkan pada aluminium substrat yang tidak dirawat dan yang dirawat dengan hakisan kimia meningkat dengan peningkatan kandungan MWCNT daripada 5 wt.% kepada 6 wt.% dan kekuatan ricih ECA menurun dengan peningkatan kandungan MWCNT daripada 6 wt.% kepada 7 wt.%. ECA yang gagal dengan lekatan-kohesif menunjukkan kekuatan ricih yang lebih tinggi berbanding ECA yang gagal pada lekatan. Kajian morfologi terhadap permukaan ECA dengan 7 wt.% kandungan MWCNT yang gagal setelah dikenakan tegangan ricih menunjukkan permukaan yang padat dengan struktur berlubang yang mungkin disebabkan berlakunya timbunan MWCNT, seterusnya mengurangkan kemampuan lekatan pada substrat. Secara keseluruhan, aluminium substrat yang dikenakan rawatan hakisan alkali/asid mempunyai kebolehbasahan dan kekasaran permukaan yang tertinggi berbanding permukaan substrat yang lain, seterusnya menyumbang kepada permukaan efektif pada sambungan yang terluas antara permukaan ECA/substrat, justeru, kekuatan ricih yang tertinggi pada ECA tercapai. Sementara itu, permukaan aluminium yang dicanai dengan kertas pengikis SiC grit 180 mempunyai kebolehbasahan permukaan yang terendah dan kekasaran permukaan lebih sedikit berbanding permukaan substrat aluminium yang tidak dirawat, seterusnya menyumbang kepada kekuatan ricih yang terendah pada ECA. Hal ini disebabkan oleh kebolehbasahan permukaan yang rendah menyebabkan permukaan efektif pada sambungan menjadi rendah, seterusnya menyebabkan pautan tidak mencukupi oleh ECA untuk melekat pada permukaan substrat.

ACKNOWLEDGEMENT

iii

TABLE OF CONTENTS

LIST OF TABLES

UNIVERSITI TEKNIKAL MALAYSIA MELAKA

LIST OF FIGURES

UNIVERSITI TEKNIKAL MALAYSIA MELAKA

LIST OF APPENDICES

LIST OF ABBREVIATIONS

LSS   -   Lap Shear Strength

ECA   -   Electrically Conductive Adhesive

CNT   -   Carbon Nanotube

SWCNT   -   Single-Walled Carbon Nanotube

MWCNT   -   Multi-Walled Carbon Nanotube

ACA   -   Anisotropically Conductive Adhesive

ICA   -   Isotopically Conductive Adhesive

PCB   -   Printed Circuit Board

CTE   -   Thermal Coefficient of Expansion

NJ   -   New Joint

RJ   -   Repaired Joint

NaOH   -   Sodium Hydroxide

HCl   -   Hydrochloric Acid

SiC   -   Silicon Carbide

SEM   -   Scanning Electron Microscopy

LIST OF SYMBOLS

λ	-	Thermal conductivity, $W/(m.K)$
phr	-	Parts per hundred
Ra	-	Surface roughness, μm
γ_{SG}	-	Free energy per unit area of solid-gas, mJ/m^2
γ_{LG}	-	Free energy per unit area of liquid-gas, mJ/m^2
γ_{SL}	-	Free energy per unit area of solid-liquid, mJ/m^2
dA	-	Area covered by the liquid, m^2
θ	-	Contact angle
C_1	-	Percentage HCL in distilled water
V_1	-	Volume of HCL solution
C_2	-	Desired percentage of HCL in distilled water
V_2	-	Desired volume of HCL solution, $V1 + V_{Distilled\ Water}$
Vm	-	Matrix volume fraction
Vf	-	Filler volume fraction
R_s	-	Sheet resistance $(\frac{\Omega}{sq})$
G	-	Correction factor = 1.9475

V	-	Voltage
I	-	Input Current
τ_{Lap}	-	Lap Shear Strength, LSS (MPa)
F_{Max}	-	Maximum tensile force (N)
A	-	Adhesive overlap area (m^2)
R_f	-	Filler resistance
R_t	-	Tunnelling resistance
R_c	-	Constriction resistance
d	-	Particle diameter
D	-	Contact diameter
ρ	-	Intrinsic resistivity
ρ_t		Tunnelling resistivity
ε	-	Dielectric of the thin film
s	-	Thickness of the thin film
Φ	-	Work function of the metal fillers
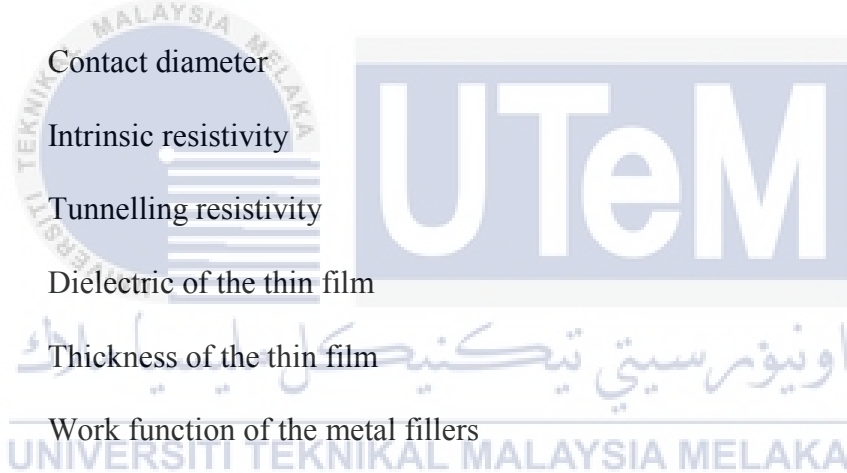
CHAPTER I

INTRODUCTION

1.1   Background

Electrically conductive adhesives (ECAs) are basically made up from combination of adhesives such as epoxy-resin and metallic or carbon conductive filler. The contact between substrate and ECA allow current flow through them which conductive fillers, allowing electron movement by their contact between their suspended particles in the adhesives (Yi, Daniel, & C.P., 2010). High volume of conductive filler in ECA will give good electrical conductivity but will reduce the mechanical strength of the ECA and vice versa (H. P. Wu et al., 2007). There are few advantages of using ECA as compared to lead-based solder for electronic component interconnection, the adhesives are lead-free, less and simple processing steps which reduce production cost, and finer pitch due to the small particles of filler (Mantena, 2009).

ECA is divided into two types which are isotopically conductive adhesive (ICA) and anisotropically conductive adhesive (ACA). ICA has capability to conduct electric at all direction while ACA able to conduct electric at single direction which normally at z-axis. Various kind of ICA are made up from thermosetting resin. Thermosetting resin has several advantages on its properties such as high adhesives strength, and high resistance to chemical and corrosion. Conductive filler usually used in ICAs are nickel, copper, gold and carbon with different size and shape. ACAs are made up from pastes or films of thermoplastic which need high pressure and heat during bonding process to substrate. ACAs are not electrically conductive

1

before bond to substrate as the ratio of conductive filler to adhesives is low and below the percolation threshold (D. D. Lu & Wong, 2009).

In ICA, conductive pathways consist of genuine conduction and percolation. Genuine conduction is conduction by particle-to-particle contact in ICAs while percolation conduction is by dielectric breakdown of the matrix which electron is transmitted by quantum-mechanical electron tunnelling between nearby particles. Besides, ICA electrical conductivity performance also contributed by the uniform dispersion of filler particles in order to create excellent conductive pathway (Mantena, 2009).

1.2 Problem statement

The use of lead-based solder for electronic components interconnection in printed circuit board (PCB) are widely used in microelectronic industry. As the awareness to environment increase, the use of lead material for component interconnection is not recommended; hence a substitute material, that is lead-free electrically conductive adhesive (ECA) is introduced. Other alternative besides the ECA is lead-free solder alloys; nonetheless one of the main concern is on its melting temperature, which exceeds the design temperature of various types of circuit board (Brien, Us, & Ashmead, 2005). Moreover, compared to lead and lead-free solder, the processing temperature of ECA is the lowest and below the design temperature of many circuit board.

ECA is typically consist of polymer matrix binder such as epoxy resin and conductive filler material. In the last couple of years, the carbon nanotube (CNT) has been introduced to replace the use of metallic material as conductive filler. The use of CNT can increase the performance and properties of ECA. The improvements of ECA when using CNT as a filler instead of metallic material are in terms of an improved strength and modulus, high thermal

2

conductivity and good thermal stability, and high capacity of current flow (Kwon, Yim, Kim, & Kim, 2011).

The critical aspect in fine-pitch interconnection field is the adhesion strength of the ECA. This is because ECA is detrimental to shock encountered during handling, assembly and lifetime which require excellent adhesion bond between ECA/substrate interface. Basically, the overall adhesion strength of ECA is from two types of adhesion mechanisms; these being the chemical and physical bonding.

Chemical bonding requires chemical reaction between polymer and substrate which involve the formation of ionic or covalent bonds to link between the substrate and the polymer while physical bonding involve mechanical interlocking between ECA/substrate interface. The formation of inter-diffusion layer established as the interaction of polymer molecule that is highly compatible with the molecules of substrate occur. Besides, the polymer is expected to has good adhesion strength towards the substrate with a rougher surface in which rougher surface provide more contact surface area between polymer/substrate interface to establish excellent interfacial mechanical interlocking (Yi et al., 2010).

However, surface roughness may not establish good adhesion strength at the polymer/substrate interface if the polymer does not penetrate well into the rough surface asperities, which results in a decrease in the effective bond area and generate stress risers at the interface (Boutar, Naïmi, Mezlini, & Ali, 2016). Therefore, good spreading of ECA towards the substrate surface is essential to promote excellent adhesion properties.

In this research project, multi-walled carbon nanotubes (MWCNT) is used as a conductive filler in ECA composites to study effect of MWCNT filler loading on ECA electrical performance, and to study the effect of substrate surface conditions on mechanical performance of ECA with varying MWCNT filler loading.

3

1.3   Objective

The objectives of this research project are:

   i.   To study the effect of MWCNT filler loading on the electrical conductivity performance of the electrically conductive adhesive.

  ii.   To study aluminium substrate surface topography, surface morphology and surface wettability.

 iii.   To study the effect of different substrate surface conditions on mechanical properties of the electrically conductive adhesive.

 iv.   To study the surface morphology of fractured surface of lap shear test samples via scanning electron microscopy (SEM).

1.4   Scope of project

The scope of this research projects is listed as below:

   i.   Formulation and fabrication of electrically conductive adhesives.

  ii.   Conditioning of the substrate materials with and without surface treatment.

 iii.   ECA sheet resistance measurement by conducting a four-point probe test on printed ECA.

 iv.   ECA mechanical testing via lap shear test.

  v.   Surface roughness and contact angle measurement on surface of aluminium substrate.

 vi.   Morphological study on substrate surface and fractured surface of the ECA.

1.5   Planning and execution

Research activities for PSM I are scheduled in Figure 1.1 which include research title selection, literature review, experiment design, surface treatment on aluminium substrate,

aluminium substrate surface topography characterization and wetting performance, formulation and fabrication of ECA, ECA sheet resistance measurement and lap shear test on ECA. The completion of the tests followed by data analysis, report writing, report submission and PSM I presentation. The research activities are continued in PSM II which consists of aluminium substrate morphology characterization through substrate surface profile measurement with 3D profilometer and morphology characterization through microscopic image of substrate surface by optical microscopy, morphological study on surface of fractured ECA through micrograph image by using scanning electron microscopy (SEM), and report writing for PSM II. Research activities of PSM II are scheduled in Figure 1.2.

WEEK / ACTIVITIES	1	2	3	4	5	6	7	8	9	10	11	12	13	14
Research Title Selection	■	■												
Literature Review	■	■	■	■	■	■	■	■	■	■	■	■	■	■
Experiment Design			■	■										
Aluminium Substrate Surface Treatment			■	■	■									
Measuring Substrate Surface Topography				■	■									
Substrate Surface Wettability Test				■	■									
Formulation and Fabrication of ECA				■	■									
ECA Electrical Conductivity Test						■	■							
ECA Lap Shear Test						■	■	■	■	■	■			
Data Analysis						■	■	■	■	■	■	■		
Report Writing						■	■	■	■	■	■	■	■	
Report Submission													■	
PSM 1 Seminar														■

Figure 1.1: Gantt chart of research activities for PSM 1.

6

WEEK / ACTIVITIES	1	2	3	4	5	6	7	8	9	10	11	12	13	14
Literature Review	■	■	■	■	■	■	■	■	■	■	■	■	■	■
Experiment Design	■	■												
Morphological Study on Substrate Surface through 3D Profile Image		■	■	■	■	■								
Morphological Study on Substrate Surface through Microscopic Image						■	■	■						
Morphological Study on Surface of Fractured ECA									■	■	■			
Data Analysis						■	■	■	■	■	■	■		
Report Writing							■	■	■	■	■	■	■	
Report Submission													■	
PSM 2 Seminar														■
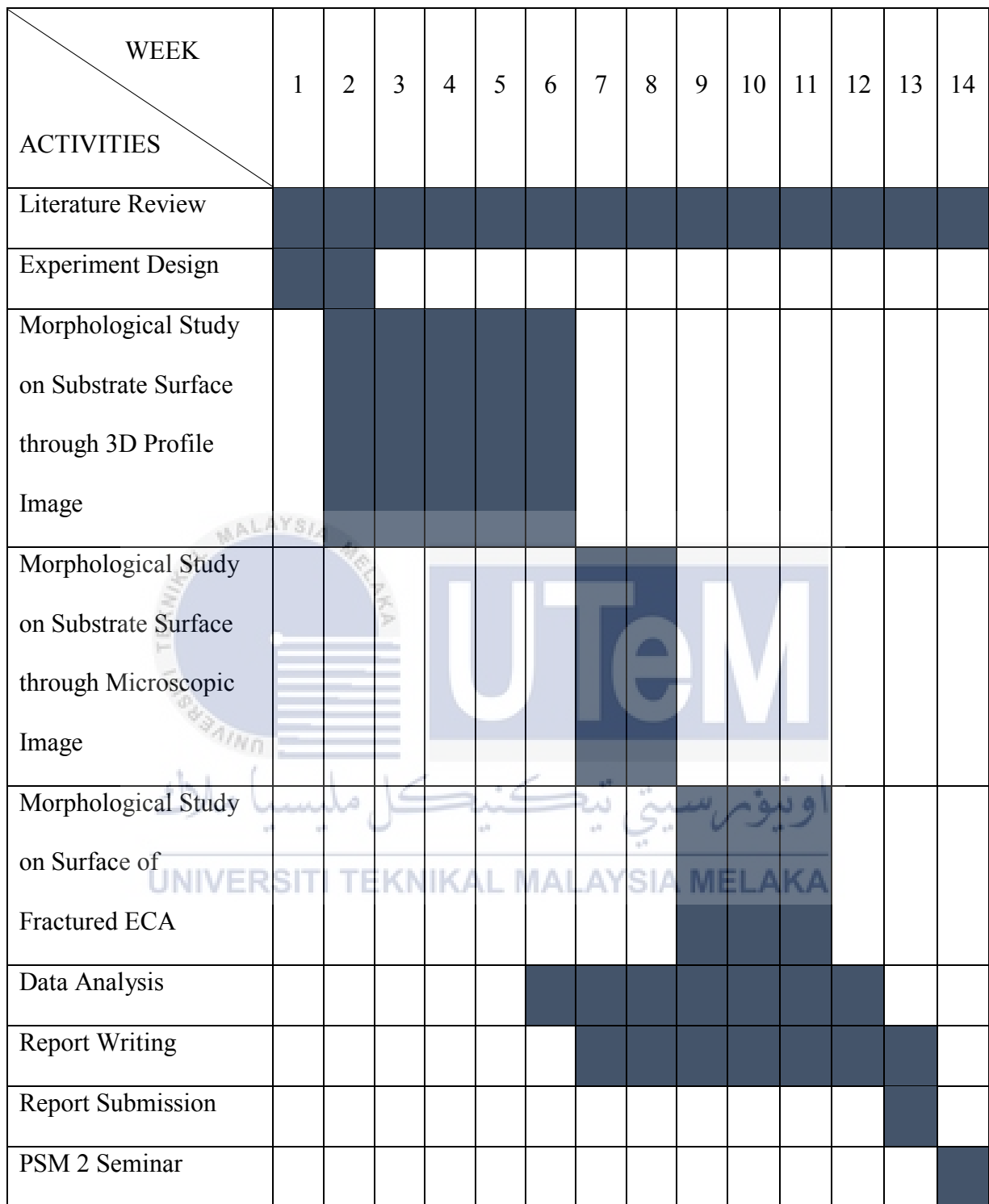
Figure 1.2: Gantt chart of research activities for PSM 2.

CHAPTER II

LITERATURE REVIEW

2.1   Introduction

A review of some related topics towards the project are included in this chapter based on previous study. The main topics reviewed in this section are on the composition of electrically conductive adhesive, mechanical and electrical properties of ECA, substrate surface characterization, ECA mode of failure and surface treatment of substrate.

2.2   Electrically conductive adhesive (ECA)

Instead of using lead/tin solder for electrical interconnection, ECA which lead free is one of alternative for latter purpose since the environmental awareness increase. ECA consists of polymeric matrix such as epoxy and conductive fillers such as CNT which polymeric matrix provide the mechanical and physical strength for ECA while conductive fillers offer electrical conductive ability (D. D. Lu & Wong, 2009; Luo et al., 2016). Polymeric matrix is come out with thermoplastics or thermosets while metallic or non-metallic materials are used as conductive filler for the ECA. Besides its properties of environmental friendly, there are several other advantages when using ECA as electrical interconnection such as low processing temperature, excellent to withstand fatigue effect and good flexibility (Z. Wu, Li, Timmer, Lozano, & Bose, 2009).

8

2.2.1 Polymer matrix for ECA composites

There are several properties required to have ideal polymeric matrix of ECA which are easy and fast curing, high glass transition temperature, good adhesion and adequate moisture resistivity. Polymeric matrix of ECA is divided into two types which are thermosets and thermoplastic. Thermoplastic-based ECA provides better reworkability as compared to thermoset-based ECA but former ECA performance decrease in several aspects such as mechanical and adhesion properties as an increased of temperature. Thermoset-based ECA provide better adhesion performance and has higher resistance to thermal and chemical (Amoli, 2015).

2.2.1.1 Thermoplastic

Thermoplastic polymer consists of long, unlinked polymer molecules and usually has high molecular weight. The structure of thermoplastic is depending on dipole-dipole interaction, aromatic ring stacking or van der Waals force since there is no molecular chains linked. Typical thermoplastics produce a crystalline structure after drop to a certain temperature which contributes to the smooth surface finish and enhance the structural strength. As the temperature elevated, the thermoplastics become soften and when reached at specified temperature, thermoplastics melt (Mayer, 2018). In ICA application, the main thermoplastic used is polyimide resin. The utilization of thermoplastic in ICA offer the reworkable advantage, thus, ICA can be easily repaired. Despite the advantage offered, the high temperature subjected to thermoplastic ICA yield to adhesion performance deterioration. Furthermore, the solvent contained in polyimide-based ICA generate the voids when undergoes high temperature condition as the solvent evaporates (Yi et al., 2010).

9

2.2.1.2 Thermosets

Thermosets consist of 3-dimensional structure of polymer. To cure the thermosets material, chemical reactions is essential to form chemical cross links between the polymer chains. The reaction has contributed to the high thermal resistance of thermosets. Typically, thermosets do not require solvent which solvent has possibility to create air bubbles and voids during curing process. Several disadvantages of thermoset are low performance against the mechanical impact and poor conductivity (Mantena, 2009).

2a.1   Epoxies

In electronic industries, epoxies are the preferred polymeric materials as the materials promote high resistance against chemical and corrosion, excellent physical and electrical properties, good adhesion, thermal insulation, low shrinkage and reasonable cost of material. Preparation of epoxies usually based on bisphenol-A which become bisphenol-A epoxy after reacting with epichlorohydrin as illustrated in Figure 2.1 (Yi et al., 2010).
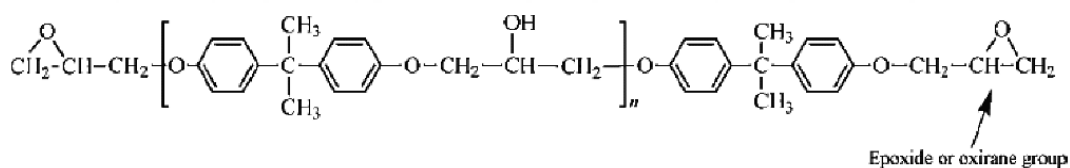
Figure 2.1: Reaction process to produce bisphenol-A epoxy (Yi et al., 2010).

The repletion number is different from zero (liquid) to approximately 30 (hard solid). The viscosity of epoxy is determined by the reactant's ratio which the ratio is between bisphenol-A against epichlorohydrin. There are some epoxy curing agents used such as amines, anhydrides, dicyanodiamides, melamine formaldehydes, urea formaldehydes, phenol-

10

formaldehydes and catalytic curing agents which anhydride and amines are the most common curing agents used (Yi et al., 2010).

The curing agents are chosen based on the curing condition, application techniques, pot-life requirement and specified physical properties. The curing agents give impact on the epoxy formulations' viscosity and reactivity while allow the process to determine the degree of cross linking and the formulation of chemical bonds in the cured epoxy system. In some condition, the accelerator such as tertiary amine is used to accelerate slow chemical reaction between anhydrides and epoxies. There are two type of epoxies which are "Novolacs" and "Resole". Novolac epoxy is formaldehyde acid-catalyzed epoxy polymer which offer high temperature and chemical resistance due to the methylene bridge linked the phenolic group inside the epoxy. Resole epoxy which is a base-catalyzed phenol-formaldehyde offers excellent chemical resistance and requires high temperature to cure (Yi et al., 2010).

High purity epoxies are utilized in device encapsulation and moulding compounds as the polymers reduced the amount of chloride and mobile ions. Besides, to reduce the polymer's thermal coefficient of expansion (CTE), small, well-controlled spherical silica with fine distribution are to be mix into the polymer systems as fillers. The addition of small amount of elastomeric materials into the rigid epoxy enhancing the epoxy toughness and greatly reduced epoxy elastic modulus and thermal stress. The low stress polymer has great ability to suit with several applications such as conductive adhesives and moulding compound (Yi et al., 2010).

2.2.2 Fillers for ECA composites

Conductive fillers in ECA provide the electrical conductivity since the polymer matrices bond to the fillers are dielectric materials. There are two types of conductive filler for ECA which are from metal and non-metal material. Besides, the conductivity performance of ECA

must be high as possible which the conductive fillers loading must reach or over than percolation threshold (Yi et al., 2010).

2.2.2.1 Metal

The movement of electrically charged particles produce the electrical conductivity in metal material. The valence electrons of metal able to move freely which allow the electric current to flow through the metal. The electrons knocked each other and passing and electric charge as electrons move. Less electrical resistance of metal will provide better electrical conductivity performance which require the metal that has less valence electron such as silver, gold and copper (Bell, 2017). Due to the high loading of metal conductive filler required to achieve good electrical conductivity in ECA, there is problem on the strength to weight ratio and reliability of the ECA (Li, Lumpp, Andrews, & Jacques, 2008) .

2b.1   Gold

Gold is the one of most expensive metal which has good electrical and heat conductivity. However, copper and silver have better electrical conductivity but since the gold is difficult to distort and corrode, in some application, the usage of gold is preferable. The resistivity of gold is 0.022 $\mu\Omega$. m at 20 ℃ and thermal conductivity is 310 W/mK at 20 ℃. This material is greatly malleable which 1 ounce of gold can be rolled into translucent wafer with thickness of 0.000013 cm (AZoM, 2010).

2b.2   Silver

Silver is widely used as conductive filler of ICA since the material provide high electrical conductivity, reasonable material cost and good chemical stability (Durairaj, 2016). The weight

12

percentage of silver flakes must in the range of 70 wt.% to 90 wt.% to ensure good electrical and mechanical properties of ECA obtained. Besides, as compared other kind of metals, silver is the highest thermal and room temperature electrical conductivity. Furthermore, silver oxide is electrical conductive while oxide of most metals is not electrical conductive which will reduce the electrical conductivity of metal filler inside the ECA. Silver oxide which is electrical conductive has given advantage to pure silver filled composite as the electrical conductivity of the composite improve when subjected to elevated temperature and humidity or thermal cycling (Yi et al., 2010). Overloading of silver flakes in ECA contribute to poor impact strength, increase in viscosity and high material consumption cost (Xuechun & Feng, 2004).

2b.3   Copper

Copper is one of the metallic materials with excellent electrical conductivity of 58 MS/m which offer low electrical resistance. In term of thermal conductivity, copper has good thermal conductivity as high of $\lambda = 380 \frac{W}{m.K}$. However, it has poor mechanical properties which the tensile strength is below 225 MPa (Coddet, Verdy, Coddet, & Debray, 2016). Besides, copper conductive filler is easily oxidised when subjected to high temperature and humidity which contribute to an increase of electrical resistivity in the ECA. Organic material coating and inorganic material coating are the approaches for copper conductive filler surface treatment and oxidation prevention in ICA application. Inorganic material coating has ability to prevent oxidation of copper, however, effectiveness of most inorganic material coating reduced when subjected to curing condition which is high temperature (Yi et al., 2010).

2.2.2.2 Non-metal

Commonly, non-metal material exists in three states of matter which is gas, liquid and solid. The solid non-metal is comprising with soft and hard materials. As example, sulphur is soft while diamond is hard. Most of non-metal are not lustre as most of the material does not have loose electron and some of them does. In electricity conductive aspect, graphite as a non-metal material which has high performance to conduct electricity while most of non-metal material have low electrical conductivity (Prasad, 2017).

2c.1   Carbon nanotube (CNT)

Carbon nanotubes are made up from molecular-scale tubes of graphitic carbon which have high stiffness, excellent mechanical strength, chemically stable and good conductor of electric (Mantena, 2009). High aspect ratio CNT has a length between the range from several hundred nanometres to several hundred micrometres. As illustrated in Figure 2.2, there are two types of CNT which are single-walled carbon nanotube (SWCNT) with diameter of 0.4-2 nm and coaxial multi-walled carbon nanotube (MWCNT) with diameter of 2-100 nm (Yi et al., 2010). The bonding structure of CNTs are stronger than bonding structure of diamond which former chemical bonding is made up from carbon-carbon bond. In term of mechanical properties, CNTs' tensile strength up to 200 GPa with Young's modulus of 1.2 TPa which make CNTs among the stiffest and strongest materials on earth (Ma, Siddiqui, Marom, & Kim, 2010). The number of shells and the conducting channels for every shell are the factors to determine conductance of single-walled carbon nanotube (SWCNT) and multi-walled carbon nanotube (MWCNT) (Yi et al., 2010).
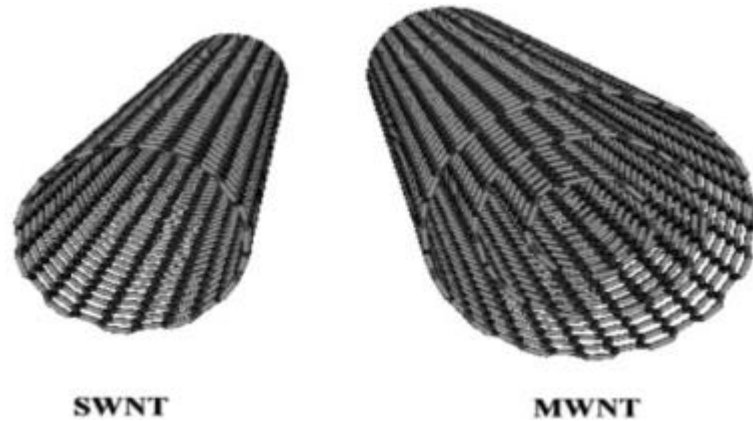
Figure 2.2: Illustration of single-walled and multi-walled carbon nanotube (Mantena, 2009).

2c.1.1 Single-walled carbon nanotube (SWCNT)

Single-walled carbon nanotube (SWCNT) offer better electric properties as compared to multi-walled carbon nanotube. SWCNTs utilization in development of first intramolecular field effect transistors (FETs) is the one of useful applications of the SWCNTs. SWCNTs are consume high cost to manufacture while the improvement of synthesis technique to become affordable is essential for the development of CNT technology (Mantena, 2009).

2c.1.2 Multi-walled carbon nanotube (MWCNT)

Multi-walled carbon nanotube (MWCNT) is made up from the several layers of graphite rolled which become a tube shape. Each layers of graphite rolled have distance approximately 0.34 nm which the layers are joint to each other via van der Waals force. In other hand, the combination of SWCNTs with different diameter, properties and length in concentric position form a MWCNT. The percolation threshold can be achieved for ECA at the low weight percentage of high aspect ratio of MWCNT. MWCNT has outstanding strength to weight ratio which able to enhance the mechanical strength of ECA (Mantena, 2009). The use of MWCNT

15

instead of metal fillers in the ECA promote potential advantage in term of corrosion resistant. Low critical volume of ECA is possible to achieve with utilization of high aspect ratio and high surface area of MWCNT as a conductive filler. ECA with 12 wt.% MWCNT filler loading able to reduce the thermal diffusivity of the epoxy by a factor of 2 to 3 and enhance the electrical performance with 10 Ω cm reduce of electrical resistivity. However, a decrease of lap shear strength reported as the increase of MWCNT filler loading (Li et al., 2008).

2.3   Properties of ECA

The main functional properties of ECA can be characterized especially in terms of its electrical and mechanical characteristics.

2.3.1   Electrical conductivity
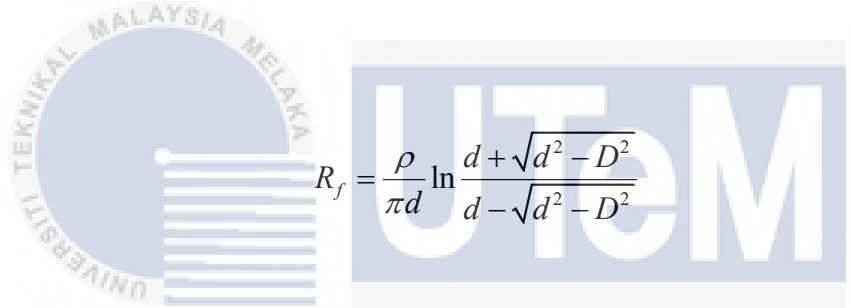
In ECA, the main criteria to be concerned is electrical conductivity performance. The electrical resistivity of the ECA is an inverse of its electrical conductivity. A proper electrical resistivity measurement technique is necessary to determine the electrical conductivity efficiency in the ECA. One of the typical technique utilized to measure resistivity of ECA is four-point probe test.

The resistivity of the ECA is depends on the volume fraction of conductive filler as to induce the formation of electrically conductive path in the ECA which related to percolation theory. As the volume fraction of conductive filler increase, the resistivity of ECA decrease gradually. Further increase of volume fraction of conductive filler in ECA results to volume fraction of percolation threshold achieved which at this point, the formation of continuous linkages between conductive fillers obtained and can be thought as a series of resistors as depicted in Figure 2.3. The total resistance in ECA is consists of filler resistance (R_f) and

16
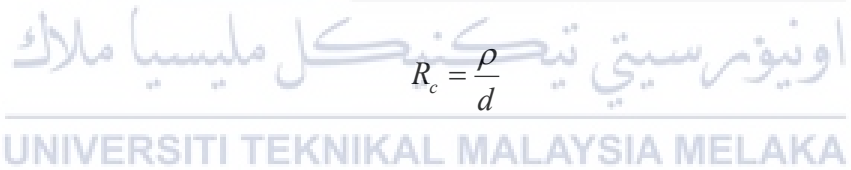
interparticle contact resistance. Latter is composed of tunnelling resistance (R_t) and constriction resistance (R_c). Former resistance occurs as current flow through a small contact area between the particles interface while latter resistance occurs due to the intermediate layer between the metal surfaces. The total resistance of ECA, R_{total}, expressed in Eq. (2.1) (Wong, Zhang, & C. Agar, 2011).

$$R_{total} = R_f + R_t + R_c \qquad (2.1)$$

where,

$$R_f = \frac{\rho}{\pi d} \ln \frac{d + \sqrt{d^2 - D^2}}{d - \sqrt{d^2 - D^2}} \qquad (2.2)$$

$$R_c = \frac{\rho}{d} \qquad (2.3)$$

$$R_t = \frac{\rho_t}{\pi \left(\dfrac{d}{2}\right)^2} \qquad (2.4)$$

$$\rho_t(s, \Phi, \varepsilon) = \frac{10^{-22}}{2} \frac{A^2}{1 + AB} e^{AB} \qquad (2.5)$$

$$A = 7.32 \times 10^{-5} \left(s - \frac{7.2}{\Phi}\right) \qquad (2.6)$$

17

$$B = 1.265 \times 10^{-6} \sqrt{\Phi - \frac{10}{s\varepsilon}} \qquad (2.7)$$

where Eq. (2.2) and Eq. (2.3), d is the particle diameter, D is the contact diameter while ρ is the intrinsic resistivity. In Eq. (2.4), (2.5), (2.6), (2.7), ρ_t is the tunnelling resistivity, ε is the dielectric of the thin film, s is the thickness of the thin film between the conductive fillers and Φ is the work function of the metal fillers.
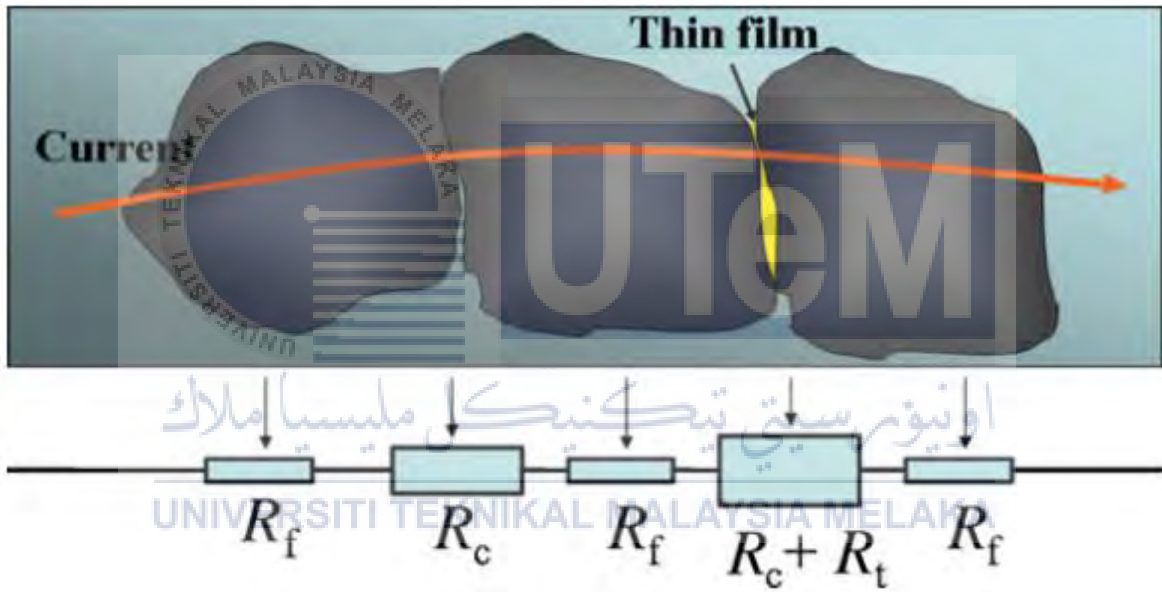
Figure 2.3: Series of resistance in ECA which consist of constriction resistance (R_c), tunnelling resistance (R_t) and filler resistance (R_f) (Wong et al., 2011).

The conductive filler particles could be separated by a thin layer of polymer, lubricants or oxide which the thickness of the layer is depend on the physiochemical properties of the filler, polymer matrix, filler concentration, and the condition of ECA preparation. Besides, the formation of thin polymer interlayers between conductive filler contact regions is significantly

depends on the filler-polymer interaction energies as the filler-filler interaction energy is lower than polymer matrix, most of conductive fillers will be covered with a thin polymer layer. In other hand, the aggregation of conductive fillers is thermodynamically favoured as the filler-filler interaction energy is greater than filler-polymer interaction energy (Wong et al., 2011).

The oxide layer and the thin layer of lubricant on conductive fillers could be removed or reduced when the ECA is subjected to curing process due to the internal stress caused by cure shrinkage. The aspects should be concerned as to enhanced ECA conductivity are the surface properties of conductive fillers (interlayers between conductive fillers), ECA composition (such as filler volume fraction), physiochemical properties of polymer matrix (interaction between conductive fillers and polymer matrix, and cure shrinkage), temperature, interlayer thickness, processing condition of ECA. Volume fraction of conductive fillers in ECA must equal or higher than the critical volume fraction to achieve conductivity, however, too high filler content in ECA cause the degradation of mechanical integrity of adhesive joint (Wong et al., 2011).

Li and Lumpp (2006) conducted an experiment on the electrical characterization of carbon nanotube (CNT) filled adhesive with different CNT loading. The experiment result showed that an increase in CNT filler loading in the adhesive composite reduced the mean value and variance of contact resistance in the composite.

Trinidad, Chen, Lian, and Zhao (2017) investigated the impact of solvent on ECA electrical conductivity. They conducted bulk resistivity test on ECAs with different formulation, in which 40 wt.% Ag/0.75 wt.% Gr(s) and 60 wt.% Ag/0.75 wt.% Gr(s). Based on Figure 2.4, it was reported that the bulk resistivity on solvent-assisted method is eighteen times smaller than the solvent-free method for ECA with 40 wt.% Ag/0.75 wt.% Gr(s). There is no significant different in the bulk resistivity for ECA with 60 wt.% Ag/0.75 wt.% Gr(s) between solvent-free and solvent-assisted which both have bulk resistivity values of $1 \times 10^{-2}\Omega$. cm.

19
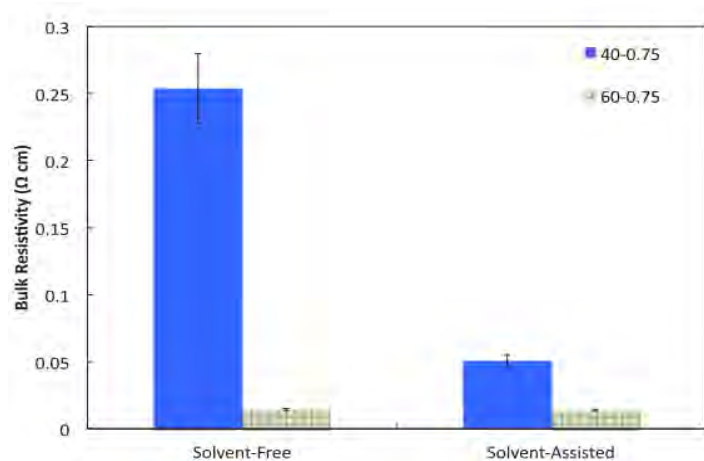
Figure 2.4: Bulk resistivity of solvent-free and solvent-assisted ECAs with different

formulation which are 40 wt.% Ag/0.75 wt.% Gr(s) and 60 wt.% Ag/0.75 wt.% Gr(s)

(Trinidad et al., 2017).

Xuechun and Feng (2004) studied on the improvement of the properties of silver-containing adhesives by the addition of carbon nanotube. First, they measured bulk resistivity of MWCNT/epoxy resin composites from 0% MWCNT loading up to 4.0 phr of MWCNT and the results showed that the bulk resistivity reduced as the increased of MWCNT loading in the composites. In the second condition, bulk resistivity test carried out on the Ag/epoxy resin composites and at 45 wt.% Ag, the bulk resistivity is high as 10^8 Ω. cm and only has good conductivity at 72 wt.% Ag which the bulk resistivity is 1.5×10^{-3} Ω. cm. In another condition, bulk resistivity test was measured for 45 wt.% Ag/epoxy resin with addition of varying MWCNT loading which the result showed that the bulk resistivity decreased as the MWCNT loading increased at the range between 0 phr to 3 phr. However, the bulk resistivity starts to increase when MWCNT loading at 5 phr. Since the 45 wt.% Ag/epoxy resin composite is below percolation threshold, MWCNT provide the electrical network between silver particle which contribute to low bulk resistivity of the composites. When comparing between 4 phr of MWCNT

20

loading in epoxy and 45 wt.% Ag/epoxy composites, latter bulk resistivity is higher since the silver contain form high viscosities composite which obstruct the dispersion of MWCNT. Then, the conductive adhesives' bulk resistivity was measured for 45 wt.%, 52 wt.%, 57 wt.%, 66.5 wt.% and 72 wt.% Ag with various MWCNT loading or without MWCNT loading and the result is presented in Figure 2.5. From the results, at 66.5 wt.% Ag/epoxy resin with addition of 0.27 wt.% MWCNT, is approximately 1,000,000 times lower bulk resistivity as compared to similar composite formulation with no addition of MWCNT.

Ag(wt %)	45	52	57	66.5	72
bulk resistivity of Ag/Ep composites (ρ_1) (ohm·cm)	$\gg 10^8$	6.91×10^6	1.04×10^6	1.01×10^4	1.5×10^{-3}
CNTs (wt%)	1. 35	1. 0	0. 4	0. 27	0. 24
bulk resistivity of CNTs/Ag/Ep composites (ρ_2) (ohm·cm)	4.8×10^3	3.82×10^1	2.4×10^{-2}	6.47×10^{-3}	1.43×10^{-3}

Figure 2.5: Bulk resistivity for 45 wt.%, 52 wt.%, 57 wt.%, 66.5 wt.% and 72 wt.% Ag with various MWCNT loading or without any MWCNT added (Xuechun & Feng, 2004).

Li et al. (2008) studied on aspect ratio and loading effects of multiwall carbon nanotube in epoxy for electrically conductive adhesive. From the study, lower percolation threshold of the MWCNT filled ECA is achieved as compared to metal filled ECA. The dramatic reduction of volume resistivity at 0.25 wt.% MWCNT filler loading, an indication of the conductive fillers starts to generate conductive path between the filler particles before reaching 0.25 wt.% MWCNT filler loading. Besides, the volume resistivity decreases as the ECA subjected to preliminary accelerated aging test with 85°C/85% RH exposure. The contact resistance between

21

MWCNTs and the intrinsic conductivity of the MWCNTs influence the ECA conduction mechanism. Besides, distance between particles, shrinkage of the polymer and work function of the MWCNTs play an important role to determine contact resistance of the composite.

In 2009, Mantena (2009) revealed that the volume resistivity in ECA decrease as the weight percentage of MWCNTs increase. There was a small change of volume resistivity from 8 wt.% to 12 wt.% MWCNTs filler loading which means that the processability is limited beyond 8 wt.% filler loading. With increasing MWCNT filler loading, the number of conductive paths increases and the reliability on resistivity measurement enhanced as the variance reduced in the ECA system. The ECA was too viscous to process as the MWCNT filler loading reached more than 12 wt.%.

The effect of CNT filler loading on the electrical properties of isotropical conductive adhesive (ICA) were studied by H. P. Wu et al. (2007) which they found that an increase of conductive filler content result to decreasing of bulk resistivity. As the filler loading achieve percolation threshold, the CNT provide little effect on the bulk resistivity. Besides, the cured pressure of resin generates the conductive network in ICA. The cured pressure is very high at high filler concentration in ICA, hence, the very well conductive particles contact achieved, resulting the bulk resistivity slightly change.

2.3.2 Mechanical properties

Mechanical properties are material properties that react to applied force. A study of mechanical properties of material is essential to determine the functionalities and strength of the materials. Effect of temperature, rate of force applied, and other conditions contribute the change of material mechanical properties ("Mechanical Properties," n.d.). There are several mechanical

properties of ECA are to be concerned in this project which are lap shear strength and mode of failure.

Lap shear strength (LSS) is measured through the shear or tensile test which the ECA is subjected to shear load. The lap shear test which involve adhesives on metal substrates, usually, the implementation of the test is based on ASTM D1002. Sample and adhesives are illustrated in Figure 2.6 and the test is conducted by gripping and pulling the test grips area which lead to shear stress subjected on the adhesive between the overlap area (Yi et al., 2010). There are some factors affect the static behaviour of single-lap bonded joint such as adhesive and substrate thickness, surface pre-treatment and surface roughness (Pereira, Ferreira, Antunes, & Bártolo, 2010). Besides, the adhesive bond strength is influenced by key and lock interactions attributed to penetration of epoxy resin into the porous oxide structure, hence, the low viscosity of resin can be utilized to provide well penetration into the porous layer (Pethrick, 2015).
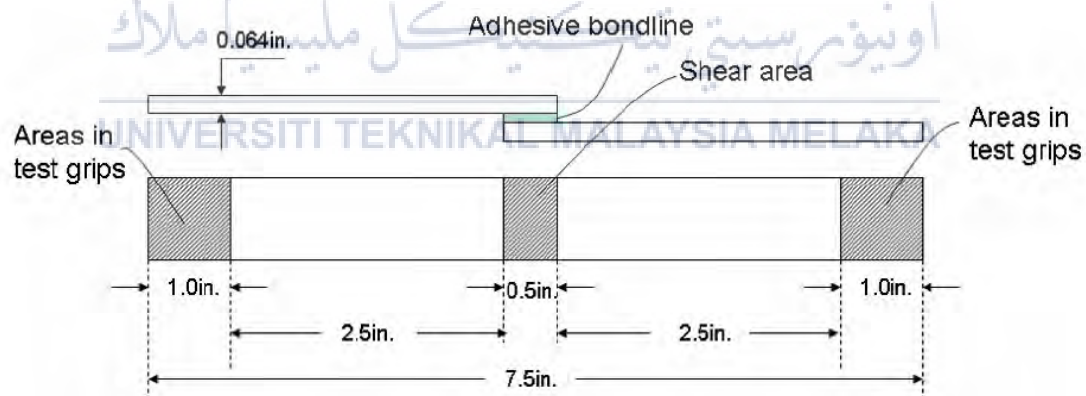
Figure 2.6: Substrate and adhesives of lap shear test method based on ASTM D1002 as a standard guideline (Yi et al., 2010).

23

2.3.2.1 Effect of ECA filler loading on ECA mechanical properties

Trinidad et al. (2017) reported on a study focusing on LSS of solvent-free and solvent assisted ECAs with different Ag and Gr(s) loading. In solvent-free ECAs, the increased of Ag fillers caused the ECAs' LSS reduced and when no addition of Gr(s), the ECAs' LSS significantly decreased as the Ag fillers increased. In the other condition, solvent-free ECAs have highest LSS when Gr(s) is 0.75 wt.% with same Ag weight percentage and start to reduce LSS when applied 1.5 wt.% Gr(s) since aggregation started to occur on Gr(s). In condition of solvent-assisted ECAs, LSS started to reduce significantly for 0.75 wt.% and 1.5 wt.% Gr(s) with 20 wt.%, 40 wt.% and 60 wt.% Ag as compared to solvent-assisted ECA with no present of Gr(s). The shear strength of ECAs reduced due to the residual solvent which supposedly to completely evaporate and desiccate. The residual solvent able to create the formation of hollow structures and voids within the ECA, and between ECA/substrate interface. Due to this, the poor mechanical bonding properties between ECA/substrate interface obtained.

Srivastava (2011) conducted lap shear test to study the effect of MWCNT on adhesives shear strength. The experimental result showed that an increase of bonding strength when epoxy resin loaded with MWCNT as compared to neat epoxy. Such observation could be attributed by the presence of MWCNT particles which enhance the strength and fracture toughness, and enhancement of stiffness due to resistance of crack initiation and propagation in ECA. Besides, an increase of fracture toughness is due to void nucleation and localised inelastic matrix deformation, fibre/particle debonding and deformations. Furthermore, the high surface area of MWCNT provide high load transfer efficiency at interface region.

Li and Lumpp (2006) conducted experiment to characterize the mechanical properties of carbon nanotube filled adhesive. The result from a shear strength test with copper substrate showed that no significant deterioration on mechanical properties of the adhesive with 0.8 wt.%

CNT filler loading. Moreover, no cracks observed on the fracture surface despite the failure is due to polymer/CNT composite loosing contact with the substrate surface. There is 20% loss of shear strength as compared to the neat adhesive shear strength which is due to the low interfacial bond strength between CNT and copper.

Dispersions of MWCNT in the polymer matrix with different MWCNT filler loading were investigated by Yim and Kim (2015). The addition of functionalized MWCNT into the polymer matrix enhance the mechanical properties of the polymer composites and assist load transfer from polymer matrix as the formation of hydrogen bonds between functional groups on the MWCNT and polymer chain improve the interfacial adhesion between them. However, the pristine MWCNTs tend to become entangled during fabrication process due to their high surface energy, the intrinsic van der Waals force between their particles, and their small size. The tendency of agglomeration between MWCNTs may contribute to mechanical properties deterioration of MWCNT/polymer nanocomposites. Degradation of mechanical properties and inefficient load transfer in MWCNT/polymer composites may due to the aggregation of MWCNTs and lack of interfacial adhesion between MWCNT/polymer. Hence, MWCNTs must be well dispersed in the MWCNT/polymer composites to enhance the interfacial interactions with the polymer chains. Furthermore, the size of MWCNT aggregate structures increases with increasing of filler loading in the composites. This is due to an increase of MWCNT loading cause an increase of MWCNT/polymer composites viscosity which reduces the mobility of MWCNTs in the composites. Therefore, the number of partially aggregate MWCNT bundles increase.

Shen, Huang, Wu, Hu, and Ye (2007) studied about the reinforcement role of different amino-functionalized MWCNT/epoxy composites which they found that the well dispersed of MWCNT in epoxy matrix provide high conductive filler surface area available and prevents

MWCNT from aggregate between them. The aggregate MWCNT can acting as stress concentrators and contribute to slippage of filler when load is subjected to MWCNT/epoxy composites. Besides, the small agglomerates and occasional voids may have great effect on the mechanical and thermal properties of the composites. The high surface area of MWCNT and high MWCNT loading in MWCNT/epoxy mixture resulting to high viscosity of the composites, create bubbles and agglomerates in the epoxy which affect the filler dispersion in epoxy. Besides, the poor dispersion of MWCNT in epoxy matrix contribute to higher standard deviation of flexural strength. High MWCNT loading in the composites contribute to increasing of composites viscosity which yield to low energy dissipating in the composites, and the removal of voids and aggregates becomes difficult.

Previous research by Qiao, Bao, Li, Jin, and Gu (2014) found that tensile-shear strength of ECAs decrease as the increase of silver conductive filler content. The factor influences the finding is the epoxy unable to be in continuous form and will not able to provide good polymer network as the epoxy contents decrease with the increase of silver fillers in ECAs.

The effect of CNT filler loading on the mechanical properties of isotropical conductive adhesive (ICA) were studied by H. P. Wu et al. (2007) which they found that the trend of increases and then decreases of shear strength of ICA with increasing of CNT filler loading. In conductive composite materials, mechanical and electrical properties are incompatible. In other words, to obtain good electrical conductivity, it would sacrifice mechanical properties. Besides that, CNT filled ICA provide excellent mechanical and electrical properties at low CNT loading.

Zandiatashbar, Picu, & Koratkar (2012) studied on the behaviour of epoxy-graphene platelets nanocomposites and found that the quality of dispersion is strongly influence the nanocomposites properties. The larger degree of aggregates graphene platelet (GPL) occur at higher GPL concentration in the composites and suggest that the better dispersion of GPL filler

26

in the epoxy is at lower filler concentration. The aggregation of GPL in the composites can lead to mechanical properties degradation of the composites.

Reinforcement efficiency of carbon nanotubes were studied by Loos and Manas-Zloczower (2012). The experimental data showed that large improvement of mechanical properties obtained up to certain CNT filler loading in polymer composites (typically at the percolation threshold), in which beyond this, a dramatic decrease in mechanical strength acquired with further increase of the filler loading.

2.3.2.2 Effect of surface conditions on ECA mechanical properties

The modification of surface topography to the shallow open structure of deep pits from sharp edged or those with recessed angle enhance the capability of resin to fill in. In addition, high stresses in hardened resin occur which is attributed to the sharp asperities. Although an increase in the surface roughness can enhance the ability of adhesives to spread, however, there is a tendency of air entrapment between the asperities which can reduce the wettability and enhance stress concentration (Jennings, 1972; Zielecki, Pawlus, PerŁowski, & Dzierwa, 2013). Therefore, the roughness should be random to avoid single line crack propagation between air pockets (trapped air between asperities). Some advantages of surface roughening toward joint strength are increase surface bonding area, provide a scarf-like surface geometry, remove surface contamination, and enhance of good spreading of adhesive on the substrate surface (Jennings, 1972).

A study on the effect of surface treatment on adhesively bonded aluminium-aluminium joints by Correia, Anes and Reis (2018) found that the new joint (NJ) has high shear strength as compared to repaired joint (RJ) in which both substrate surface of NJ were anodized and painted with primer. Meanwhile, for RJ, only one substrate surface undergoes both surface treatment

27

and another substrate surface solely cleansed with solvent. Besides, the type of failure gives significant effect on the joint strength. Based on the lap shear test results, the specimens with adhesives failure (occur on untreated surface) have lower shear strength while specimens with adhesive-cohesive failure (occur on treated surface) have higher shear strength. The adhesive failure usually occurs due to lack of adherence in untreated substrate surface. In term of surface treatment, it was argued that anodizing surface treatment create a stable coating on a substrate surface in a various electrolyte, induce the formation of an oxide layer on the surface. At the microscopic level, the enhancement of bond area obtained with the appearance of "whiskers". Four types of anodizing method can be utilized; these being phosphoric acid anodizing, chromic acid anodizing, boric-sulfuric acid anodizing and sulfuric acid anodizing. The first two anodizing treatment release the carcinogen substance which can harm human health. Sulfuric acid anodizing can create very thin oxide layer, resulting the improvement of bond strength. Besides, the primer was utilized to prevent the moisture breaching into the adhesive and the substrate inter-phase which can deteriorate the joint strength.

A study on the effect of surface roughening of aluminium plates on the bond strength by Yasuda and Saito (2014) found that an increase of surface roughness, Ra, of aluminium surface through chemical etching process enhanced the average bonding shear strength. Low surface roughness is due to presence of small density of etch pits which cause insufficient anchoring of adhesive to substrate surface. An increase in immersing time of the aluminium substrate in the chemical solution yield to an increase in the surface roughness and providing large interfacial area between aluminium and polyphenylene sulphide (PPS). As the low temperature thermosonic bonding utilized, no interfacial interatomic reaction can be expected.

Prolongo and Uren (2009) were conducted study on the effect of surface pre-treatment on the adhesive strength of epoxy-aluminium joints. It was reported that corrosion process

28

(alkaline or acid environment) is usually utilized to treat surface of aluminium substrate as to activate and clean aluminium surface, to dissolve natural alumina layer, and to induce the formation of porous alumina layer which will enhance the adhesion ability. Furthermore, formation of high porous oxide on aluminium surface indicate high surface contact area and enhance the mechanical interlocking with the adhesives. Based on result of surface treatment of aluminium substrates, they confirmed that the surface of chemically etched substrates is more bumpy and rugged as compared to abraded substrates. The experiment result shows that the higher shear strength of adhesive is when aluminium was surface treated with sulphuric acid-ferric sulphate solution as compared to dichromate-sulphuric acid etching treatment due to the higher porosity introduced by the formed of oxide layer. In another comparison, the shear strength of adhesives bonded to abraded-substrate is lower than adhesive bonded to chemically etched substrate (acid or alkaline etching) as the existence porous and oxide layer enhance the adhesive strength. Chemically etched aluminium A2024 alloy usually promote better adhesion strength towards ECA as compared to chemically etched aluminium A1050 alloy. This is due to former aluminium was more affected by chemical etching treatment as the existence of different allowing elements and intermetallic compounds, with different electrochemical potential influence the electrochemical corrosion process. Due to the process, a porous oxide layer formed, with large and deep voids, which yield an increase of adhesion strength. Besides, one of the most crucial parameters is viscosity as high viscosity of adhesive could reduce wettability and impregnation process, resulted to decrease of actual contact area.

The effect of surface pre-treatment on surface characteristics and adhesives bond strength of aluminium alloy were studied by Leena, Athira, Bhuvaneswari, Suraj, and Rao (2016). Three types of aluminium substrate were considered in this experiment which were subjected to different surface treatment method. The kind of aluminium are Al-SD (treat with

29

solvent degreasing), Al-SDFPL (treat with solvent degreasing, Forest Product Laboratory etching) and Al-SDFPLP (combine of first two treatment method followed by priming of substrate). Based on contact angle experiment, they found that the absorption of adhesive on substrate is depends on geometry of the pores, surface energy of adhesive and substrate, the time since application of adhesive on the substrate, and rheology of the adhesive. Although the oils and organic contaminants are removed from the Al-SD surface, the weakly bound of oxide layer reduce the capability of adhesive to spread. Al-SDFPL substrate provide uniform porosity and high surface energy when subjected to chromic etching which yield in lower contact angle and good wetting as the more penetration of adhesive into the surface pores. Although Al-SDFPLP substrate has lower surface energy, but, adhesive show good wetting on substrate surface due to an increase interaction of primer/epoxy interface. Besides, Al-SDFPL showed higher work adhesion as compared to Al-SD, indicate the fresh and porous aluminium oxide layer on the surface after application of surface treatment. For the lap shear test, Al-SD showed the lowest shear strength while Al-SDFPL has the highest shear strength although Al-SDFPLP provide highest theoretical work of adhesion. This condition is attributed by several factors such as interfacial contact area, surface roughness, surface energy and chemical composition of adherent and adhesive. In term of surface topography with utilizing AFM imaging, Al-SD surface showed less random, compact surface with uniform peaks while Al-SDFPL showed an ideal random porous texture with predominant pits and provide highest surface roughness which attributed to the oxide protrusions resulted to excellent interfacial interaction and serve the mechanical interlocking with the adhesive. For Al-SDFPLP, surface topography is mostly like Al-SDFPL surface topography, but it has lower surface roughness. As a conclusion, the combination of high surface roughness and high surface energy of substrate, and good wettability of adhesive yield to excellent joint strength.

30

From the previous study, NaOH etching process on aluminium substrate generate a micro-rough structure to the surface. Surface of chemically (NaOH solution) etched aluminium is much cleaner and possibly free from organic contaminant as compared to the untreated surface. In wettability measurement, the contact angle of chemically etched aluminium is lower than untreated aluminium which latter condition has low surface energy. As information, the high surface energy of the substrate yield to stronger attraction between substrate surface and molecule of the liquid, result to good adhesion. Wettability of substrate is influenced by the surface roughness which the high surface roughness (in micro scale) of substrate will has low contact angle. In other hand, the contact angle is inversely proportional to the surface roughness. The hydrophilic surface with high surface roughness has a greater interface area resulting to lower contact angle and higher surface energy. The flow of resin into each micro-pores or micro-grooves on the substrate surface indicate the good wetting condition. Thus, the complete wetting can be achieved by having the maximum contact between resin and substrate surface while an increase of micro-grooves yields to more surface area of contact between resin and substrate. Therefore, an increase of shear strength can be obtained at low contact angle which attributed to the liquid follow the topography or it spread inside the solid texture. Lap shear test result showed an increase of shear strength of adhesive bonding with increasing of surface roughness and decreasing of contact angle which attributed to good adhesion when an adhesive penetrates the holes, pores, crevices and other irregularities of substrate surface and then, locks mechanically to the substrate. Besides, the friction coefficient, matrix stiffness and cohesive bond significantly influence the interlocking effect between two surfaces (Muhammad, Hj, & Suzana, 2014).

A study on effect of surface treatment on adhesive joining aluminium was conducted by Borsellino, Bella, and Ruisi (2009) and the experiment result showed a significant enhancement

31

of joint strength from untreated to the treated aluminium surface (mechanical abrasion surface treatment) due to latter generate surface topography and remove the contaminated outer layer of substrate. Besides, the formation of chemical bond between substrate and adhesive during the curing process contribute to the bond strength enhancement. Despite that, the use of epoxy adhesive which contain an alkaline curing agent will react with moisture and form a strong alkaline. An improvement of stability of Mg oxide contain in aluminium oxide can be obtained and enhance the epoxy adhesion as Mg oxide is thermodynamically passive at high pH. Lastly, the joint resistance is increase until a specified topography obtained when subjected by mechanical abrasion surface treatment, then, no significant improvements with further increase surface roughness

Ghumatkar and Sekhar (2017) carried out study about the different aluminium substrate surface roughness on adhesive bond strength. They found that the highest shear strength is when the surface roughness is $2.05 \pm 0.19\ \mu m$ which 12.14% increase of shear strength compared to as-received surface roughness which is $1.55 \pm 0.15\ \mu m$. However, due to wettability performance of adhesive decreased at specified surface roughness, the higher surface roughness of aluminium substrates which are $3.46 \pm 0.20\ \mu m$ and $3.71 \pm 0.17\ \mu m$ result to lower shear strength of adhesive bond. The increase and then decrease trend of adhesive shear strength with increasing of aluminium surface roughness obtained in the experiment.

Based on study on the effect of surface treatment on shear strength of aluminium adhesive single-lap joint, the contact angle of water drop is inversely proportional to adhesive shear strength (Boutar et al., 2016). Polished aluminium substrate with p1000 has contact angle of 62° while with p50, the contact angle is 80.3°. Polishing aluminium with p50 promote to the high surface roughness, however, the micro geometric barrier effect generated due to surface morphology could prevent the spreading of drop on the surface which result to low wettability.

32

This is due to the gas molecules can be trapped in the asperities valleys and cause the liquid unable to penetrate well the rough surface asperities. Therefore, the continuous interface between solid-liquid cannot be achieved and alternate the interface to the gas-liquid interface. As the valleys and grooves does not penetrated by adhesive due to low wettability and remain air entrapped between adhesive and substrate, the effective bond area decreases and produces stress riser at the interface.

Uehara and Sakurai (2002) carried out study of bonding strength of adhesives and surface roughness of joined part where they found that an optimum surface roughness yield to the maximum tensile strength of adhesive. A peak of the adhesive shears strength is virtually unobservable in the graph of shear strength against surface roughness which mean no clear relationship between surface roughness and adhesive shear strength.

2.3.2.3 Mode of failure

There are four types of ECA bond mode of failure in single-lap-joint test which are cohesive, adhesive, adhesive-cohesive and substrate failure as illustrated in Figure 2.7. Cohesive failure occurs when ECA break while adhesive failure occurs is due to failure of joint between substrate and ECA. When the previous two types of failure occur concurrently, this result present the adhesive-cohesive failure. For the rare case of single-lap-joint test, the substrate failure occurs due to substrate mechanical strength not capable to withstand the applied load and start to yield and break (Correia et al., 2018).
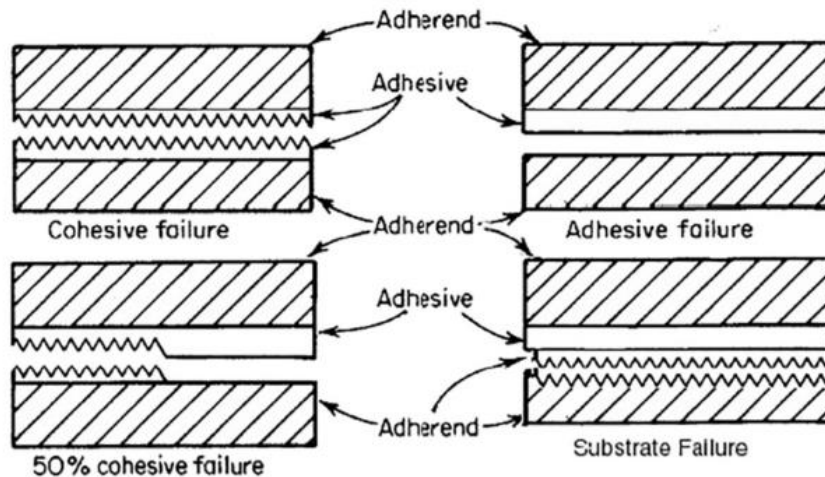
Figure 2.7: Four different type of failure in single-lap-joint test (Correia et al., 2018).
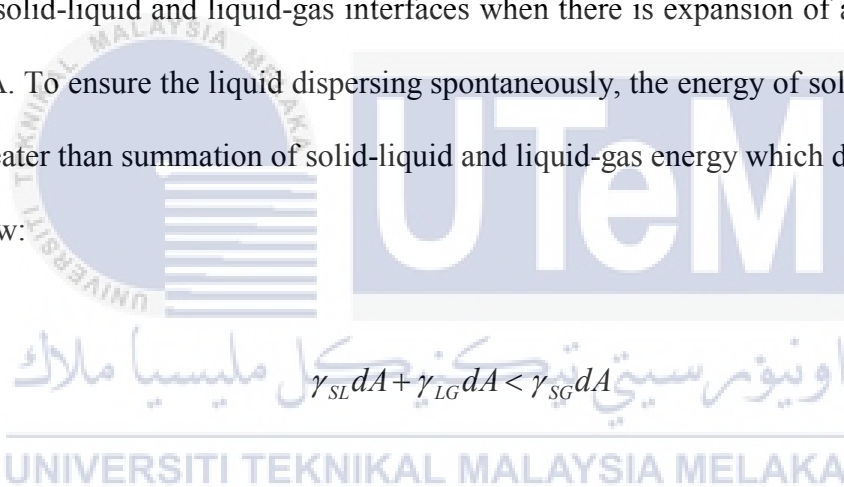
An indication of poor bonding between the substrate and adhesives can be reflected from the formation of adhesive bonding and can be specifically addressed by surface treatment prior to bonding (Pethrick, 2015). A stronger bond at interface between substrate and adhesive result to a cohesive failure, thus, contribute to excellent properties in shear strength and delamination resistance of the joint. However, in some case, the adhesive-substrate joint may fail adhesively but has a greater strength than a similar joint with a weaker adhesive that fails cohesively (Muhammad et al., 2014).

2.4   Properties of aluminium substrate

This section consists of review on literature with explanation on theoretical knowledge which related to wettability, surface morphology and surface topography of the substrate.

2.4.1 Wettability

Wettability is the ability of liquid to disperse over the solid surface. High performance of wettability means that the liquid capable to flow over the solid surface and has the maximum contact area on the surface which covering all voids and bump and removing trapped air inside the void. Wetting only occur in two conditions, firstly, the liquid must not in high viscosity and secondly, free energy of the system reduce after undergoes wetting process. Every surface has their own free energy and the free energy per unit area of solid-gas, liquid-gas and solid-liquid interfaces are present as $\gamma_{SG}, \gamma_{LG}, \gamma_{SL}$ respectively as illustrated in Figure 2.8. More energy is required for solid-liquid and liquid-gas interfaces when there is expansion of area covered by the liquid, dA. To ensure the liquid dispersing spontaneously, the energy of solid-gas interface should be greater than summation of solid-liquid and liquid-gas energy which described by Eq. (2.8) as follow:

$$\gamma_{SL}dA + \gamma_{LG}dA < \gamma_{SG}dA \tag{2.8}$$

Energy per unit area is as expressed in Eq. (2.9) below:

$$\gamma_{SL} + \gamma_{LG} < \gamma_{SG} \tag{2.9}$$

Then, the spreading coefficient is defined as given in Eq. (2.10):

$$SC = \gamma_{SG} - (\gamma_{SL} + \gamma_{LG}) \tag{2.10}$$

35

The spreading coefficient should be in greater than zero for liquid wetting. For example, surface energies of epoxy resin with γ_{LG} = 40 mJ/m² is expected to be able to wet aluminium surface which has γ_{SG} = 1100 mJ/m² but the matrix not be able to wet the low surface energies of solid-gas interface such as polyethylene with γ_{SG} = 30 mJ/m².
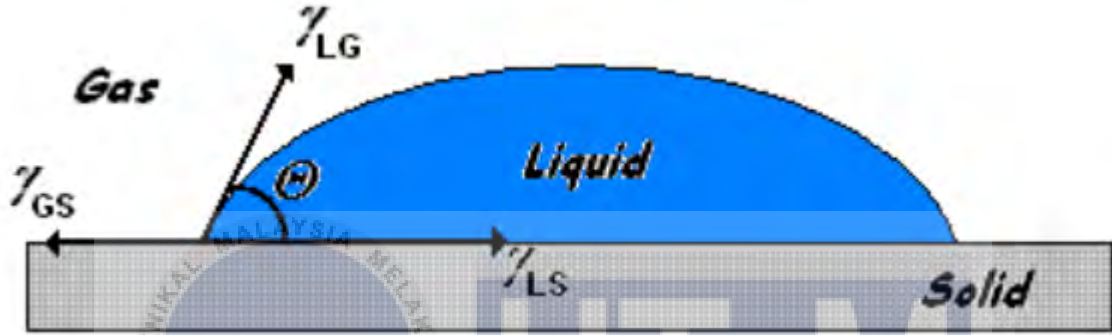
Figure 2.8: Liquid wet on solid surface with surface energies of solid-liquid, liquid-gases and solid-gases interfaces which described as $\gamma_{SG}, \gamma_{LG}, \gamma_{SL}$ respectively (Dr. Reinhard Miller & Dr. Alexander Makievski GbR, 2011).

Since the surface energies is equal to surface tension which is force per unit length, the force can be resolved horizontally in Eq. (2.11):

$$\gamma_{SG} = \gamma_{SL} + \gamma_{LG} \cos\theta \qquad (2.11)$$

Rearrange Eq. (2.11) gives contact angle, θ, equation, and expressed in Eq. (2.12):

$$\cos\theta = \frac{(\gamma_{SG} - \gamma_{SL})}{\gamma_{LG}} \qquad (2.12)$$

36

Contact angle, θ, use to measure degree of wettability which θ=180° indicate the dropped liquid do not wet the solid surface and form the spherical shape while for the perfect wetting, contact angle is θ=0°. The increment of contact angle indicates the reducing of wettability and vice versa (F.L. Matthews and R.D. Rawlings, 1999).

2.4.2 Surface roughness

Borsellino et al. (2009) studied on the effects of resin and surface treatment. They found that the joint resistance enhanced with an increase in surface roughness up to specific surface topography, then, the joint resistance reaching plateau as further increase in surface roughness. Besides, an increase in surface roughness yield to higher wettability for EPO resins while VE resin is vice versa. It means that, the type of resin influenced the wettability performance.

A study on effect of grit blasting on surface properties for adhesions were conducted by Harris and Beevers (1999) and they found that rougher surfaces exhibited lower surface energies due to effect of geometric features of the surfaces on the ability of liquid drop to wet the surfaces. They suggested that the ridges, peaks and asperities form barriers which hinder the spreading of the liquid. Spreading and wetting properties are more influenced by the amount of effective surface area than the surface texture characteristics (Harris and Beevers 1999; Wenzel, 1936)

The effect of surface roughness on surface wettability were studied by Hitchcock, Carroll, and Nicholas (1981) which argued that a decrease in surface wettability subjected to surface roughening except for the surface texture is very rough or the liquid is inherently excellent wetting.

37

2.5   Substrate surface treatment

Surface treatment is the method to change the substrate surface condition which play an important role to enhance the mechanical strength of adhesive of epoxy-aluminium joint (Prolongo & Uren, 2009). The oxide layer and adsorbed contamination which cover the aluminium surface should be removed to improve the durability of joint between adhesives and metal. An excellent mechanical strength can be obtained by removal of gross contamination. Furthermore, surface treatment is the most crucial process to enhance the adhesive-bonded joint durability and strength while reduce the rate degradation of joint when subjected under stressed conditions.

Despite that, the high porosity oxide layer formed of treated surface influenced the bond strength (Pereira et al., 2010). Although the presence of passive oxide layer on aluminium surface could yield to good adhesion, however, for bonding purpose, it is not optimal. Besides, an increase in the joint strength was reported for as-received substrate as compared to treated substrate (Borsellino et al., 2009). ECA which consist of epoxy resin and conductive filler as reinforced material will fail in different mode which depend on the strength of the interface. Weak interface enhances the ability of ECAs to resist fracture but reduce stiffness and strength while for the strong interface is vice versa (F.L. Matthews and R.D. Rawlings, 1999).

2.5.1   Chemical etching

Chemical etching surface treatment is one of the alternatives to enhance surface roughness of the aluminium substrate. The treatment may consist of acid etching and alkaline etching. By immersing the aluminium substrate at specified temperature of sodium hydroxide solution, the dissolution reactions occur on the surface of the substrate. The NaOH solution reaction on the aluminium substrate is expressed in Eq. (2.13) and Eq. (2.14):

38

$$Al_2O_3 \text{ (s)} + 2\,NaOH \text{ (aq.)} + 3H_2O \rightarrow 2Na[Al(OH)_4] \text{ (aq.)} \qquad (2.13)$$

$$2Al \text{ (s)} + 2NaOH \text{ (aq.)} + 6H_2O \rightarrow 2Na[Al(OH_4)] \text{(aq.)} + 3H_2 \text{ (g)} \qquad (2.14)$$
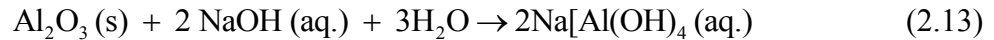
The complete reaction from the alkaline etching will produce the matte finish of aluminium surface which is due to presence of nucleation sites of pits. After that, aluminium substrate immersed into the hydrochloric acid solution and the reaction occur is expressed in Eq. (2.15):

$$2Al \text{ (s)} + 6HCl \text{ (aq.)} \rightarrow 2AlCl_3 \text{ (aq.)} + 3H_2 \text{ (g)} \qquad (2.15)$$
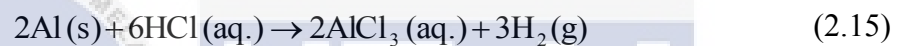
The reaction between aluminium nucleation sites of pits and hydrochloric acid form the pits in rectangular shape. The rectangular pits grow rapidly to round-shaped crater when immerse the aluminium substrate into the NaOH solution again due to high rate of anodic dissolution when cathodic second phase expose on the substrate surface (Yasuda & Saito, 2014).

Yasuda and Saito (2014) conducted chemical treatment on the aluminium surface by using three different condition which result to the different surface roughness. In the first condition (C1), the aluminium substrate was immersed into sodium hydroxide (5 wt.% aq. solution) for 2 minutes at 40 °C and followed by hydrochloric acid (3 wt.% aq. solution) for 5 minutes at 40 °C. In the second condition (C2), aluminium substrate immersed into sodium hydroxide (5 wt.% aq. solution) for 2.5 minutes at 40 °C after C1. As for the third condition (C3), the aluminium substrate was immersed into sodium hydroxide (5 wt.% aq. solution) for 5 minutes at 40 °C after C1. Following this, the surface roughness, Ra, was measured using a

39

scanning laser microscopy, with the values of 3.2 µm, 4.8 µm, 15.5 µm and 25.5 µm for as-received, C1, C2 and C3 respectively. Aluminium surface subjected to C3 treatment exhibit the highest surface roughness with highest hemispherical pits as shown in Figure 2.9 (c) and (d), in which the substrate experienced the longest period of chemical etching process.
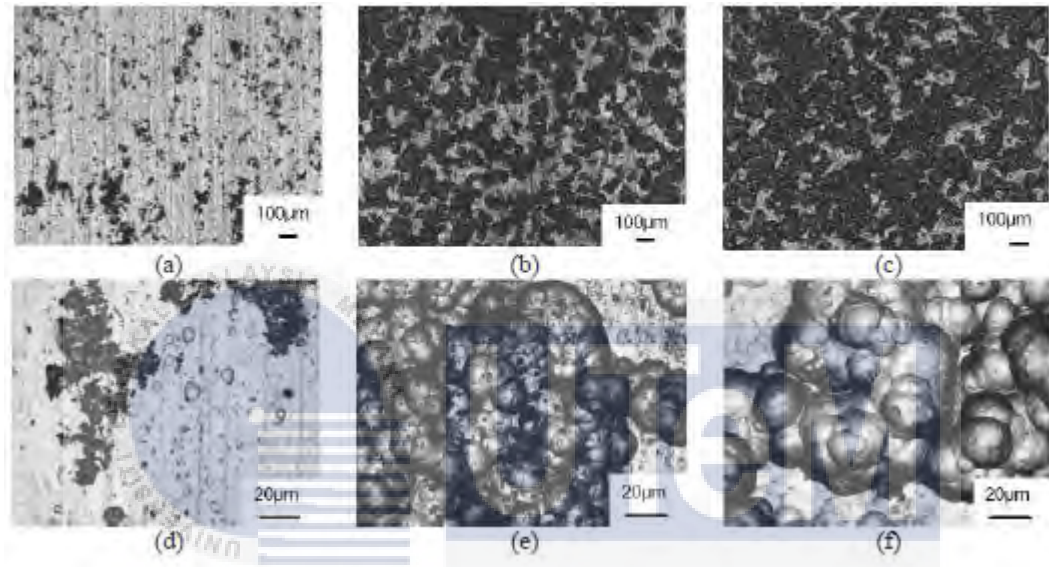
Figure 2.9: Aluminium surface after undergoes alkaline/acid etching process: C1 ((a), (d)); C2 ((b), (e)); and C3 ((c), (f)) (Yasuda & Saito, 2014).

In another study, AA6061 aluminium alloy underwent ultrasonic immersion in sodium hydroxide solution following surface treatment using acetone followed by characterization of aluminium alloy by Saleema, Sarkar, Paynter, Gallant and Eskandarian (2012). The chemical reaction between the aluminium substrate and NaOH solution produced a microrough structure on the treated surface. An increase immersion time from 30 minutes to 60 minutes results in an increase in substrate surface roughness and exposed the grain boundaries which produced another degree of surface roughness. The NaOH treatment on aluminium surface generated a

40

new stable form of oxide of the form Al_2O_3 (form after aluminium hydroxide dehydration) to create microrough surface after removal of the weak native oxide layer.

2.5.2 Grinding with silicon carbide (SiC) abrasive paper

The purpose of grinding process is to remove damage from cutting, planarize sample surface and remove material located on surface of interest area. Silicon carbide (SiC) is widely used as an ideal abrasive for grinding due to its hardness and sharp edge. In preparation of metallographic specimen, abrasive grinding papers are coated with SiC abrasives with coarse from 60 grit to 1200 grit sizes ("Grinding & Polishing," 2013).

Grinding of soft non-ferrous metals is suggested to start with 320 grit followed by 400, 600, 800 and 1200 grit SiC paper. Since the soft non-ferrous material does not able to distort the performance of abrasive paper easily, grinding process can be start with 320 grit SiC abrasive paper which allow the adequate removal rates and minimizing initial deformation. For very soft materials, the abrasive paper is recommended to be coated with a paraffin wax to prevent SiC embedded on the soft material surface ("Grinding & Polishing," 2013).

Contaminated or poor adhering of substrate outer layer could be removed by mechanical abrasion to expose the new oxidised aluminium bulk material and provide suitable surface layer to directly bonded to adhesives. As mechanical abrasion process conducted by Borsellino et al. (2009) to treat aluminium surface prior bonded with adhesive, the substrate thickness was removed about 2.5% to obtain regular surface before proceeding to mechanical abrasion process with grinding paper. Then, the surfaces were cleaned by soft clean cloth and air in pressure to remove residual particle remaining.

41

CHAPTER III

METHODOLOGY

3.1   Overview of research

This chapter describes the experimental work involved in this project, which consists of preparation of ECA, substrate surface treatment and various types of testing involved. The methodology of this study is summarized in Figure 3.1 which represent the workflows of experiments and research activities for the entire project. A summary of the research activities involved in this project are as follows:

i.   The procedure of different surface treatment, preparation of ECA, fabrication of single-lap-joint adhesively bonded and fabrication of sample for four-point probe test.

ii.   Design the experiments which relate to the research study.

iii.   Experiment parameter, standards and procedures are pointed out.

iv.   Conduct surface characterization study which relate to surface topography and surface morphology of substrate.

v.   Experiment to determine the wettability of aluminium substrate towards liquid.
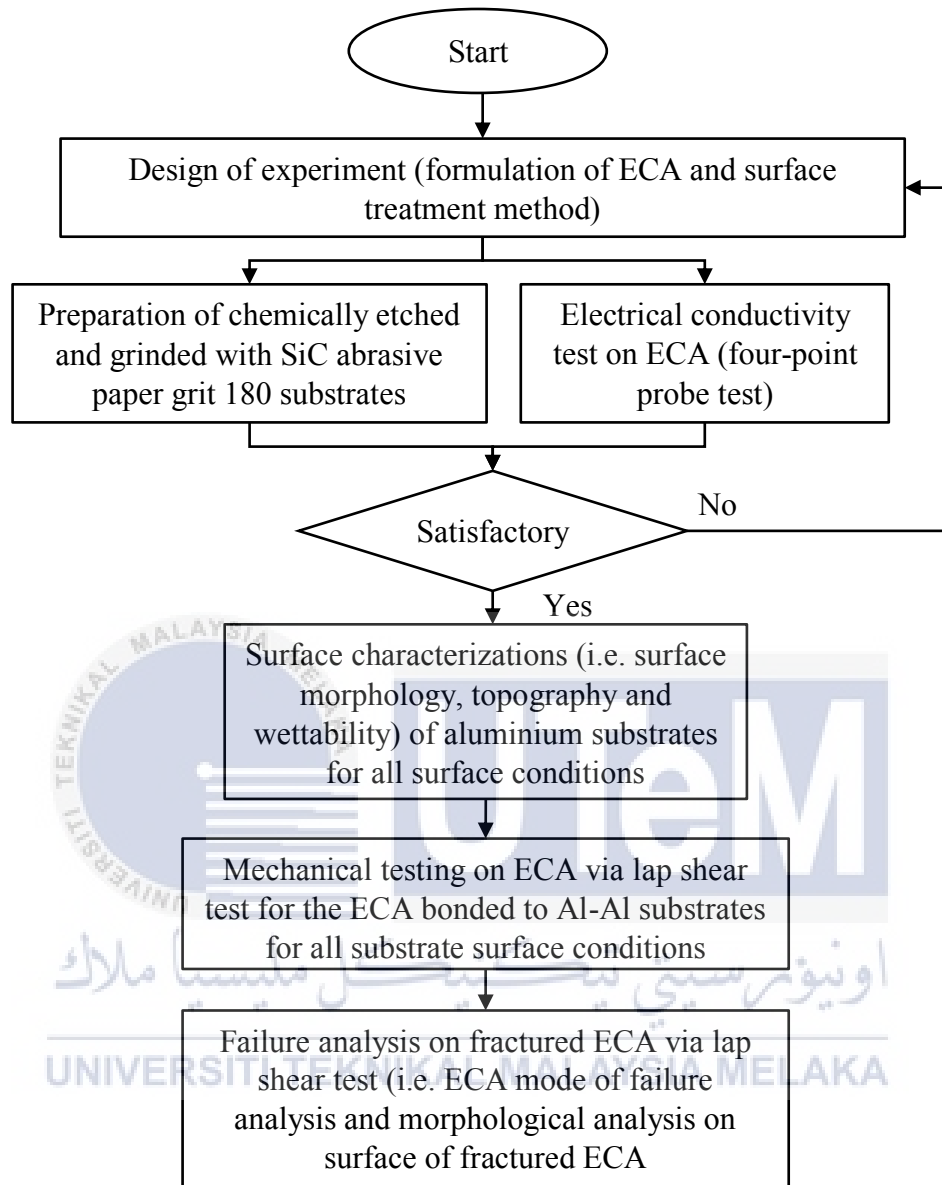
Figure 3.1: Flow chart of the research activities.

3.2 Substrate surface treatment

Surface treatment on aluminium substrate is the process to enhance adhesion of ECA towards the substrate surface (Critchlow & Brewis, 1996). High area of contact between ECA/substrate interface will enhance the mechanical interlocking of ECA towards substrate surface (Yasuda & Saito, 2014). Hence, surface treatment on aluminium substrate were

43

conducted to provide larger substrate surface area and may attained sufficient anchoring of ECA towards the substrate surface.

3.2.1 Surface roughening with SiC abrasive paper grit 180

The purpose of surface grinding is to rougher the substrate surface which different value of abrasive paper grit size will contribute to different effect. Usually, high grit size will have good ability to smoother the surface while low grit size will rougher the surface.
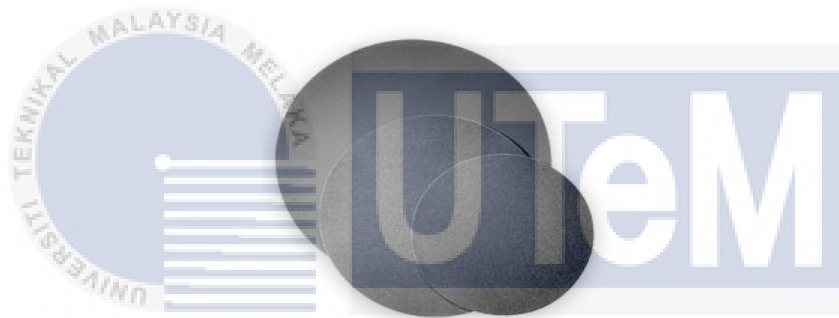
Figure 3.2: Water prove SiC abrasive paper was used for mechanical abrasion surface treatment ("Grinding Consumables," 2017).

As to roughen the substrate surface, the abrasive paper with silicon carbide grit 180 was used. The abrasive paper was placed on the rotating disc and tight them by bracket. Then, the speed was set to 100 rpm, rotation was set to anti-clockwise and water tap was opened to allow water flow onto the abrasive paper. Aluminium substrate was put onto the abrasive paper and overlap area part of the substrate was pressed evenly towards the abrasive paper. 'Run' button was hit, and the machine start to grind the substrate surface for 30 second. When reached 30

second, the machine was stopped, and the rotation mode was change to clockwise. Substrate was grinded again for 30 second with the new grinding direction.

Figure 3.3: Grinder and polishing machine for substrate surface treatment.

3.2.2 Chemical etching

The purpose of chemical etching is to roughen the substrate surface by producing high density of nucleation sites of pits. Sodium hydroxide solution and hydrochloric solution were utilized to etch aluminium substrate surface as to enhance surface roughness of the substrate surface.

Table 3.1: Chemical etching material and function.

Material	Function
Sodium Hydroxide (5 wt.% aq. solution)	• Chemical etching solution for
Hydrochloric Acid (3.6 wt.% aq. solution)	aluminium surface treatment
Distilled Water	• Clean substrate
	• Chemical dilution

45

Calculation for NaOH solution concentration in Eq. (3.1):

$$NaOH \ concentration = \frac{Mass \ of \ NaOH \ granules}{Mass \ of \ Distlled \ Water} \times 100\%$$
(3.1)

Calculation for HCl solution concentration in Eq. (3.2):

$$C_1V_1 = C_2V_2$$
(3.2)

where C_1 is percentage HCl in distilled water, V_1 is volume of HCl solution, C_2 is desired percentage of HCl in distilled water, and V_2 is desired volume of HCl solution which comprised of V1 + volume of distilled water.

As to prepare 5 wt.% NaOH solution from NaOH granule, 5 g of granule was mixed with 100 ml of distilled water inside the round bottom flask as shown in Figure 3.4. The mixture was shake until the solution was cleared from undiluted granule. Then, the well shake diluted NaOH solution was poured into 250 ml beaker.

Figure 3.4: NaOH granules was mixed with distilled water inside the round bottom flask.

Then, 100 ml of 3.6 wt.% HCl solution was poured into 250 ml beaker which make the height of the solution in the beaker was more than 12.7 mm which as a requirement to adequately etch the substrate surface overlap area. Both of beakers which contain different solutions were partially immersed into water inside the ultrasonic bath. The thermometer was set up with retort stand and was partially immersed into the solution (without touch the bottom of the beaker) to measure the actual temperature of the solution as shown in Figure 3.5.
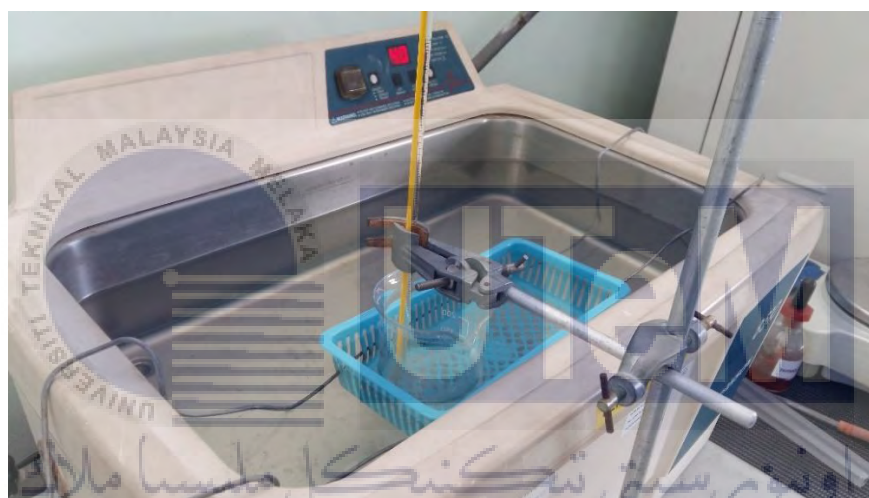
Figure 3.5: Thermometer was partially submerged into NaOH solution.

The water temperature inside the ultrasonic bath was set to 40 ℃ with no ultrasonic vibration used. Prior of chemical etching process, the aluminium substrates were completely immersed in the heated distilled water inside the beaker which the beaker was heated by water inside the ultrasonic bath as shown in Figure 3.6. The purpose to heat up the substrate prior of etching process is to reduce the heat loss in the chemical solution during immersing the substrate which will affect the etching efficiency. In other words, at low temperature of chemical solution, the etching rate of the chemical solution on the surface of aluminium substrate is low.

Figure 3.6: The complete set up of chemical etching process.

As both solution reached thermal equilibrium of 40 ℃, 5 aluminum substrates were immersed partially into NaOH solution for 120 s as shown in Figure 3.7 and were cleansed by distilled water prior to acidic etching in beaker containing HCl solution for 300 s. Then, the substrates were immersed again in NaOH solution for 300 s. Every interchange and after chemical etching process, the substrates were cleansed with distilled water as illustrated in Figure 3.8.

Figure 3.7: Air bubbles formed as the NaOH solution react to aluminium surface.
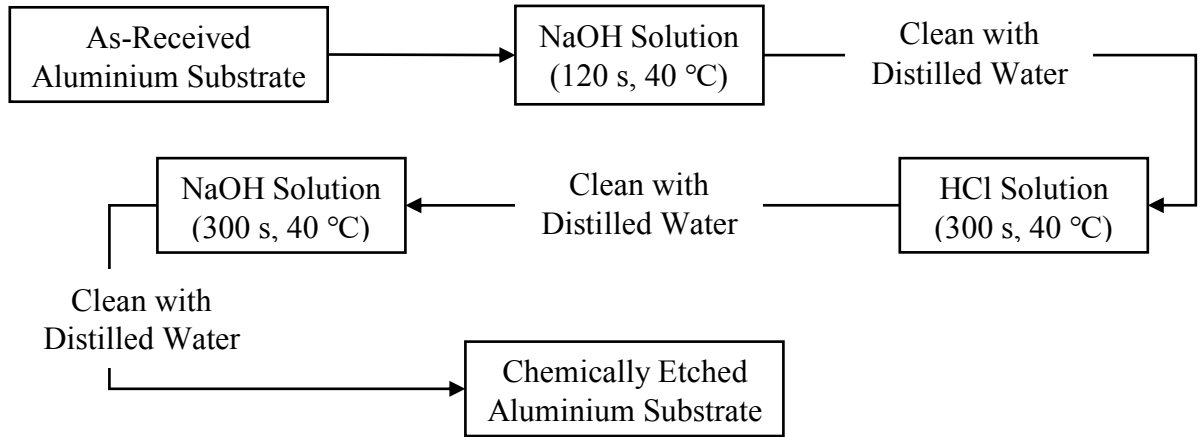
Figure 3.8: Flow diagram of chemical etching process on aluminium substrate.

3.3   Surface analysis

This section comprises of explanation on several surface characterization methods which are surface morphology and topography characterizations, and wetting performance of substrate towards liquid through contact angle test.

3.3.1   Surface morphology

In surface morphology, there are two aspects to be differentiated which are structure and microstructure. Structure is the crystallography of defect-free surfaces while microstructure is the deteriorate of ideal crystallization by line and distribution defects. Surface consists of high symmetry singular surfaces and vicinal surfaces. Latter consist of singular terraces divided by steps while high symmetry singular surfaces are cusped and discontinuous first derivatives of orientation surface free energies (Shay, Porter, & Prescott, 1974). In this research project, surface morphology and topography characterizations were conducted on aluminium substrate with different surface conditions. Besides, the morphological study on surface of fractured ECA was carried out through micrograph image captured from scanning electron microscopy.

49

3.3.1.1 Scanning electron microscopy (SEM)

Basic operation of scanning electron microscopy is by scanning an electron beam on the surface of the sample and interpreting the interaction of electron with the surface into image. The electron that release through the beam hit the on the sample's surface and the ejected the weakly bound electrons on the surface to form secondary electrons. The ejected electron then measured and calculated by the detector which then produce colour for each pixel of SEM image. Electromagnetic force tends to disturb the trajectory of the secondary electrons which will affect the accuracy of SEM image and as counter measure, the sample surface must be conducting. The conducting surface prevent the charge build-up which produce electromagnetic force. In the case of measuring non-conductive sample, the thin layer of metal can be coating over the sample surface as SEM measurement require the conductive surface.

There are several advantages of using SEM in measuring surface morphology such as provides high resolution of image surface features and the scanning process is faster than scanning probe microscopy. However, SEM surface measurement has some difficulties and disadvantages such as the sample must be conductive (at least, surface is coated by conductive material for non-conductive sample), require vacuum condition, unable to measure the height and chemical properties sample surface (Yi et al., 2010).

Some of samples are beam-sensitive which will damage as high energy electron beam interact on them. Part of energy from electron beam transfer to the sample in the form of heat and as the sample material is beam-sensitive, the sample surface structure will damage. Therefore, sputter-coating play an important role to prevent the problem occur and act as the protective layer as the conductive material coated the material are not beam sensitive. For non-conductive material, the material need to undergo sputter coating as the material surface tend to trap electron and cause the electron to accumulate on the material surface. The accumulation of

50

electron can influence the micrograph image information as the formation of white region by the trapped electron. The trapped electron can be removed by reducing the vacuum level inside the chamber since the presence of the positively-charged molecules in low vacuum level create the interaction toward the electron and remove the charging effect. However, there will be interaction between primary electron and introduced air particle which deteriorate the quality of micrograph image. Therefore, sputter coating technique is favourable to remove the charging effect since the conductive coating material act as a channel to remove the trapped electron (Antonis Nanakoudis, 2017).

Surface morphology analysis on the of fractured ECA is crucial to find the potential defects and surface behaviour of the ECA cross section. Scanning the surface of ECA with electron beam of scanning electron microscopy (SEM) generates the micrograph image of the scanned part. Since the polymer matrix in ECA is not conductive material, the ECA need undergoes sputter coating process.

Initially, the samples of weakest and strongest fractured ECA which bonded to chemically etched substrate were cut into small pieces to fit the space of specimen holder of SEM. Then, both samples were placed on the specimen holder as shown in Figure 3.9 and they were placed inside the auto-fine coater machine brand JEOL JEC-3000FC as shown in Figure 3.10 to be sputtered by conductive material to create the negative cathode. The vacuum pump was operated to obtained desired operating pressure with the admitted of inert gas to the chamber by a fine control valve (Quorum Technologies, 2002).

51
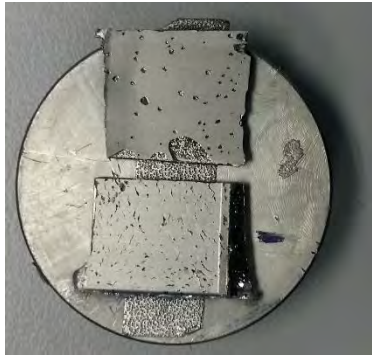
Figure 3.9: Samples of fractured ECA on specimen holder.

Figure 3.10: Auto-Fine Coater brand JEOL JEC-3000FC.

Then, the coated samples were place inside SEM specimen chamber and scanned to capture the micrograph image of interest. The specimen chamber was vacuumed to ensure the air particle not impeded the electron movement during the scanning process.

3.3.1.2 Optical microscope

There are two important functions of optical microscope which are magnified image of a sample and illuminating a sample. The process to magnify image requires 3 principle criteria

52

of obtaining clear and sharp image, changing a magnification and bringing into focus. In illumination process, there are several criteria required such as supplying light, collecting light and changing light intensity. This illumination optical system illuminate the sample by efficiently collecting emitted light from the light source ("Microscope Basic Functions and Optical System Configuration," n.d.).

Figure 3.11: Low power microscope brand ZEISS Axioskop 2 MAT.

The low power microscope brand ZEISS Axioskop 2 MAT as shown in Figure 3.11 was utilized to capture microscopic image of the aluminium substrates surface for all surface conditions. Initially, the surface of interest (overlap area) of each substrate were clean with acetone to remove any contamination on the surface as to obtained good representative of substrate surface morphology. Then, the substrate was placed on the mechanical stage and the

53

surface of interest was aligned below and normal to the objectives lens. The objective lens with lateral magnification 20x were used to obtain the desired images magnification and the total magnification is 200x as eyepiece has 10x magnification. Then, the mechanical stage height was adjusted by turning the fine and coarse knob until the clear image acquired. Stage control was turned to adjust the stage horizontal position as to capture microscopic image of the specific area of interest.

3.3.1.3 3D optical profilometer

3D profilometer utilized non-contact metrology technique which able to measures variety of surface finishes and materials including large steps, steep slopes, rough and super smooth surface. There is relation between the surface morphology and adhesion performance of ECA towards substrate, therefore, 3D profiles of treated and untreated substrate surface were measured.

Figure 3.12: 3D optical profilometer brand Shodensha GR3400.

3D optical profilometer brand Shodensha GR3400 as Figure 3.12 was utilized to obtain 3D profiles image of the surface morphology for all substrate surface conditions. As to obtained clean overlap area of aluminium substrate surface, the acetone was utilized prior to surface 3D profile measurement. Then, the substrate was placed on the mechanical stage with the overlap area of substrate aligned and normal to objective lens. WinROOF 2015 software was launched to operate the profilometer. Mechanical stage was adjusted in vertical orientation until the clear image of substrate surface obtained. As to merge focus the images, the initial and end vertical position of lens, and distance interval of image capture were set. Finally, 'execute' command was clicked, and the profilometer was operated to generate 3D profile image.

3.3.2   Surface topography

One of the most important parameter for surface physical characteristic is surface topography. Quantitative techniques are used to measured surface topographical properties. (Thwaite, 1982). In this research project, stylus profilometer was used to measure aluminium substrate surface topography in term of surface roughness. Surface roughness, Ra, is a set of average of surface profile height deviation from the mean line, recorded within the line of interest.

3.3.2.1 Stylus profilometer

There are two main parts of profilometer which are sample stage and detector. The profilometers consist of two different types which both profilometers use different techniques to measure surface topography. One of them are stylus profilometers which use a physically moving probe along the surface line of interest to measure surface height. The surface measurement requires the feedback loop from movement of probe along the sample surface

55

which the different surface height push the probe upward. In the other hand, stylus profilometer measure the change of Z position of the probe which at different position will indicate different force subjected to probe. Another type of profilometers are optical profilometry which instead of usage of probe, it uses light. The light is directing as it can detect surface in 3D ("How a Profilometer Works," 2017).

In this research project, stylus profilometer brand Mitutoyo SJ-410 as shown in Figure 3.13 was used to measure aluminium substrate surface roughness. Prior to surface roughness measurement, the lap-joint or overlap area of substrate was divided into 3 parts by making black line on them which every single part will undergoes surface roughness measurement process. Then, the profilometer configuration was set with stylus head speed of 0.5 mm/s and was set to move through a straight line with distance of 4.0 mm. After that, the profilometer was calibrated and the thermal paper roll was placed inside the printing component of the profilometer as to print the data of the surface roughness after the measurement process.

Figure 3.13: Mitutoyo SJ-410 profilometer used to measure surface roughness of aluminium substrate (*SURFTEST SJ-410 Series*, 2015).

To begin the analysis, aluminium substrate was placed on 3-axis adjustment table and one of divided part of aluminium surface was aligned to profilometer probe. Then, column stand

which hold the detector was adjusted its height until the stylus head touch the substrate surface at specified force as shown in Figure 3.14. After that, 'START' button was hit, and the probe begin to move in a straight-line route and was move back at initial position once it reach the last point. The measurement result was showed on profilometer screen interface and was printed. The column stand was adjusted its height to higher position to prepare for surface measurement on another part. The process was repeated for every divided part for 5 samples for each substrate surface condition. Surface roughness, Ra, data for all samples were recorded and were averaged for each surface condition.

Figure 3.14: Stylus head touch on the substrate surface.

3.3.3 Contact angle test

The purpose of contact angle test on substrate is to determine wetting properties of liquid on different aluminium substrate surface conditions. The contact angle test was following ASTM D5725 as a standard guideline.

Before proceeding to contact angle test, overlap area of aluminium substrate was divided into three equal parts to get average of surface contact angle. The overlap area was wiped with lint free cotton and the experiment was set up as Figure 3.15, which dry substrate was place on

57

the 3-axis stage next to digital microscope (Panrico MSP-3080) with white wall surrounded to ensure the homogenous distribution of light towards the water droplet. The digital microscope was connected to processing image device (in this case is personal computer) through USB cable and Digital Microscope's software generate real time image on the PC screen.

Figure 3.15: Surface contact angle experiment was set up inside the box.

Microliter pipette (Eppendorf Research plus) was set to drop water droplet at volume of 0.5 µl and the pipette tips was installed on the tip cone. Distilled water inside the beaker was drawn into the pipette through the pipette tips. Then, the water droplet was dropped at position normal to the first part of substrate surface. The image of droplet was snap for 3 times as the drop of water touch the substrate surface and was save in the hard drive. The contact angle of the water droplet image was measured for the left and the right side as demonstrated in Figure 3.16. The experiment was repeated for other parts of surface interest for all substrate surface conditions. The data of contact angle were averaged for each surface condition.
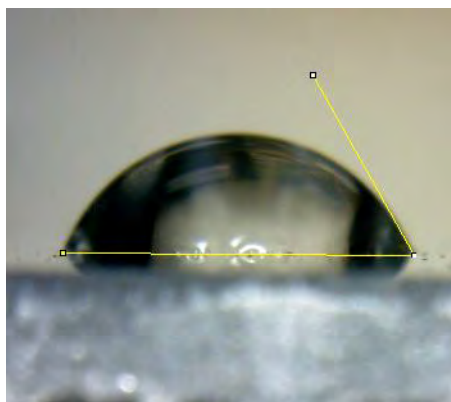
Figure 3.16: Contact angle measured at the right side of water droplet.

3.4 ECA preparation

Based on Table 3.2, ECA consists of polymer binder (epoxy resin) and conductive filler (multiwalled-carbon nanotube). In this project, ECA were prepared with varying MWCNT filler loading. The effect of varying MWCNT filler loading on ECA electrical resistance and shear strength are discussed in Chapter 4.

Table 3.2: ECA components and function details.

Component	Function
Epoxy Resin	Matrix Material (Binder)
Polyetheramine D230	Hardener
MWCNT (Amorphous Materials)	Conductive Filler for ECA

Table 3.3: Epoxy resin specifications.

Araldite 506 Epoxy Resin	
Criteria	Specification
Brand	Sigma-Aldrich
Product Number	A3183
Component	Bisphenol-A (epichlorohydrin) and Epoxy Resin (no. average molecular weight <=700)
CAS-No.	25068-38-6
EC-No.	500-033-5
Index-No.	603-074-00-8
Form	Semi-solid to a liquid
Colour	Colourless
Melting Point/Freezing Point	-15 – 5 °C
Flash Point	252 °C
Vapour Pressure	0,04 hPa at 77 °C
Relative Density	1,168 g/cm3
Partition coefficient: n-octanol/water	log Pow: 2,8

Hardener or epoxy curing agent brand JEFFAMINE D-230 Polyetheramine was used to cure the epoxy resin in ECA. There are other several applications of the hardener such as transforms to hot melt adhesives when reacts with carboxylic acids and capable to react quickly to isocyanates. The hardener is low viscosity, low vapor pressure, totally dissolve with many

type of solvent, and provides tough adhesives. The specifications of the hardener are provided in Table 3.4.

Table 3.4: Property and specifications of hardener.

Epoxy Curing Agent: JEFFAMINE D-230 Polyetheramine	
Property	Specification
Appearance	Colourless to pale yellow liquid
Primary amine, % of total amine	97 (minimum)
Total acetylatables, meq/g	8.3-9.1
Total amine	8.1-8.7
Total amine, % acetylatables	94 (minimum)
Water percentage, %	0.2 (maximum)
Amine hydrogen equivalent weight, g/eq	60
Equivalent weight with isocyanates, g/eq	120
Viscosity at 25 °C	9.5 cSt
Density at 25 °C	0.948 g/ml
Flash point	121 °C
pH at 5% aqueous solution	11.7

Table 3.5: MWCNT specifications.

Criteria	MWCNT
	Amorphous Material
Purity	>95%
Outside Diameter	10-20 nm
Inside Diameter	5-10 nm
Length	10-30 um
SSA	>200 m^2/g
Colour	Black
Bulk Density	0.04-0.05 g/cm^3
True Density	2.1 g/cm^3

Table 3.6: MWCNT dimension specifications with aspect ratio details.

MWCNT	Outer Diameter, OD (nm)		Length, L (μm)		Aspect Ratio, A.R. (L/OD)		
	Min.	Max.	Min.	Max	Min.	Max.	Average
Amorphous Material	10.0	20.0	10.0	30.0	500.0	3000.0	1750.0

Law of Mixture expressed in Eq. (3.3):

$$X_c = X_m V_m + X_f V_f \qquad (3.3)$$

Volume Fraction expressed in Eq. (3.4) and Eq. (3.5):

$$Matrix\ volume\ fraction: Vm = \frac{Vm}{Vc} \tag{3.4}$$

$$Filler\ volume\ fraction: Vf = \frac{Vf}{Vc} \tag{3.5}$$

Rule of ECA Mixture in Eq. (3.6) and Eq. (3.7):

$$Mass\ of\ ECA = Mass\ of\ MWCNT + Mass\ of\ Epoxy\ Resin \tag{3.6}$$

$$Mass\ of\ Hardener = 0.3 \times Mass\ of\ Epoxy\ Resin \tag{3.7}$$

Table 3.7: ECA formulation for different filler loading.

ECA mass, g	MWCNT wt.%	MWCNT mass, g	Epoxy mass, g	Hardener, g
5.00	5.00	0.25	4.75	1.425
5.00	6.00	0.30	4.70	1.410
5.00	7.00	0.35	4.65	1.395

The specified mass of MWCNT, epoxy and hardener for different MWCNT loading are referred to Table 3.7. The plastic spoons were used to collect MWCNT, epoxy and hardener, and to stir the mixture. Based on Figure 3.17, each plastic spoon used is specified to collect specific materials as to prevent from unintentional mixing between the materials. The levelling screw of digital weight balancing as shown in Figure 3.19 was adjusted to ensure it is horizontally placed on the table.
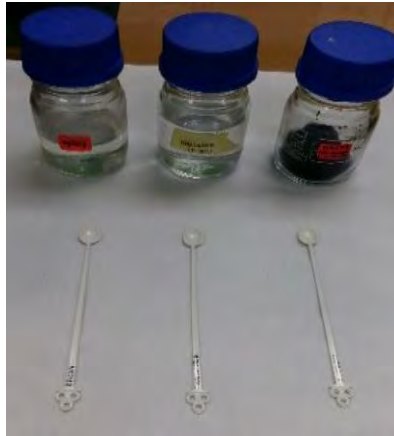
Figure 3.17: Epoxy, hardener and multiwalled carbon nanotube inside moulded glass container

align with their specified plastic spoons.
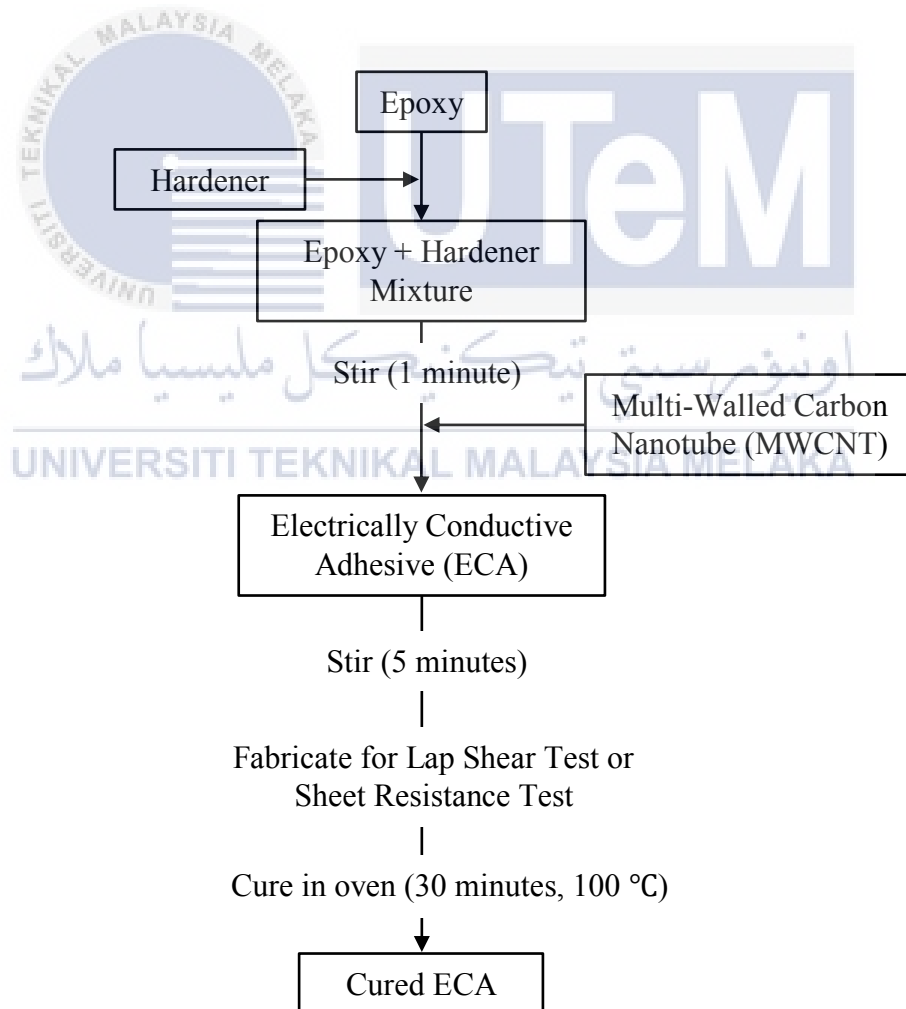
Figure 3.18: The flow process of ECA preparation.

The round plastic container was placed on the pan and the digital weight balancing measurement was set to zero. Small amount of epoxy was collected from its container and was poured carefully into the round plastic container and repeat the step until reached the specified mass. The weight balanced was set to zero again and the epoxy was mixed with specified mass of hardener. Then, the mixture of epoxy-hardener was stirred for 1 minute. After that, the weight balance was set to zero and the epoxy-hardener mixture was added with specified mass of MWCNT. Then, the mixture was stirred for 5 minutes and was fabricated on substrate of four-point probe test and on aluminium substrate of lap shear strength test. Lastly, the substrates were placed inside oven which was readily heat with 100 °C to cure the ECA for 30 minutes. The flow process of ECA preparation as illustrated in Figure 3.18.

Figure 3.19: Digital weight balancing used for high accuracy of mass measurement.

3.5 Fabrication of single-lap-joint

The fabrication process was start with the cutting process of 6096 mm x 25.4 mm x 1.65 mm aluminium flat bar into 101.6 mm x 25.4 mm x 1.65 mm and 177.8 mm x 25.4 mm x 1.65 mm. The cutting process was done by using shearing machine. Some of 101.6 mm x 25.4 mm x 1.65 mm aluminium substrates were applied surface treatment prior to single-lap-joint process.

To fabricate aluminium single-lap-joint, single-lap-joint jig was used to assist the fabrication process. Single-lap-joint jig consists of 101.6 mm x 25.4 mm x 1.65 mm aluminium flat bar, 177.8 mm x 25.4 mm x 1.65 mm aluminium flat bar and 0.1 mm steel plate and fabricated as illustrated in Figure 3.20. The joint between aluminium flat bar-aluminium flat bar and between 0.1 mm steel plate-aluminium flat bar were bonded with cyanoacrylate adhesive.
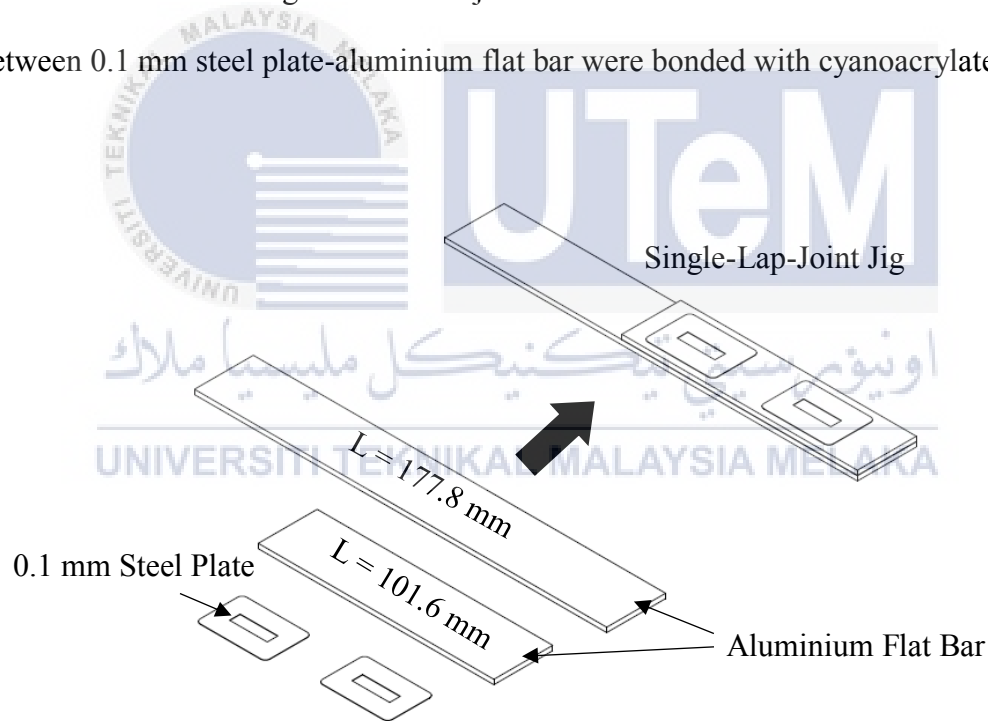
Figure 3.20: Fabrication process of single-lap-joint jig.

Once the jig was completely fabricated, the jig and the steel plate surface were wiped with the release agent (EXTEC 14705-R) to ease the dismantle process between jig and single-lap-joint sample after curing process of ECA. The overlap area of substrates was cleansed with

66

acetone and then, the ECA was applied on each aluminium overlap area as illustrated in Figure 3.21.

Then, the samples and the jig were gripped by three metal clips to ensure the uncured ECA has homogeneous thickness between the aluminium substrates. Then, the samples with the jig were placed on the metal pan as showed in Figure 3.22 and were put into oven which readily heated at 100 ℃. The samples were heat steadily at 100 ℃ for 30 minutes and were drawn out from oven and were underwent curing process at ambient temperature for 24 hours.
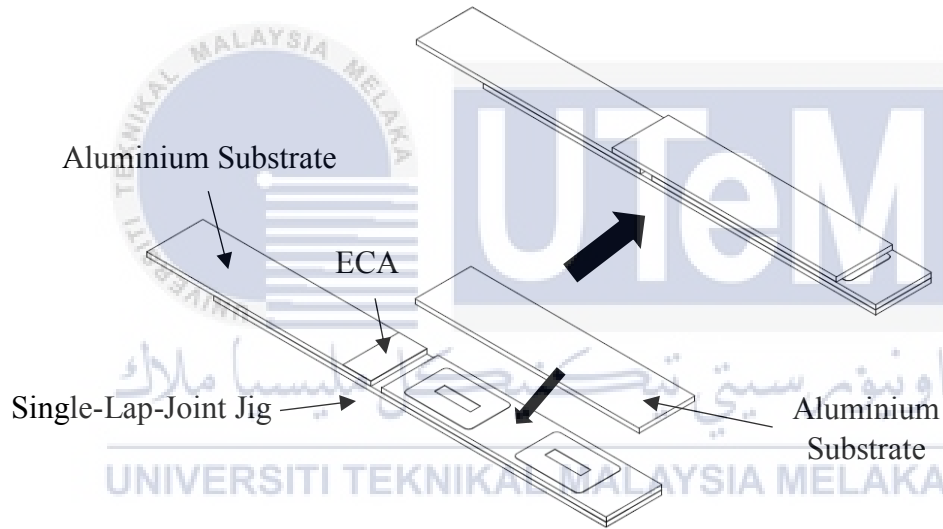
Figure 3.21: Illustration of the process to fabricate aluminium single-lap-joint adhesively bonded.

Figure 3.22: Single-lap-joint adhesively bonded samples are put into oven for ECA curing process.

3.6 Fabrication of printed ECA on substrate

Substrates sheet utilized for four-point probe test are made from polycarbonate material with dimension of 114.3 mm x 88.9 mm x 3 mm as shown in Figure 3.23. The polycarbonate sheet was cut into the specified substrate dimension by using laser cutter (trotec® Speedy 300™ Flexx).
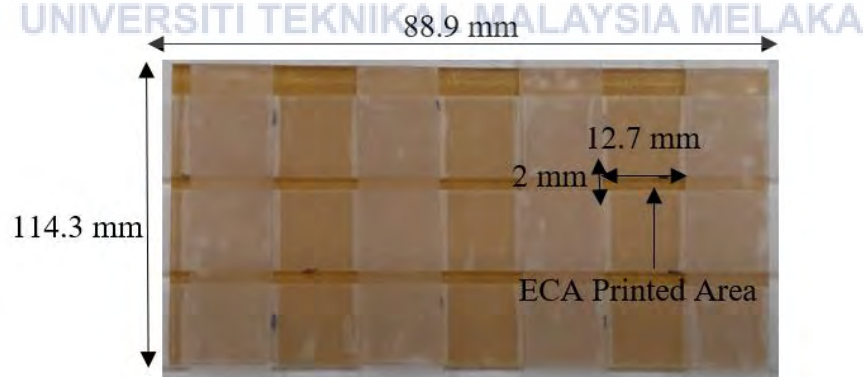
Figure 3.23: Polycarbonate substrate with dimensions.

Then, the 3M Scotch tape was applied on the substrate to form ECA printed area with depth of 2 layer of scotch tape thickness. The uncured ECA were applied into printed and were squeezed and flattened by sheet metal as shown in Figure 3.24. After that, the substrate was place into readily heated oven at 100 ℃ for 30 minutes and was taken out to be cured for 24 hours at ambient temperature.
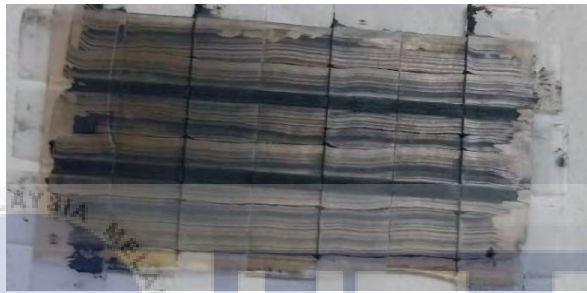
Figure 3.24: The dispersion of ECA on polycarbonate substrate.

The scotch tapes were removed and form the printed ECA as shown in Figure 3.25. Now, the printed ECA are ready to be tested by four-point probe equipment to measure the ECA sheet resistance.

Figure 3.25: Printed ECA on polycarbonate sheet.

3.7   Conductivity performance

As interconnect material, electrical conductivity is the main properties in ECA system. Therefore, the ECA was underwent four-point probe test to measured ECA sheet resistance. The low ECA resistance is desired which is an indication of excellent electrical conductivity.

3.7.1   Four-point probe test

By testing the printed ECA resistivity, electrical conductivity can be analysed and concluded. Resistivity test was conducted by using JANDEL In-Line Four-Point Probe as shown in Figure 3.27 with following ASTM F390 as a standard guideline. Six printed ECA are prepared on the polycarbonate sheet surface which based on dimension as illustrated in Figure 3.26.
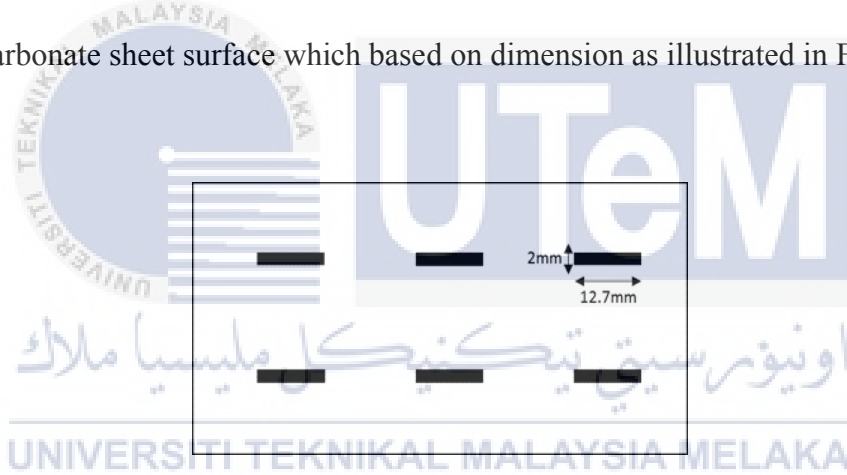
Figure 3.26: Illustration of 6-printed ECA on substrate with dimensions.

The current flow through the probe was set at specified ampere prior of resistivity test. Then, each of printed ECA were placed align and under four-point probe head and the probe head was lifted down until touched the printed ECA. The sheet resistance calculation is expressed in Eq. (3.8):

$$R_s = G.\frac{V}{I} \tag{3.8}$$

70

where R_s is sheet resistance $(\frac{\Omega}{sq})$, G is correction factor $= 1.9475$, V is voltage, I is input current.

The resistivity test was done at three positions (left, middle, right) of each printed ECA, and the resistivity results were recorded and were averaged for each ECA with varying filler loading.

Figure 3.27: JANDEL In-Line 4 Point Probe test equipment.

3.8   Mechanical properties

3.8.1   Lap shear test

The purpose of lap shear test is to test lap shear strength of ECA. High ECA shear strength means a good mechanical strength of bond and excellent mechanical interlocking of ECA towards substrate surface. Different filler loading with high aspect ratio of ECA was used in this experiment by following ASTM D1002 as a standard guideline with the dimensions as illustrated in Figure 3.28.
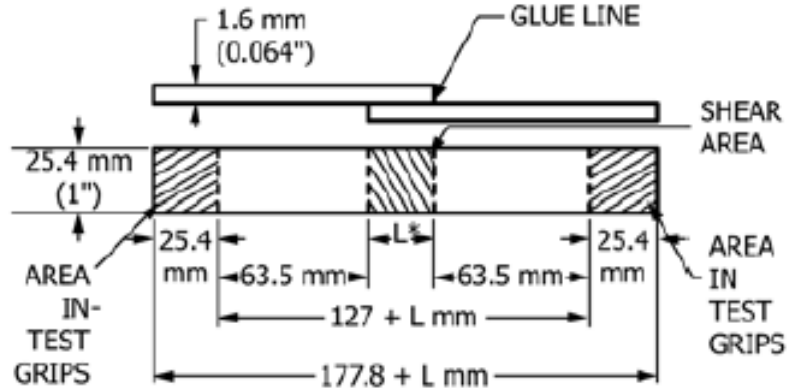
Figure 3.28: Dimension of single-lap-joint ECA bonded to Al-Al substrates (Method, 2010).

Single-lap-joint of ECA bonded to aluminium substrates was subjected to lap shear tensile test by using Universal Material Testing which the substrates were pull oppositely to create shear stress on the ECA bonded to aluminium substrates until the ECA failed. Lap shear strength expressed in Eq. (3.9):

$$\tau_{Lap} = \frac{F_{Max}}{A} \tag{3.9}$$

where τ_{Lap} is lap shear strength, LSS (MPa), F_{Max} is maximum tensile force (N), A is adhesive overlap area (m^2).

After the ECA was completely cured under ambient temperature, the clips and the jig were removed, and the test grips area were joint with small aluminium plate with the same thickness as illustrated in Figure 3.29 to ensure centric load subjected on the ECA during the lap shear test.

72
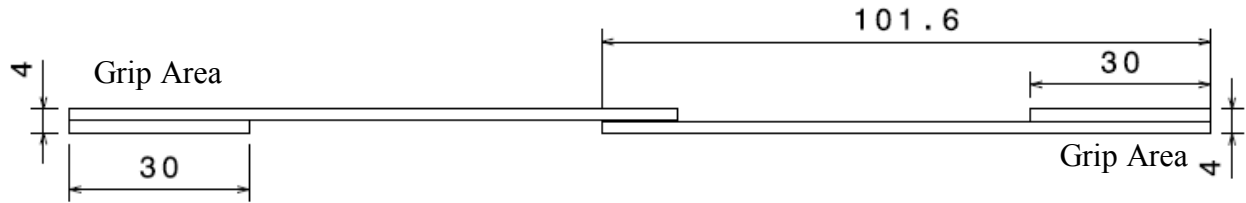
Figure 3.29: The dimension (in mm) of single-lap-joint sample with small aluminium plate placed on the grip area.

The complete samples were brought to Universal Material Testing (AG-10kNX) as shown in Figure 3.30 to begin tensile test. Prior of tensile test, the jig speed was set to 1.3 mm/min and the measured force was set to zero. The double layer side (grip area) of sample was entirely gripped by the tensile machine jig and the jig was tighten strongly as to prevent slippage during testing process. Then, the 'Start' button was clicked to begin the tensile test. The machine was stop after each failure of ECA joint and the maximum tensile force subjected to samples were recorded and were calculated to get maximum shear strength of the ECA.

Figure 3.30: Universal Material Testing (AG-10kNX) used for lap shear test.

73

3.8.2   Analysis on failure mode

There are 3 modes of failure typically occur for the lap shear test which are cohesive, adhesive and mix of adhesive-cohesive. The relation between mode of failure and ECA shear strength are discussed in Chapter 4.

CHAPTER IV

RESULTS AND DISCUSSION

4.1   Introduction

This chapter are discussed based on the four main objectives, with the focus on ECA performance with varying filler loading as well as using varying substrate surface conditions, particularly in terms of their electrical performance, interlayer strength and the corresponding mode of failure.

4.2   Electrical performance of ECA with varying filler loading

In this section, the electrical performance of ECA with varying MWCNT filler loading is explained based on sheet resistance measurement using JANDEL In-Line Four-Point Probe as per ASTM F390 standard guideline. The electrical performance play an important role in ECA field of study since this interconnect material is created to perform the electrical interconnection between the components which low electrical resistance is desired.

From Ohm's Law, the electrical conductivity performance of ECA is inversely proportional to the resistivity towards current flow. Therefore, to enhance the conductivity, the conductive fillers in the ECA should in contact between them as to form three-dimensional network. The epoxy act as an insulator material which promote high electrical resistivity and MWCNT added into the adhesive reduce the resistivity gradually. At volume fraction coincident with the critical filler concentration, Vc, the resistivity drops dramatically and reaching a plateau with further increases MWCNT volume fraction (Yi et al., 2010).

75

4.2.1 The effect of filler loading on ECA sheet resistance

The sheet resistance of ECA was measured with varying MWCNT filler loadings. Table 4.1 shows the result of average sheet resistance of the ECA with varying filler loading.

Table 4.1: MWCNT filler loading and average sheet resistance of ECA.

Filler Loading, wt.%	Average Sheet Resistance, kΩ/sq.
5	37.39 ± 9.46
6	15.32 ± 2.76
7	2.59 ± 0.35
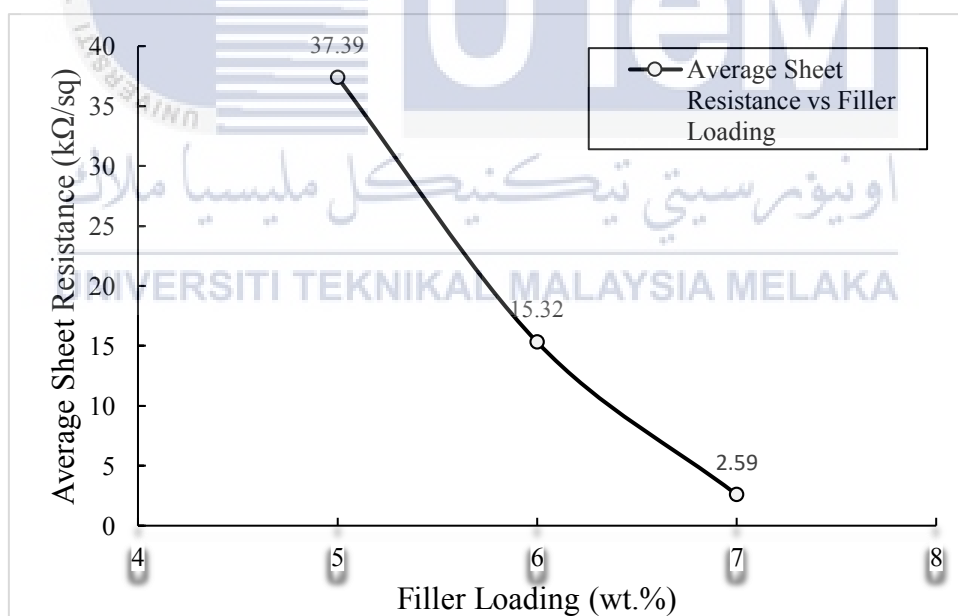
Figure 4.1: Graph of ECA average sheet resistance against percentage of MWCNT filler loading.

Based on the experimental results in Figure 4.1, sheet resistance decreases when filler loading is increase from 5 wt.% to 7 wt.%. As expected, an increase of MWCNT loading contribute to lower electrical resistivity in ECA due to an increase of contact, an increase of probability of continuous linkage and an enhancement formation of three-dimensional network between MWCNT conductive particles in ECA (Wong et al., 2011; Yi et al., 2010). The result is in agreement with increasing of MWCNT reduce bulk resistivity of MWCNT/epoxy composites as demonstrated by Xuechun and Feng (2004).

Besides, the standard deviation of sheet resistance significantly decreases with an increase of filler loading in ECA, an indication of more reliable measurement of sheet resistance obtained (Li & Lumpp, 2006; Mantena, 2009).

The rate of decrease of ECA sheet resistance before and after 6 wt.% MWCNT filler loading shows a significant difference which are 22.07 kΩ/wt.% and 12.73 kΩ/wt.% respectively. This is due to the rate of decrease of ECA resistivity with an increase filler loading is reduced as filler concentration is beyond the critical filler of concentration, V_c, in ECA (H. P. Wu et al., 2007; Yi et al., 2010) as depicted in Figure 4.2. In other hand, the cured pressure of epoxy is high as the MWCNT filler loading reach the volume of percolation threshold, resulted to significant number of percolated linkages are formed, hence, the ECA resistivity slightly change with further increase of MWCNT filler loading (Kwon et al., 2011; D. Lu, Tong, & Wong, 1999; H. P. Wu et al., 2007; Yu, Tong, & Critchlow, 2010).
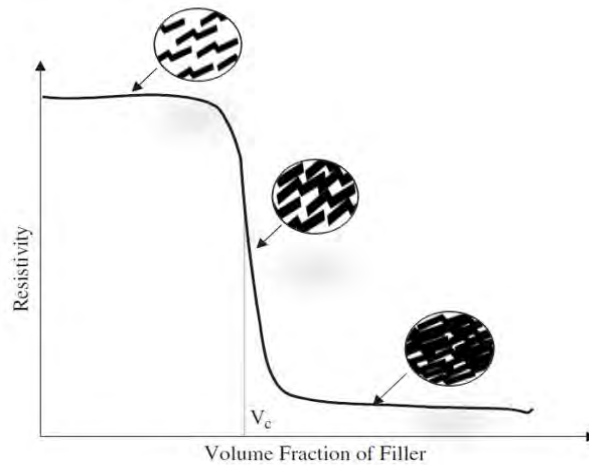
Figure 4.2: Effect of volume fraction of MWCNT filler on the resistivity of ECA system.

Prior to the curing process, ECA with high conductive filler loading (at filler volume of percolated threshold) has high total resistance between percolated linkage due to a thin layer of epoxy resin cover MWCNT particle surface, however, the total resistivity reduces with shrinkage of epoxy resin after curing process result to conductive filler particles closer together. Hence, large contact area and reduction of the insulating film thickness between filler particles interface was obtained yield to a decrease of constriction resistance and a decrease of tunnelling resistance respectively between the percolated linkages (Lu et al., 1999).

4.3   Aluminium substrate surface characterizations

This section consists of results and discussion on aluminium substrate surface characterization in terms of surface morphology, surface topography and surface wettability. Thus, the relation between the substrate surface characteristic and the ECA shear strength can be made.

78

4.3.1 Optical microscopy

Microscopic images of different substrate surface conditions showed in Table 4.2 with total magnification of 200x. Based on the images, treated and untreated substrate exhibit different surface morphology which affect surface wettability and surface roughness as well ECA shear strength. Initially, aluminium substrate for each surface conditions were solely wiped with acetone to remove surface contamination prior to capturing process of microscopic image.
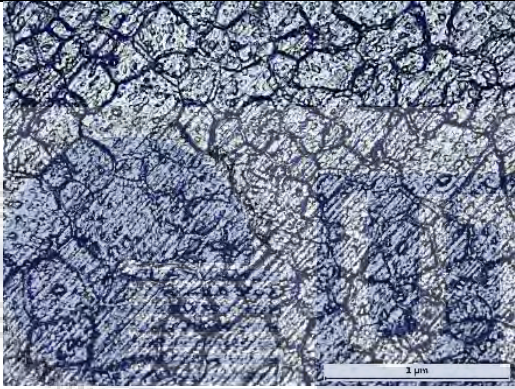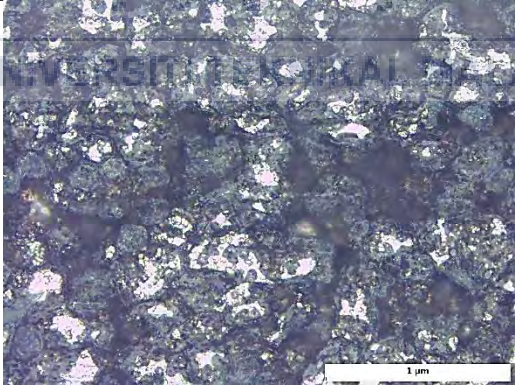
At the microscopic level, as-received aluminium substrate surface exhibits formation of aluminium oxide crack with small voids. This kind of surface can contribute to some degree of surface roughness due to presence of crack structure and voids. With no treatment applied on the substrate except wiped with acetone, the aluminium surface may consist of aluminium oxide/hydroxide film and stubborn oils and greases which will affect the adhesion of ECA towards the substrate surface.
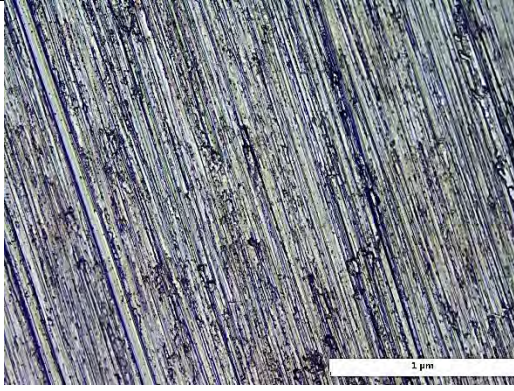
Chemically etched aluminium substrate exhibits highly dense round shaped crater which provides micro-rough structure on the surface. The large voids on the substrate surface can enhance the tendency of ECA to flow into the voids (Jennings, 1972) and induce optimum area of contact between ECA/substrate interface. Thus, an enhancement of mechanical interlocking can be attained and providing good adhesion properties between the ECA/substrate interface.

For the aluminium substrate which underwent mechanical abrasion process with silicon carbide paper G180, the smooth micro-groove with low dense of small voids observed. The grooves formation was attributed to friction between rotating silicon carbide paper and the aluminium surface. Sharp edges of grooves and small voids on the substrate surface may hinder the spreading of liquid (ECA or water) and may generate air pocket between liquid/substrate interface (Jennings, 1972). Therefore, good wetting properties of liquid towards substrate may

79

not be attained. In addition, the sharp edge of groove or sharp asperities will contribute to high stress towards the ECA results to a lower shear strength (Zielecki et al., 2013).

Table 4.2: Microscopic images of surface morphology of different substrate surface conditions.

Surface Treatment	Microscopic Image	Explanation
As-Received	 200x magnification	• The surface exhibit the crack structure of natural surface oxide with low dense of small voids.
Chemical Etching	 200x magnification	• High density of round-shaped crater on surface. • Chemical etching process create micro-rough structure and high porous of new alumina layer on surface.
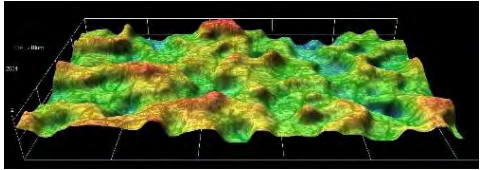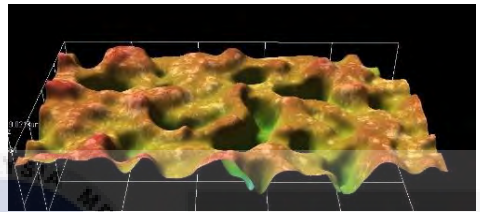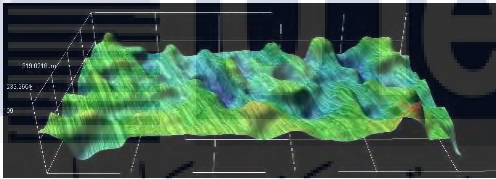
Surface Treatment	Microscopic Image	Explanation
Grinding with SiC Abrasive Paper G180	 200x magnification	• Smooth sharp grooves with low dense of small voids.

4.3.2   3D surface profile

3D profile images of all aluminium substrates surface conditions were obtained with utilization of optical 3D profilometer. The profile images of the substrates are provided in Table 4.3. Based on the images, comparison of surface morphology in term of density of voids, high of bumps and deep of valleys can be made between different substrate surface conditions.

3D profile image of the as-received aluminium substrate exhibits uniform low peaks and shallow valleys throughout the surface. Meanwhile, the chemically etched aluminium substrate has perfectly random porous texture with predominant deep valleys and high peaks observed which attributed to long etching time at specified temperature. For the aluminium substrate that was grinded with silicon carbide paper G180, the 3D profile exhibits uniform low peaks with slightly deeper valleys than on as-received aluminium substrate surface as the resulted of silicone carbide particle mechanically abrade the surface.

81

Table 4.3: 3D profile image of different substrate surface conditions.

Surface Treatment	3D Profile Image	Explanation
As-Received		• Highly dense presence of voids with shallow valleys.
Chemical Etching		• Presence of highly dense voids. • Highly dense of deep valley.
Grinding with SiC Abrasive Paper G180		• Low density of void with groove lines on the surface.

4.3.3 Surface roughness

Result of surface roughness measurement by stylus profilometer on as-received and surface treated aluminium substrates as given in Table 4.4. The results of surface roughness for each surface conditions came from the average of surface roughness of 5 samples for each surface condition.

Based on the result, the chemically etched substrate exhibits the highest surface roughness up to 2.60±0.30 µm which attributed to deep valleys and high peaks distribute throughout the substrate surface observed in 3D profile image.

As-received aluminium substrate has the lowest surface roughness due to no surface treatment applied and with the oxide layer presence on the substrate surface provide uniform shallow valleys and low peaks on the entire surface.

Grinded aluminium substrate with silicon carbide paper G180 has slightly higher surface roughness in the range of 0.52 ± 0.05 µm as compared to as-received surface roughness, 0.36 ± 0.02 µm. This is due to the friction between moving silicon carbide paper and aluminium substrate surface remove part of aluminium oxide layer and generate higher asperities surface.

Table 4.4: Aluminium substrate surface conditions with the average surface roughness.

Surface Treatment	Average Surface Roughness, Ra (µm)
As-Received	0.36 ± 0.02
Chemical Etching	2.60 ± 0.30
Grinding with SiC Abrasive Paper G180	0.52 ± 0.05
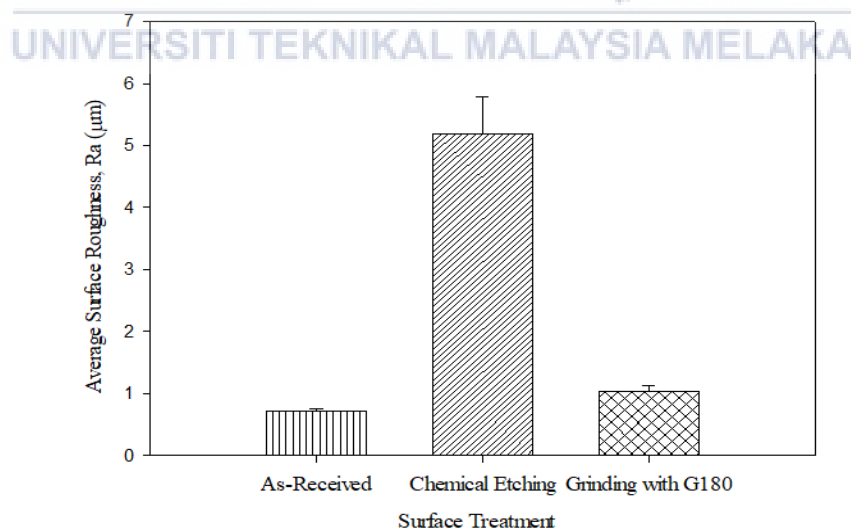
Figure 4.3: Graph of surface roughness against type of surface treatment applied on aluminium substrate surface.

83

Based on Figure 4.4, the chemically etched substrate exhibits less compact peaks per distance and exhibits high peaks protrusion. Former condition may influence the tendency of liquid (ECA for lap shear test or water for contact angle measurement) to flow into the micro-rough surface while latter condition to provide larger contact area between ECA/substrate interface for better mechanical interlocking of ECA toward substrate.
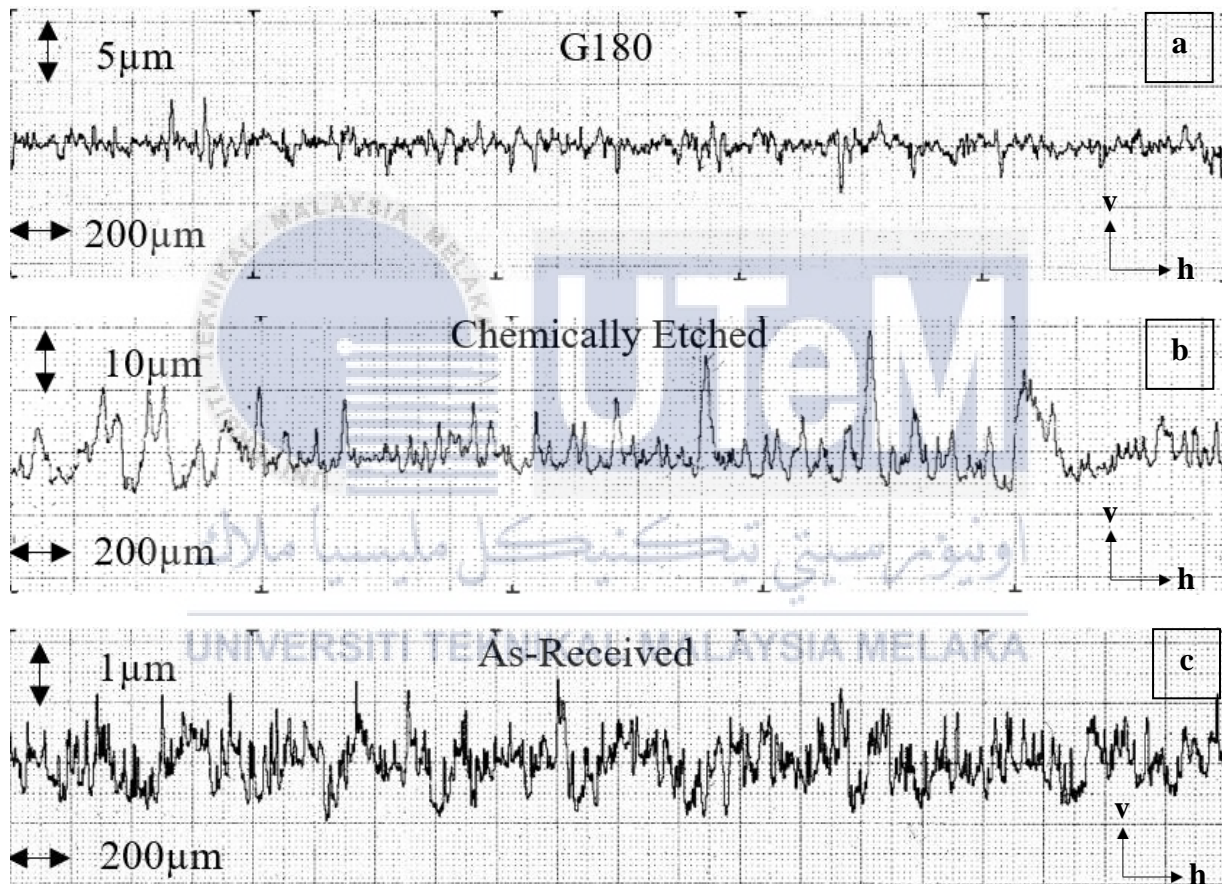
Figure 4.4: Surface profile of aluminium substrates: (a) grinded with silicon carbide paper G180, (b) chemically etched, and (c) as-received.

Meanwhile, grinded and as-received aluminium substrate surface profile exhibits much compact of sharp peaks per distance, an indication of low tendency of liquid to flow into the

84

voids/grooves (Jennings, 1972). Furthermore, for grinded aluminium substrate surface, higher downward peaks profile as compared to as-received exhibited, give an indication of series of deeper valleys on the substrate surface, thus, the penetration of fluid into the valleys/grooves become harder.

4.3.4 Contact angle test
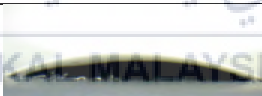
Based on the theory on wettability as described by Matthews et al. (Matthews and Rawlings, 1999), the low contact angle experienced by liquid in specified surface indicates that the liquid has good wettability toward the surface. The wettability will give an impact on surface adhesion performance between ECA and substrate. This is due to an excellent wettability is influenced by the excellent ability of ECA to cover all bumps and voids which results to great adhesion properties of the bond.

Based on the results from contact angle measurement in Table 4.5, the chemically etched substrate has the lowest contact angle, an indication of excellent surface wettability since higher surface roughness promote better spreading of liquid to the substrate surface (Leena et al., 2016). Furthermore, the open structure of voids or crevices on the surface contribute to high tendency of the water to fill in and reduce the contact angle (Jennings, 1972).

Besides, the grinded substrate with SiC abrasive paper G180 yield in the highest contact angle, an indication of poor surface wettability. Although, the grinded substrate surface has the higher surface roughness as compared to the as-received substrate, the former contact angle is higher than the latter surface condition due to the asperities on the grinded surface may form geometric barriers which led to an increase of contact angle (Boutar et al., 2016). The sharp edge asperities and deep voids on grinded surface may hinder the ability of water to penetrate the space between the asperities or voids resulted to low substrate surface covered by the water.

85

As-received substrate has smooth surface indicating the low surface area to be covered by water. Therefore, the substrate has significant higher contact angle than chemically etched substrate. However, the surface contact area between water/substrate is much higher than grinded substrate as the tendency formation air-pocket between water/substrate interface is lower for smoother surface. Therefore, as-received substrate has better wetting performance as compared to grinded substrate.

Table 4.5: Water droplet behaviour on different substrate surface conditions and the average contact angle.

Surface Treatment	Water Droplet Behaviour	Average Contact Angle (°) (θ)
As-Received		74.47 ± 5.29
Chemical Etching		16.78 ± 4.40
Grinding with SiC Abrasive Paper G180		85.66 ± 6.42

4.4 Interlayer strength of ECA

4.4.1 The effect of filler loading on ECA shear strength

The ECA with MWCNT filler loading of 0 wt.%, 5 wt.%, 6 wt.% and 7 wt.% were subjected to lap shear test and the result is illustrated in Figure 4.5. Based on the result, shear

strength of ECA is greatly increase when the filler loading is increase from 0 wt.% to 5 wt.% MWCNT loading and increase slightly from 5 wt.% to 6 wt.% since the addition of MWCNT filler into the epoxy enhance the mechanical properties of the composite due to a reinforcement of MWCNT filler in the composites contribute to an increase of ECA toughness and resist the formation of crack growth in the composites (Srivastava, 2011). Moreover, the presence of MWCNT in ECA induce the formation of new surface which increase the energy absorbed (Zohar et al., 2011) and the mechanical load from epoxy can be transferred to the high stiffness MWCNT.

However, when further increase of filler loading from 6 wt.% to 7 wt.% has result to a decrease of shear strength in ECA. At this point, the MWCNT filler which is high surface energy tend to aggregate resulting poor dispersion and reduce mechanical strength in the ECA (Shen et al., 2007; Trinidad et al., 2017; Zandiatashbar et al., 2012). This is due to an increase of MWCNT filler loading in ECA contribute to the increasing of viscosity of ECA prior to curing process which reduce the mobility of MWCNT in the epoxy and affect the dispersion of MWCNT in the ECA. Therefore, the partially aggregated MWCNT bundles increase which the aggregation of MWCNT can act as stress concentrators which reduce the interfacial adhesion between MWCNT/epoxy, resulted to slippage of filler when the load is subjected to the ECA (Shen et al., 2007; Yim & Kim, 2015; Zohar et al., 2011).

Moreover, high viscosity of ECA reduce the adhesion strength of ECA towards the aluminium substrate as the high viscosity fluid is low wettability (F.L. Matthews and R.D. Rawlings, 1999), hence, reduce the tendency of ECA to penetrate the voids and reduce the effective bond area between the ECA and the substrate interface, (Hitchcock et al., 1981; Prolongo & Uren, 2009). Furthermore, high viscosity of ECA due to high filler loading create

the bubbles and reduces the ability of bubbles removal which reduce the mechanical bonding properties between ECA/substrate interface (Shen et al., 2007).

Besides, an increase of conductive filler loading in ECA means volume fraction of epoxy relatives to the total volume of ECA reduces, therefore, cause a decrease on the composites shear strength due to epoxy unable to be in continuous form and will not be able to provide good polymer network (Qiao et al., 2014; Trinidad et al., 2017). In addition, at high MWCNT filler loading, means less surface contact area between epoxy/substrate interface to provide adhesion properties (Li & Lumpp, 2006) since numerous of MWCNT exist between the epoxy/substrate interface which MWCNT does not have strong bond to the substrate.

Based on the results following lap shear test for the as-received substrate, there is a clear trend on the resultant shear strength of the ECA with increasing MWCNT filler loading, which is similar to the trend observed in an earlier studies using CNT/polymer composites as reported by Loos and Manas-Zloczower (2012), and experimental result on mechanical properties of ICA demonstrated by H. P. Wu et al. (2007).
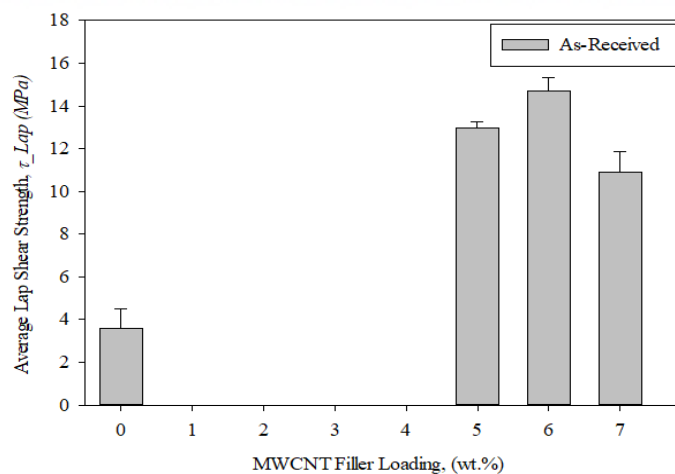
Figure 4.5: Plot of shear strength against filler loading of ECA bonded to as-received aluminium substrate.

88

4.4.2   The effect of substrate surface condition on ECA shear strength

Based on Figure 4.6, ECA bonded to chemically etched and as-received aluminium substrate shows an increase of shear strength with increasing of MWCNT filler loading from 5 wt.% to 6 wt.% and shows a decrease in the shear strength beyond 6 wt.% filler loading. This is due to an increase in the MWCNT filler loading, up to a specified limit (typically percolation threshold) of the ECA, which yield in an enhancement in the composites toughness. Nevertheless, further increase of MWCNT filler loading beyond the limit cause a reduce of reinforcement efficiency (Loos & Manas-Zloczower, 2012). Meanwhile, the ECA bonded to grinded substrate shows a decrease of shear strength with further increase of MWCNT loading, an indication that the grinded surface substrate is significantly affected by the viscosity of the ECA.
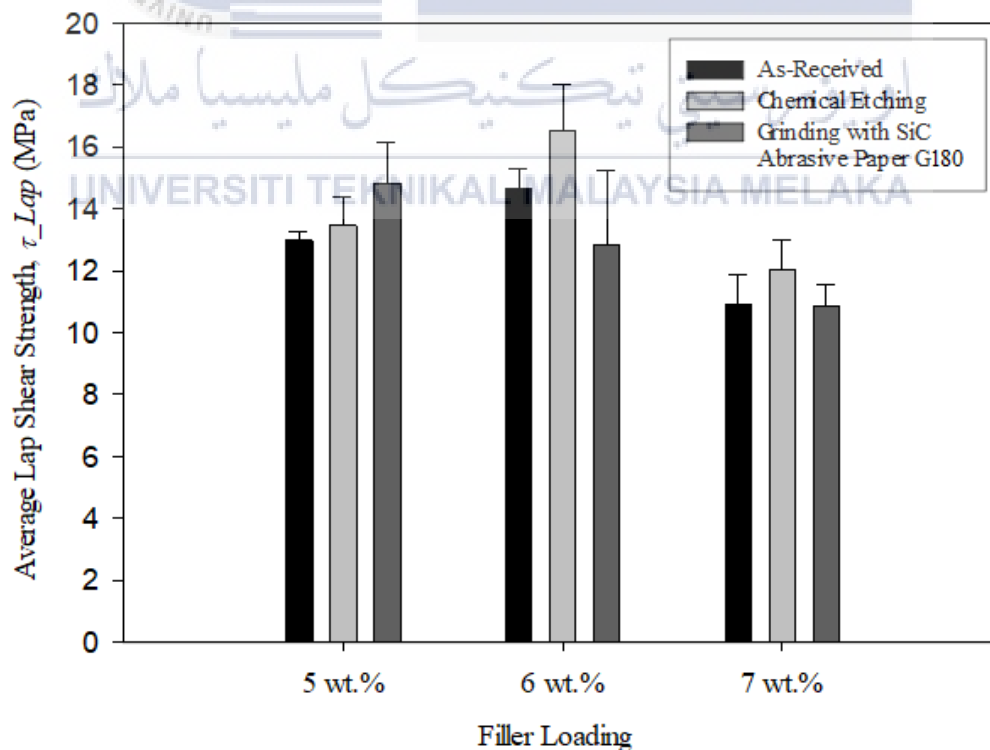
Figure 4.6: Graph of lap shear strength of ECA against MWCNT filler loading.

Table 4.6: Result of single-lap-joint, contact angle and surface roughness for different substrate surface conditions.

Surface Treatment	Average Surface Roughness, Ra (μm)	Average Contact Angle, θ (°)	Filler Loading, wt.%	Average Lap Shear Strength, MPa
As-Received	0.36	74.47	5.00	12.98 ± 0.30
			6.00	14.68 ± 0.63
			7.00	10.92 ± 0.94
Chemical Etching	2.60	16.78	5.00	13.47 ± 0.94
			6.00	16.52 ± 1.51
			7.00	12.02 ± 1.00
Grinding with SiC Abrasive Paper Grit 180	0.52	85.66	5.00	14.83 ± 1.30
			6.00	12.84 ± 2.42
			7.00	10.87 ± 0.68

By referring to Table 4.6, at 5 wt.% filler loading, ECA bonded to grinded aluminium substrate exhibit the highest shear strength, which is 14.83 MPa. Hence, at low MWCNT loading, the viscosity is low which led to better penetration of ECA into the grooves/voids of although surface morphological of grinded substrate exhibits sharp asperities and deep valleys. For 6 wt.% and 7 wt.% filler loading, ECA has the greatest shear strength when bonded to chemical etched aluminium substrate which is 16.52 MPa and 12.02 MPa respectively while weakest ECA shear strength is when bonded to grinded aluminium substrate with 12.84 MPa

and 10.86 MPa respectively. For 7 wt.% filler loading, all types of surface conditions show a lower ECA shear strength as compared to 5 wt.% and 6 wt.% filler loading.

Overall, the chemically etched aluminium substrate provides the highest ECA shear strength which attributed to the relation between liquid contact angle and ECA shear strength which chemical etching treatment on aluminium surface yield to excellent wettability since the contact angle is low which result to high shear strength. Besides, chemically etched substrate provides highest surface roughness which introduce to large interfacial area between aluminium and ECA which enhance the mechanical interlocking of the interface (Yasuda & Saito, 2014). Other factors that contribute to good adhesion are the chemical etching process activated and cleaned aluminium surface, and dissolved natural alumina layer or weakly bound oxide layer which the natural alumina can reduce the ability of adhesive to spread (Leena et al., 2016). Moreover, the chemical etching process introduced the formation of high porous oxide aluminium surface and generate more bumpy and rugged surface as compared to the other surface conditions. The combination of high surface roughness and good wettability of adhesive toward aluminium surface yield to an excellent bond strength (Leena et al., 2016).

Grinded aluminium substrate with SiC paper G180 has the lowest wettability resulted to lowest shear strength. This is due to the micro geometric barrier effect generated which prevent the spreading of ECA throughout the surface. Furthermore, the entrapped air between asperities valleys hinder the well penetration of ECA into the rough surface asperities as demonstrated in Figure 4.7. Thus, the discontinuous interface between ECA/substrate obtained and the part of the interface alternate to gas-liquid interface which latter interface does not promote to adhesion properties between ECA and substrate interface (Boutar et al., 2016). Due to this, surface area of contact between ECA/substrate reduced, hence, stress riser build up at the ECA/substrate interface (Jennings, 1972).

91
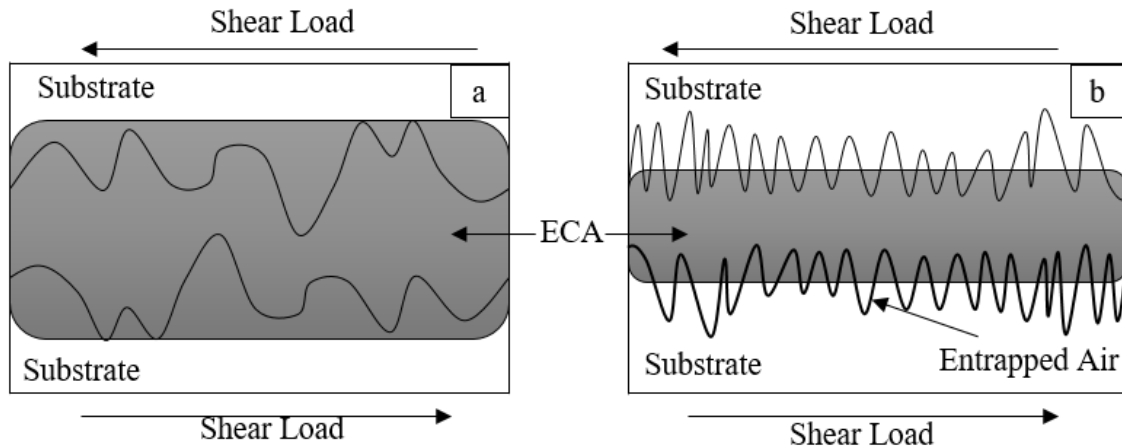
Figure 4.7: Illustration of ECA bonded to aluminium substrates with (a) voids with wide opening structures, and (b) sharp peaks and deep voids.

For the case of as-received aluminium substrate, although it has lowest surface roughness, yet it still has greater wettability than grinded aluminium substrate. Therefore, it has higher shear strength than the grinded substrate as high wettability means more contact area between ECA/substrate, resulted to high mechanical interlocking between ECA/substrate interface.

As the chemically etched substrate promote to the higher bond strength than the as-received substrate (surface wiped with acetone) in this experiment, the result is congruent to experiment of effect of surface treatment on the shear strength of aluminium adhesive single-lap-joint demonstrated by Correia et al. (2018). The experiment result revealed that the chemically treated of both aluminium substrate provides higher ECA load of failure as compared to only one substrate is chemically treated.

The result are meet with agreement of experiment made by (Ghumatkar & Sekhar (2017) on the relation between aluminium surface roughness and adhesive bond shear strength. From the experiment, the result showed that the highest of adhesive shear strength when aluminium

92

surface roughness at 2.05 ± 0.19 μm which near to the chemically etched substrate surface roughness in this project that yield the highest ECA shear strength.

4.5   ECA failure analysis

4.5.1   Mode of failure

Based on Table 4.7, Table 4.8, and Table 4.9, the ECA with 5 wt.% and 6 wt.% MWCNT loading failed in adhesive-cohesive mode while ECA with 7 wt.% MWCNT loading, adhesive mode of failure observed. Overall, adhesive-cohesive failure mode of ECA provide higher shear strength as compared to adhesive failure mode.

High shear strength of ECA with adhesive-cohesive failure give indication of high adhesion strength between ECA/substrate interface as a resulted of large surface area of contact between epoxy/substrate interface, yield to strong mechanical contact (Muhammad et al., 2014). The experimental result is congruent with experiment of effect of surface treatment on adhesively bonded aluminium-aluminium joints conducted by Correia et al. (2018) as the adhesive bond with adhesive-cohesive failure has higher failure loads as compared to adhesive bond presenting adhesive failure.

Adhesive failure at high MWCNT filler loading suggest low mechanical interlocking strength between epoxy/substrate interface which can be attributed to the presence of large amount of MWCNT particles between epoxy/substrate interface, thus, induced to low surface area of contact between the epoxy/substrate interface. Hence, the ECA bond with adhesive failure have lower shear strength than ECA bond with adhesive-cohesive failure.

Table 4.7: ECA with 5 wt.% MWCNT filler loading mode of failure.
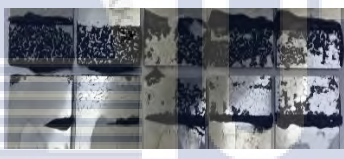
Surface Treatment	ECA Failure Behaviour	Mode of Failure	Average Shear Strength, MPa
As-Received		Adhesive-Cohesive	12.98 ± 0.30
Chemical Etching		Adhesive-Cohesive	13.47 ± 0.94
Grinding with SiC Abrasive Paper Grit 180		Adhesive-Cohesive	14.83 ± 1.30

Table 4.8: ECA with 6 wt.% MWCNT filler loading mode of failure.
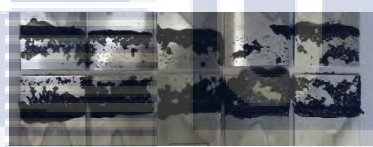
Surface Treatment	ECA Failure Behaviour	Mode of Failure	Average Shear Strength, MPa
As-Received		Adhesive-Cohesive	14.68 ± 0.63
Chemical Etching		Adhesive-Cohesive	16.52 ± 1.51
Grinding with SiC Abrasive Paper Grit 180		Adhesive-Cohesive	12.84 ± 2.42

Table 4.9: ECA with 7 wt.% MWCNT filler loading mode of failure.
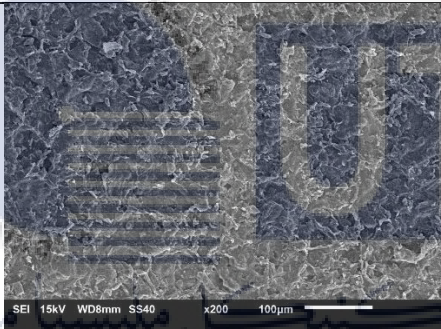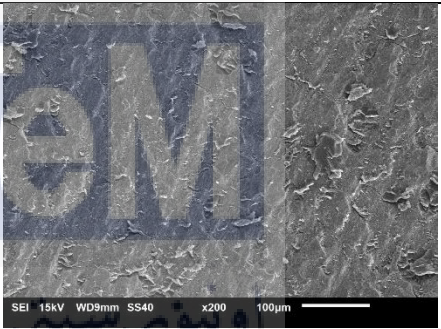
Surface Treatment	ECA Failure Behaviour	Mode of Failure	Average Shear Strength, MPa
As-Received		Adhesive	10.92 ± 0.94
Chemical Etching		Adhesive	12.02 ± 1.00
Grinding with SiC Abrasive Paper Grit 180		Adhesive	10.87 ± 0.68

4.5.2 Morphology study on surface of fractured ECA

4.5.2.1 Scanning electron microscopy (SEM)

Scanning electron microscopy (SEM) was utilized to capture micrograph images of fractured ECA. Therefore, surface morphology between weakest and strongest shear strength of fractured ECA bonded to chemically etched aluminium substrate via lap shear test can be compared.

96

Table 4.10: Comparison of ECA with different filler loading on chemically etched substrate.

	Weakest ECA	Strongest ECA
Surface Treatment	Chemical Etching	Chemical Etching
MWCNT Loading	7 wt.%	6 wt.%
Lap Shear Strength, τ_Lap (MPa)	12.02	16.52
SEM Micrograph Image	 200x magnification	 200x magnification
Surface Description	• High dense of voids • Aggregation of MWCNT hinder the smoothness of surface	• Low dense of voids • Smoother surface due to less aggregation of MWCNT.
Mode of Failure via Lap Shear Test	• Adhesive failure	• Mix of adhesive and cohesive failure

97

Based on Table 4.10, both ECA were bonded to chemically etched substrate and failed via lap shear test. Fracture surface of ECA with 7 wt.% MWCNT filler loading exhibit denser volume of voids with rougher surface than ECA with 6 wt.%. MWCNT filler loading. A reduce of 27% of ECA shear strength (bonded to chemically etched aluminium substrate) from 16.52 MPa to 12.02 MPa with an increase of MWCNT filler loading from 6 wt.% to 7 wt.% respectively. High contains of voids or hollow structure in ECA with 7 wt.% MWCNT filler loading reduce the contact area between the ECA and the substrate, hence, insufficient anchoring of epoxy towards the substrate occur (Trinidad et al., 2017). The claim is supported by the adhesive failure mode obtained on ECA with 7 wt.% filler loading via lap shear test which an indication of lack of adhesion strength between the ECA and the substrate.

Besides, high volume of voids in ECA reduce the energy dissipation in the system (Yim & Kim, 2015). The contact area between ECA and substrate play an important role to enhance the shear strength of the ECA as the ECA with low dense of voids promote large contact area of the ECA towards the substrate results to the better mechanical interlocking (Trinidad et al., 2017).

4.6 Chapter summary

In term of electrical conductivity, the higher the MWCNT filler loading in the ECA, the higher ECA electrical conductivity performance due to formation of conductive path between the fillers. In term of mechanical strength, an increase of filler loading up to the 6 wt.% yield an increase of shear strength. However, beyond 6 wt.% filler loading, the shear strength of ECA decrease despite contain higher reinforcement by the filler. This is due to the aggregation between the fillers and the low weight fraction of polymer matrix which latter is essential to promote adhesion strength between substrate and the ECA. Besides, the chemically etched

98

substrate promotes highest surface roughness and lowest contact angle results to the highest shear strength of the ECA.

CHAPTER V

CONCLUSION AND RECOMMENDATIONS FOR FUTURE WORK

5.1   Conclusion

In this study, the effect of MWCNT filler loading electrical was studied through sheet resistance measurement. In addition, the effect of MWCNT filler loading and aluminium substrate surface conditions on ECA mechanical properties were studied through surface morphology and topography analysis, contact angle testing and mechanical testing.

In terms of electrical conductivity, the ECA resistivity decrease with an increase of MWCNT filler loading in the ECA. Besides, an increase of MWCNT loading give an increase and a decrease trend of ECA shear strength which congruent with study conducted by Loos and Manas-Zloczower (2012) on reinforcement efficiency of carbon nanotubes in CNT/polymer composites and they found that a significant enhancement of the composites mechanical properties with CNT loading up to specified filler loading and a degradation of ECA mechanical properties obtained with further increase of filler loading beyond the specified loading.

As for the effect of substrate surface conditions on ECA mechanical properties, the chemically etched provide the highest ECA shear strength via lap shear test which attributed to the highest wettability and highest surface roughness which mean the large effective bond area obtained. Furthermore, the excellent wettability of the chemically etched substrate is attributed to the substrate surface morphology which consists of wide opening structure of voids/micro-roughs, an indication high tendency of liquid to flow in (Jennings, 1972).

Although grinded aluminium substrate with SiC paper G180 provide higher surface roughness as compared to as-received aluminium substrate, yet, the lower ECA shear strength obtained due to low wettability. Hence, high surface area provided is meaningless if the actual surface contact area between ECA and substrate is low as a resulted of poor wettability. This is due to the surface morphology of the grinded substrate which consist of sharp peaks and deep valleys, yield to poor spreading of ECA towards the surface and generated entrapped air between ECA/substrate interface.

As a conclusion, an increase of filler loading promotes the enhancement of ECA electrical properties and the combination of excellent wetting properties of substrate towards ECA and high surface roughness of substrate (indication of high surface area) contribute to excellent adhesion properties of the ECA towards the substrate, hence, yield to high shear strength.

5.2   Recommendation for future works

In an actual application, as interconnect material, ECA is subjected to impact or shock during handling, assembling and lifetime, hence, an excellent mechanical property is essential to ensure the ECA is robust and reliable. Therefore, the aggregation of MWCNT filler in the ECA composites must be avoided/reduced as the aggregated MWCNT filler build up stress concentrators, results to slippage when subjected to composites load. Furthermore, a well dispersed MWCNT filler in ECA contribute to a high filler surface area available to absorbed load from polymer matrix. As to counter the problem, the used of the mechanical stirrer and the ultrasound sonication is crucial. Both device utilization will improve the dispersion of MWCNT filler and latter device can break the aggregation of the filler at sub-micron level (Zohar et al., 2011). Besides, the measurement of ECA viscosity through viscometer can evaluate the

101

dispersion state of MWCNT in the ECA, hence, the peak of viscosity suspension can be determined to achieve optimum dispersion of MWCNT filler.

Besides, the used of functionalized MWCNT filler as conductive filler in ECA composites can provide some benefits such as prevention of MWCNT entanglement to provide good dispersion in ECA, good interfacial interactions between MWCNT and surrounding matrix, and induced the ECA wettability due to the fillers are not influenced by MWCNT agglomerates. Furthermore, functionalized MWCNT can improves the matrix toughness as the filler are more readily to dispersed in epoxy matrix, and MWCNT filler surface is covalently attached to the epoxy matrix results to more effective stress transfer and forms denser crosslink structure (Kwon et al., 2011).

REFERENCES

Amoli, B. M. (2015). Development of Advanced ECAs with Micro / nano Hybrid Filler System : Filler Functionalization , Dispersion , and Conductivity Improvement.

Antonis Nanakoudis. (2017). Sample preparation: how sputter coating assists your SEM imaging. Retrieved March 12, 2018, from http://blog.phenom-world.com/sample-preparation-sputter-coating-sem-imaging

AZoM. (2010). Gold - Physical, Mechanical, Thermal and Electrical Properties of Gold - World Gold Council. Retrieved from https://www.azom.com/article.aspx?ArticleID=5147

Bell, T. (2017). Electrical Conductivity in Metals. Retrieved from https://www.thebalance.com/electrical-conductivity-in-metals-2340117

Borsellino, C., Bella, G. Di, & Ruisi, V. F. (2009). Adhesive joining of aluminium AA6082 : The effects of resin and surface treatment, *29*, 36–44. https://doi.org/10.1016/j.ijadhadh.2008.01.002

Boutar, Y., Naïmi, S., Mezlini, S., & Ali, M. B. S. (2016). Effect of surface treatment on the shear strength of aluminium adhesive single-lap joints for automotive applications. *International Journal of Adhesion and Adhesives*, *67*, 38–43. https://doi.org/10.1016/j.ijadhadh.2015.12.023

Brien, J. O., Us, U. T., & Ashmead, S. D. (2005). (19) United States (12) Patent Application

Publication (10) Pub . No .: US 2005 / 0235718 A1 SOURCE (S) AGENT (S), *1*(60).

Coddet, P., Verdy, C., Coddet, C., & Debray, F. (2016). On the mechanical and electrical properties of copper-silver and copper-silver-zirconium alloys deposits manufactured by cold spray. *Materials Science and Engineering A, 662,* 72–79. https://doi.org/10.1016/j.msea.2016.03.049

Correia, S., Anes, V., & Reis, L. (2018). E ff ect of surface treatment on adhesively bonded aluminium- aluminium joints regarding aeronautical structures. *Engineering Failure Analysis, 84*(October 2017), 34–45. https://doi.org/10.1016/j.engfailanal.2017.10.010

Critchlow, G. W., & Brewis, D. M. (1996). Review of surface pretreatments for aluminium alloys. *International Journal of Adhesion and Adhesives, 16*(4), 255–274. https://doi.org/10.1016/S0143-7496(96)00014-0

Dr. Reinhard Miller & Dr. Alexander Makievski GbR. (2011). Contact angle measurement with PAT-1. Retrieved December 11, 2017, from http://www.sinterface.com/ca1.html

Durairaj, R. (2016). Investigation on the mechanical and electrical properties of multiwall carbon nanotubes (MWNCTs) based isotropic. https://doi.org/10.1108/PRT-05-2014-0037

F.L. Matthews and R.D. Rawlings. (1999). *Composite mterials: Engineering and science*. North America: Chapman & Hall.

Ghumatkar, A., & Sekhar, R. (2017). ScienceDirect Experimental study on different adherend surface roughness on the adhesive bond strength, *4*, 7801–7809. https://doi.org/10.1016/j.matpr.2017.07.115

Grinding & Polishing. (2013). Retrieved December 10, 2017, from http://www.metkon.com/en/application_grinding-polishing_12.html

Grinding Consumables. (2017). Retrieved December 14, 2017, from https://www.struers.com/en/Products/Grinding-and-Polishing/Grinding-and-polishing-consumables#contact

Harris, A. F., & Beevers, A. (1999). The effects of grit-blasting on surface properties for adhesion. *Journal Of Adhesion*, *19*(November 1998).

Hitchcock, S. J., Carroll, N. T., & Nicholas, M. G. (1981). Some effects of substrate roughness on wettability. *Journal of Materials Science*, *16*(3), 714–732. https://doi.org/10.1007/BF00552210

How a Profilometer Works. (2017). Retrieved from http://www.nanoscience.com/technology/optical-profiler-technology/how-profilometer-works/

Jennings, C. W. (1972). Surface Roughness and Bond Strength of Adhesives. *The Journal of Adhesion*, *4*(1), 25–38. https://doi.org/10.1080/00218467208072208

Kwon, Y., Yim, B. S., Kim, J. M., & Kim, J. (2011). Dispersion, hybrid interconnection and heat dissipation properties of functionalized carbon nanotubes in epoxy composites for electrically conductive adhesives (ECAs). *Microelectronics Reliability*, *51*(4), 812–818. https://doi.org/10.1016/j.microrel.2010.11.005

Leena, K., Athira, K. K., Bhuvaneswari, S., Suraj, S., & Rao, V. L. (2016). Effect of surface pre-treatment on surface characteristics and adhesive bond strength of aluminium alloy. *International Journal of Adhesion and Adhesives*, *70*, 265–270. https://doi.org/10.1016/j.ijadhadh.2016.07.012

Li, J., & Lumpp, J. K. (2006). Electrical and Mechanical Characterization of Carbon Nanotube Filled Conductive Adhesive. *Aerospace Conference IEEE*.

Li, J., Lumpp, J. K., Andrews, R., & Jacques, D. (2008). Aspect ratio and loading effects of multiwall carbon nanotubes in epoxy for electrically conductive adhesives. *Journal of Adhesion Science and Technology*, *22*(14), 1659–1671. https://doi.org/10.1163/156856108X320528

Loos, M. R., & Manas-Zloczower, I. (2012). Reinforcement efficiency of carbon nanotubes - Myth and reality. *Macromolecular Theory and Simulations*, *21*(2), 130–137. https://doi.org/10.1002/mats.201100099

Lu, D. D., & Wong, C. P. (2009). *Materials for advanced packaging. Materials for Advanced Packaging*. https://doi.org/10.1007/978-0-387-78219-5

Lu, D., Tong, Q. K., & Wong, C. P. (1999). Conductivity mechanisms of isotropic conductive adhesives (ICAs). *Proceedings - International Symposium on Advanced Packaging Materials: Processes, Properties and Interfaces*, 2–10. https://doi.org/10.1109/ISAPM.1999.757278

Luo, J., Cheng, Z., Li, C., Wang, L., Yu, C., & Zhao, Y. (2016). Electrically conductive adhesives based on thermoplastic polyurethane fi lled with silver fl akes and carbon nanotubes. *Composites Science and Technology*, *129*, 191–197. https://doi.org/10.1016/j.compscitech.2016.04.026

Ma, P., Siddiqui, N. A., Marom, G., & Kim, J. (2010). Composites : Part A Dispersion and functionalization of carbon nanotubes for polymer-based nanocomposites : A review. *Composites Part A*, *41*(10), 1345–1367. https://doi.org/10.1016/j.compositesa.2010.07.003

Mantena, K. (2009). Electrical and Mechanical Properties of MWCNT Filled Conductive Adhesives on Lead Free Surface Finishd PCB's. Retrieved from http://uknowledge.uky.edu/cgi/viewcontent.cgi?article=1617&context=gradschool_theses%5Cnhttp://uknowledge.uky.edu/gradschool_theses/613/

Mayer, M. (2018). What Is a Thermoplastic Polymer? Retrieved December 10, 2017, from https://sciencing.com/thermoplastic-polymer-5552849.html

Mechanical Properties. (n.d.). Retrieved December 11, 2017, from https://www.nde-ed.org/EducationResources/CommunityCollege/Materials/Mechanical/Mechanical.htm

Method, S. T. (2010). Standard Test Method for Apparent Shear Strength of Single-Lap-Joint Adhesively Bonded Metal Specimens by Tension Loading (Metal-to-, 10–15. https://doi.org/10.1520/D1002-10.on

Microscope Basic Functions and Optical System Configuration. (n.d.). Retrieved from https://www.olympus-ims.com/en/microscope/terms/feature10/

Muhammad, N., Hj, S., & Suzana, E. (2014). International Journal of Adhesion & Adhesives Effect of surface treatments on the durability of green polyurethane adhesive bonded aluminium alloy, *55*, 43–55.

Pereira, A. M., Ferreira, J. M., Antunes, F. V., & Bártolo, P. J. (2010). Analysis of manufacturing parameters on the shear strength of aluminium adhesive single-lap joints. *Journal of Materials Processing Technology*, *210*(4), 610–617. https://doi.org/10.1016/j.jmatprotec.2009.11.006

Pethrick, R. A. (2015). Design and ageing of adhesives for structural adhesive bonding-A review. *Proceedings of the Institution of Mechanical Engineers, Part L: Journal of Materials: Design and Applications*, *229*(5), 349–379. https://doi.org/10.1177/1464420714522981

Prasad, S. C. and S. (2017). Metals and Non-Metals. Retrieved from https://brilliant.org/wiki/metals-and-non-metals/

Prolongo, S. G. Ã., & Uren, A. (2009). Effect of surface pre-treatment on the adhesive strength
108

of epoxy – aluminium joints, *29*, 23–31. https://doi.org/10.1016/j.ijadhadh.2008.01.001

Qiao, W., Bao, H., Li, X., Jin, S., & Gu, Z. (2014). International Journal of Adhesion & Adhesives Research on electrical conductive adhesives fi lled with mixed fi ller, *48*, 159–163. https://doi.org/10.1016/j.ijadhadh.2013.07.001

Quorum Technologies. (2002). Sputter Coating Technical Brief, *2*(2), 1–13.

Saleema, N., Sarkar, D. K., Paynter, R. W., Gallant, D., & Eskandarian, M. (2012). A simple surface treatment and characterization of AA 6061 aluminum alloy surface for adhesive bonding applications. *Applied Surface Science*, *261*, 742–748. https://doi.org/10.1016/j.apsusc.2012.08.091

Shay, J. W., Porter, K. R., & Prescott, D. M. (1974). Surface Morphology. *Cell Research*, *71*(8), 3059–3063.

Shen, J., Huang, W., Wu, L., Hu, Y., & Ye, M. (2007). The reinforcement role of different amino-functionalized multi-walled carbon nanotubes in epoxy nanocomposites. *Composites Science and Technology*, *67*(15–16), 3041–3050. https://doi.org/10.1016/j.compscitech.2007.04.025

Srivastava, V. K. (2011). Effect of carbon nanotubes on the strength of adhesive lap joints of C/C and C/CSiC ceramic fibre composites. *International Journal of Adhesion and Adhesives*, *31*(6), 486–489. https://doi.org/10.1016/j.ijadhadh.2011.03.006

SURFTEST SJ-410 Series. (2015). Mitutoyo America Corporation www.mitutoyo.com. Retrieved from https://www.struers.com/en/Products/Grinding-and-Polishing/Grinding-and-polishing-consumables#contact

Thwaite, E. (1982). Surface topography measurement and analysis. *Australian Journal of Physics*, *35*(6), 777–784. Retrieved from http://www.publish.csiro.au/?paper=PH820777

Trinidad, J., Chen, L., Lian, A., & Zhao, B. (2017). Solvent presence and its impact on the lap-shear strength of SDS-decorated graphene hybrid electrically conductive adhesives. *International Journal of Adhesion and Adhesives*, *78*(May), 102–110. https://doi.org/10.1016/j.ijadhadh.2017.06.012

Uehara, K., & Sakurai, M. (2002). Bonding strength of adhesives and surface roughness of joined parts, *127*, 178–181.

Wenzel, R. N. (1936). Resistance of solid surfaces to wetting by water. *Industrial and Engineering Chemistry*, *28*(8), 988–994. https://doi.org/10.1021/ie50320a024

Wong, C. P., Zhang, R., & C. Agar, J. (2011). Conductive polymer composites. *Encyclopedia of Polymer Science and Technology*.

Wu, H. P., Wu, X. J., Ge, M. Y., Zhang, G. Q., Wang, Y. W., & Jiang, J. (2007). Properties investigation on isotropical conductive adhesives filled with silver coated carbon nanotubes. *Composites Science and Technology*, *67*(6), 1182–1186.

https://doi.org/10.1016/j.compscitech.2006.05.010

Wu, Z., Li, J., Timmer, D., Lozano, K., & Bose, S. (2009). International Journal of Adhesion & Adhesives Study of processing variables on the electrical resistivity of conductive adhesives, *29*, 488–494. https://doi.org/10.1016/j.ijadhadh.2008.10.003

Xuechun, L., & Feng, L. (2004). The improvement on the properties of silver-containing conductive adhesives by the addition of Carbon Nanotube, 17–19.

Yasuda, K., & Saito, R. (2014). Effect of surface roughening of aluminum plates on the strength of bonds formed between aluminum and polyphenylene sulfide by thermosonic bonding Effect of surface roughening of aluminum plates on the strength of bonds formed between aluminum and polyphen, 61. https://doi.org/10.1088/1757-899X/61/1/012007

Yi, L., Daniel, L., & C.P., W. (2010). *Electrical Conductive Adhesives with Nanotechnologies*. New York: Springer Science+Business Media.

Yim, B. S., & Kim, J. M. (2015). Electrical and mechanical properties of multiwalled carbon nanotubes-reinforced solderable polymer nanocomposites. *Journal of Materials Science: Materials in Electronics*, *26*(3), 1678–1689. https://doi.org/10.1007/s10854-014-2592-9

Yu, S., Tong, M. N., & Critchlow, G. (2010). Use of carbon nanotubes reinforced epoxy as adhesives to join aluminum plates. *Materials and Design*, *31*(SUPPL. 1), S126–S129. https://doi.org/10.1016/j.matdes.2009.11.045

Zandiatashbar, A., Picu, R. C., & Koratkar, N. (2012). Mechanical Behavior of Epoxy-Graphene Platelets Nanocomposites. *Journal of Engineering Materials and Technology*, *134*(3), 31011. https://doi.org/10.1115/1.4006499

Zielecki, W., Pawlus, P., Perłowski, R., & Dzierwa, A. (2013). Surface topography effect on strength of lap adhesive joints after mechanical pre-treatment. *Archives of Civil and Mechanical Engineering*, *13*(2), 175–185. https://doi.org/10.1016/j.acme.2013.02.005

Zohar, E., Baruch, S., Shneider, M., Dodiuk, H., Kenig, S., Tenne, R., & Wagner, H. D. (2011). The effect of WS2 nanotubes on the properties of epoxy-based nanocomposites. *Journal of Adhesion Science and Technology*, *25*(13), 1603–1617. https://doi.org/10.1163/016942410X524138

112
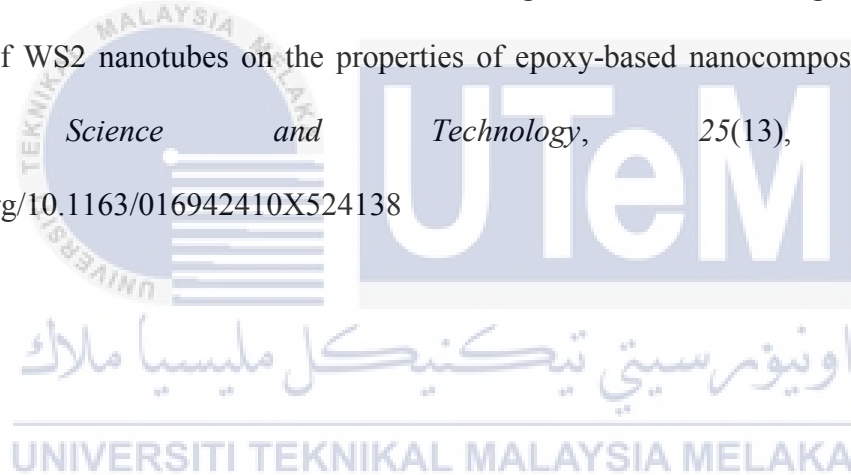
APPENDIX

A. Results of contact angle test

Table (a): Average contact angle on surface of as-received aluminium substrate.

As-Received															
	Sample 1					Sample 2					Sample 3				
	Left	Right	Average	Total Average		Left	Right	Average	Total Average		Left	Right	Average	Total Average
P1	75.38	73.92	74.65	74.71	P1	86.73	80.82	83.77	83.33	P1	77.83	84.66	81.24	82.51
	73.01	73.83	73.42			84.52	80.13	82.33			83.92	84.47	84.20	
	79.13	73.01	76.07			82.73	85.04	83.88			77.26	86.92	82.09	
	Left	Right	Average	Total Average		Left	Right	Average	Total Average		Left	Right	Average	Total Average
P2	75.99	74.64	75.32	74.26	P2	70.37	70.50	70.44	73.72	P2	69.82	75.16	72.49	73.04
	75.49	72.50	74.00			77.44	72.42	74.93			73.16	78.44	75.80	
	72.97	73.98	73.47			74.90	76.72	75.81			68.02	73.64	70.83	
	Left	Right	Average	Total Average		Left	Right	Average	Total Average		Left	Right	Average	Total Average
P3	68.85	75.00	71.93	71.30	P3	67.48	72.05	69.77	69.48	P3	62.06	72.79	67.43	67.92
	66.93	72.92	69.92			65.21	67.30	66.25			64.83	70.48	67.65	
	67.03	77.08	72.05			70.65	74.17	72.41			69.43	67.91	68.67	

Table (b): Average contact angle on surface of grinded with SiC abrasive paper aluminium substrate.

Grinding with SiC Abrasive Paper Grit 180															
	Sample 1					Sample 2					Sample 3				
	Left	Right	Average	Total Average		Left	Right	Average	Total Average		Left	Right	Average	Total Average
P1	79.47	77.72	78.60	79.99	P1	90.33	88.56	89.45	88.89	P1	90.26	86.89	88.58	89.52
	89.20	74.91	82.06			87.92	89.14	88.53			92.29	88.79	90.54	
	83.15	75.50	79.32			89.84	87.52	88.68			91.53	87.36	89.44	
	Left	Right	Average	Total Average		Left	Right	Average	Total Average		Left	Right	Average	Total Average
P2	91.68	87.88	89.78	89.17	P2	79.95	76.97	78.46	76.94	P2	85.57	85.69	85.63	84.54
	88.48	89.36	88.92			78.45	71.49	74.97			83.10	83.45	83.27	
	90.70	86.92	88.81			76.94	77.84	77.39			85.79	83.66	84.73	
	Left	Right	Average	Total Average		Left	Right	Average	Total Average		Left	Right	Average	Total Average
P3	87.76	86.76	87.26	86.89	P3	87.45	91.06	89.25	87.79	P3	91.13	87.47	89.30	87.23
	88.47	85.05	86.76			90.29	82.35	86.32			85.91	85.51	85.71	
	86.21	87.11	86.66			88.16	87.41	87.78			90.31	83.06	86.69	

113

Table (c): Average contact angle on surface of chemically etched aluminium substrate.

						Chemical Etching								
		Sample 1					Sample 2					Sample 3		
	Left	Right	Average	Total Average		Left	Right	Average	Total Average		Left	Right	Average	Total Average
P1	17.03	25.82	21.42		P1	8.73	7.26	7.99		P1	27.08	24.83	25.96	
	17.95	18.94	18.44	19.10		11.59	7.68	9.63	8.70		28.45	23.42	25.93	23.88
	15.88	18.99	17.44			8.39	8.56	8.47			18.50	21.03	19.77	
	Left	Right	Average	Total Average		Left	Right	Average	Total Average		Left	Right	Average	Total Average
P2	32.46	26.44	29.45		P2	9.36	13.93	11.65		P2	14.98	14.75	14.86	
	26.57	32.39	29.48	29.26		11.15	13.83	12.49	11.63		17.91	16.15	17.03	15.83
	28.47	29.24	28.86			10.20	11.31	10.76			16.87	14.34	15.61	
	Left	Right	Average	Total Average		Left	Right	Average	Total Average		Left	Right	Average	Total Average
P3	15.05	15.89	15.47		P3	14.94	15.55	15.24		P3	10.15	14.50	12.32	
	16.35	15.31	15.83	15.42		10.88	16.61	13.75	14.89		12.81	13.08	12.95	12.32
	14.59	15.34	14.97			12.68	18.68	15.68			10.39	13.01	11.70	

B. 3D profiles of aluminium substrate surface

Line	Name	Height [um]	Width1 [um]	Area [um^2]	Diagonal [um]	Surface Length [um]	RoughnessRa [um]
1	Profile	5.5951	154.6325	701.9711	154.7337	154.6466	0.3351
2	Profile	5.5951	154.6325	642.2872	154.7337	154.7549	0.3428
3	Profile	5.5951	154.6325	482.4021	154.7337	154.6732	0.3278
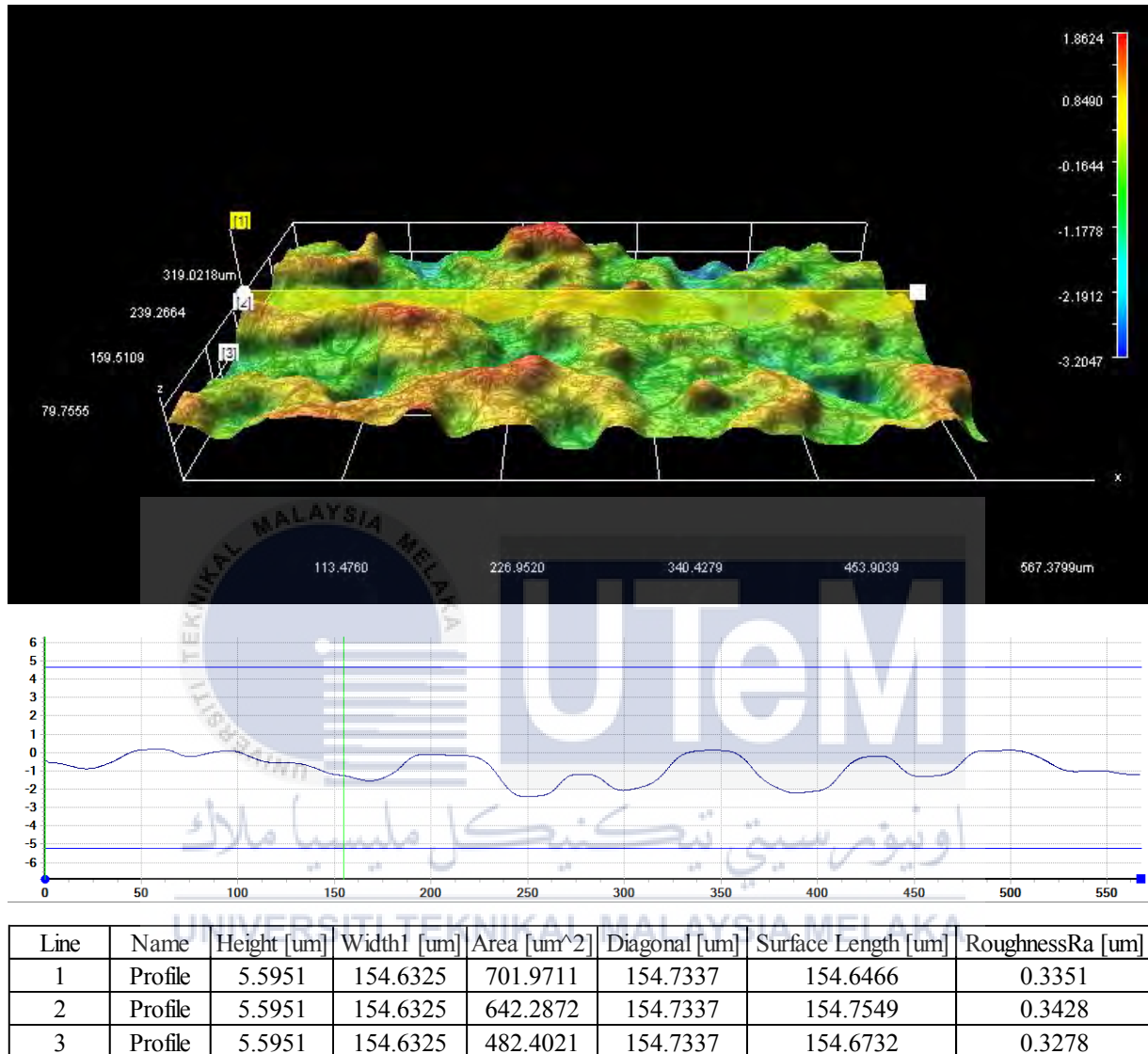
Figure (a): Results of non-contact 3D profile measurement on surface of as-received aluminium substrate.
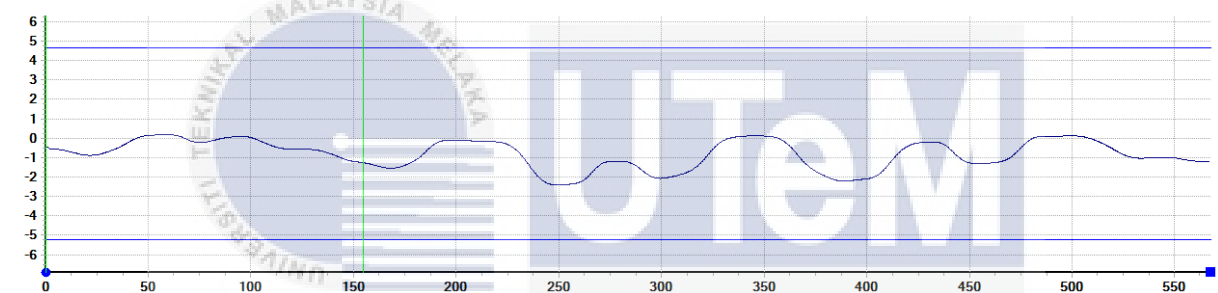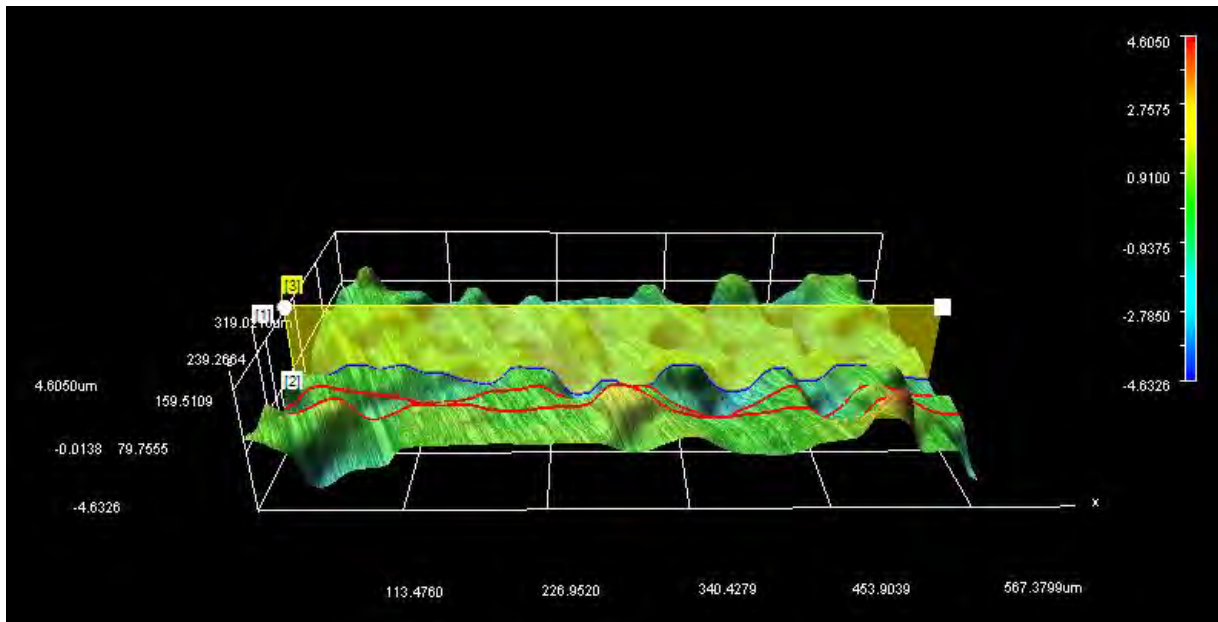
115

Line	Name	Height [um]	Width1 [um]	Area [um^2]	Diagonal [um]	Surface Length [um]	RoughnessRa [um]
1	Profile	9.9037	154.6325	842.6734	154.9493	154.7678	0.4792
2	Profile	9.9037	154.6325	706.6211	154.9493	154.7125	0.6173
3	Profile	9.9037	154.6325	748.8737	154.9493	154.6962	0.581

Figure (b): Results of non-contact 3D profile measurement on surface of grinded with SiC abrasive paper grit 180 aluminium substrate.

Line	Name	Height [um]	Width1 [um]	Area [um^2]	Diagonal [um]	Surface Length [um]	RoughnessRa [um]
1	Profile	17.1703	154.6325	2225.5147	155.5828	155.6711	2.7215
2	Profile	17.1703	154.6325	2011.2848	155.5828	157.0022	2.9976
3	Profile	17.1703	154.6325	2415.3026	155.5828	154.8795	2.1826
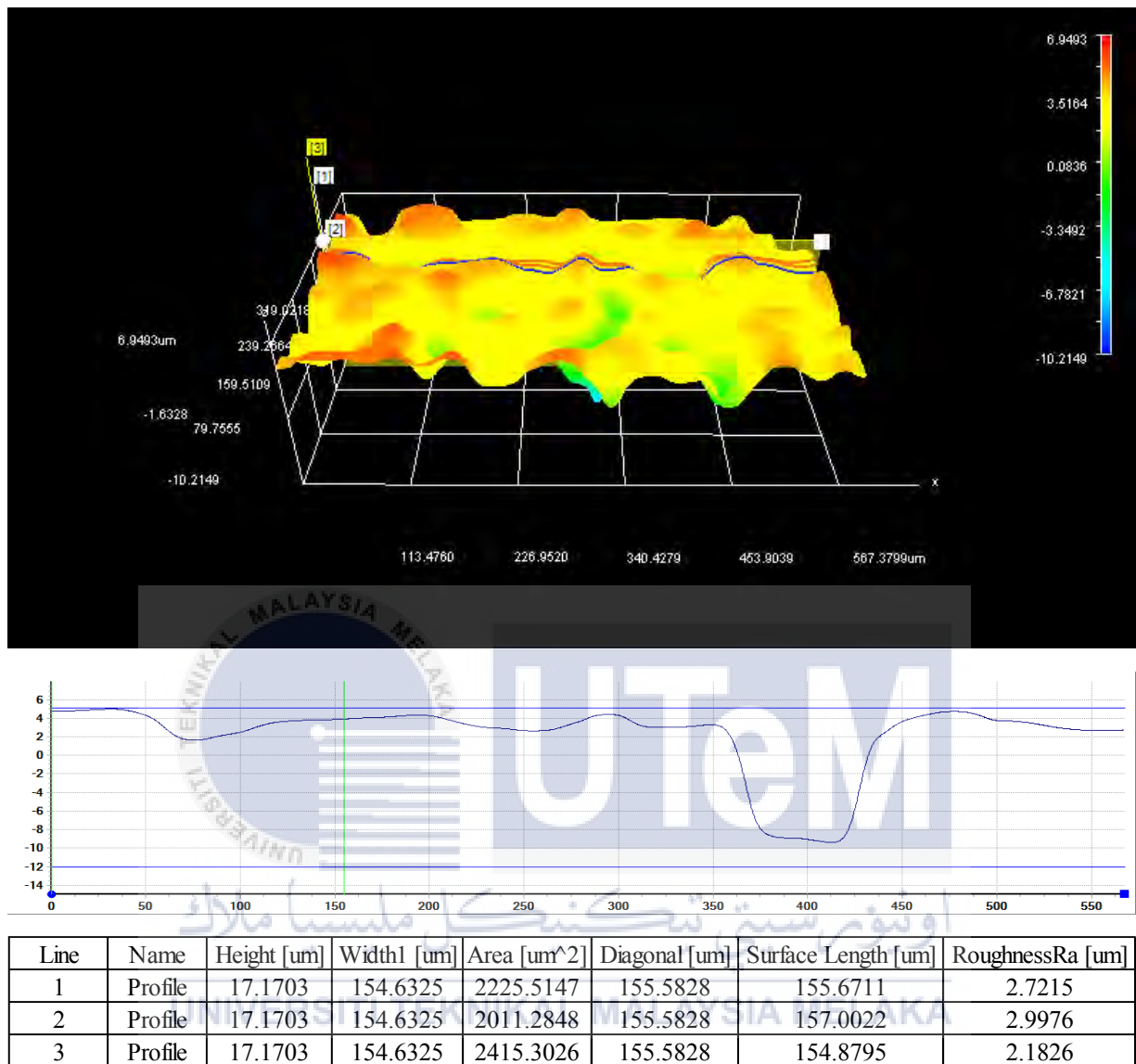
Figure (c): Results of non-contact 3D profile measurement on surface of chemically etched aluminium substrate.

117

SIGMA-ALDRICH

SAFETY DATA SHEET

1.   SECTION 1: Identification of the hazardous chemical and of the supplier

1.1   Product identifiers

Product name   :   Araldite® 506 epoxy resin

Product Number   :   A3183
Brand   :   Sigma-Aldrich

1.2   Other means of identification

No data available

1.3   Recommended use of the chemical and restrictions on use

For R&D use only. Not for pharmaceutical, household or other uses.

1.4   Details of the supplier of the safety data sheet

Company   :   Sigma-Aldrich (M) Sdn. Bhd.
                                                        A-07-11, Empire Office, Empire Subang
                                                        Jalan SS16/1, SS16
                                                        47500 SUBANG JAYA-SELANGOR DARUL EHSAN
                                                        MALAYSIA

Telephone   :   +60 (603) 563 53321
Fax   :   +60 (603) 563 54116

1.5   Emergency telephone number

Emergency Phone #   :   1-800-262-8200

2.   HAZARDS IDENTIFICATION

2.1   Classification of the hazardous chemical

Classification according to CLASS regulations 2013
Skin corrosion/irritation (Category 2)
Serious eye damage/eye irritation (Category 2)
Skin sensitisation (Category 1)
Hazardous to the aquatic environment - chronic hazard (Category 2)

2.2   Label elements

Labelling according to CLASS regulations 2013
Pictogram

Signal word   Warning

Hazard statement(s)
H315   Causes skin irritation.
H317   May cause an allergic skin reaction.

| H319 | Causes serious eye irritation. |
| H411 | Toxic to aquatic life with long lasting effects. |

Precautionary statement(s)

Prevention
P261	Avoid breathing dust/ fume/ gas/ mist/ vapours/ spray.
P273	Avoid release to the environment.
P280	Wear protective gloves/ eye protection/ face protection.

Response
P333 + P313	If skin irritation or rash occurs: Get medical advice/ attention.
P337 + P313	If eye irritation persists: Get medical advice/ attention.
P362	Take off contaminated clothing and wash before reuse.

2.3   Other hazards - none

---

3.   SECTION 3: Composition and information of the ingredients of the hazardous chemical

3.1   Substances
Chemical identity

CAS-No.   :   25068-38-6

Component	Concentration
Reaction product: bisphenol-A-(epichlorhydrin) and epoxy resin (number average molecular weight <= 700)	
CAS-No. 25068-38-6 EC-No. 500-033-5 Index-No. 603-074-00-8	<= 100 %

---

4.   FIRST AID MEASURES

4.1   Description of first aid measures

General advice
Consult a physician. Show this safety data sheet to the doctor in attendance.

If inhaled
If breathed in, move person into fresh air. If not breathing, give artificial respiration. Consult a physician.

In case of skin contact
Wash off with soap and plenty of water. Consult a physician.

In case of eye contact
Rinse thoroughly with plenty of water for at least 15 minutes and consult a physician.

If swallowed
Never give anything by mouth to an unconscious person. Rinse mouth with water. Consult a physician.

4.2   Most important symptoms and effects, both acute and delayed

4.3   Indication of any immediate medical attention and special treatment needed
No data available

---

5.   FIREFIGHTING MEASURES

5.1   Extinguishing media

Suitable extinguishing media
Use water spray, alcohol-resistant foam, dry chemical or carbon dioxide.

5.2 **Special hazards arising from the substance or mixture**
Nature of decomposition products not known.

5.3 **Advice for firefighters**
Wear self-contained breathing apparatus for firefighting if necessary.

5.4 **Further information**
No data available

6. ACCIDENTAL RELEASE MEASURES

6.1 **Personal precautions, protective equipment and emergency procedures**
Use personal protective equipment. Avoid breathing vapours, mist or gas. Ensure adequate ventilation.

6.2 **Environmental precautions**
Prevent further leakage or spillage if safe to do so. Do not let product enter drains. Discharge into the environment must be avoided.

6.3 **Methods and materials for containment and cleaning up**
Soak up with inert absorbent material and dispose of as hazardous waste. Keep in suitable, closed containers for disposal.

6.4 **Reference to other sections**
For disposal see section 13.

7. HANDLING AND STORAGE

7.1 **Precautions for safe handling**
Avoid contact with skin and eyes. Avoid inhalation of vapour or mist.

7.2 **Conditions for safe storage, including any incompatibilities**
Store in cool place. Keep container tightly closed in a dry and well-ventilated place. Containers which are opened must be carefully resealed and kept upright to prevent leakage.

7.3 **Specific end use(s)**
No data available

8. Exposure controls and personal protection

8.1 **Control parameters**

Permissible exposure limit
Contains no substances with occupational exposure limit values.

8.2 **Exposure controls**

Appropriate engineering controls
Handle in accordance with good industrial hygiene and safety practice. Wash hands before breaks and at the end of workday.

Personal protective equipment

Eye/face protection
Face shield and safety glasses Use equipment for eye protection tested and approved under appropriate government standards such as NIOSH (US) or EN 166(EU).

Skin protection
Handle with gloves. Gloves must be inspected prior to use. Use proper glove removal technique (without touching glove's outer surface) to avoid skin contact with this product. Dispose of contaminated gloves after use in accordance with applicable laws and good laboratory practices. Wash and dry hands.

The selected protective gloves have to satisfy the specifications of EU Directive 89/686/EEC and the standard EN 374 derived from it.

Full contact
Material: Nitrile rubber
Minimum layer thickness: 0,11 mm
Break through time: 480 min
Material tested:Dermatril® (KCL 740 / Aldrich Z677272, Size M)

Splash contact
Material: Nitrile rubber
Minimum layer thickness: 0,11 mm
Break through time: 480 min
Material tested:Dermatril® (KCL 740 / Aldrich Z677272, Size M)

data source: KCL GmbH, D-36124 Eichenzell, phone +49 (0)6659 87300, e-mail sales@kcl.de, test method: EN374

If used in solution, or mixed with other substances, and under conditions which differ from EN 374, contact the supplier of the CE approved gloves. This recommendation is advisory only and must be evaluated by an industrial hygienist and safety officer familiar with the specific situation of anticipated use by our customers. It should not be construed as offering an approval for any specific use scenario.

Body Protection
Complete suit protecting against chemicals, The type of protective equipment must be selected according to the concentration and amount of the dangerous substance at the specific workplace.

Respiratory protection
Where risk assessment shows air-purifying respirators are appropriate use a full-face respirator with multi-purpose combination (US) or type ABEK (EN 14387) respirator cartridges as a backup to engineering controls. If the respirator is the sole means of protection, use a full-face supplied air respirator. Use respirators and components tested and approved under appropriate government standards such as NIOSH (US) or CEN (EU).

Thermal hazards
No data available

9.   PHYSICAL AND CHEMICAL PROPERTIES

9.1   Information on basic physical and chemical properties

a)	Appearance	Form: Semi-solid melting to a liquid Colour: colourless
b)	Odour	No data available
c)	Odour Threshold	No data available
d)	pH	No data available
e)	Melting point/freezing point	-15 - 5 °C
f)	Initial boiling point and boiling range	No data available
g)	Flash point	252 °C
h)	Evaporation rate	No data available
i)	Flammability (solid, gas)	No data available
j)	Upper/lower flammability or explosive limits	No data available
k)	Vapour pressure	0,04 hPa at 77 °C
l)	Vapour density	No data available

m)	Relative density	1,168 g/cm3
n)	Water solubility	No data available
o)	Partition coefficient: n-octanol/water	log Pow: 2,8
p)	Auto-ignition temperature	No data available
q)	Decomposition temperature	No data available
r)	Viscosity	No data available

10. STABILITY AND REACTIVITY

10.1 Reactivity
No data available

10.2 Chemical stability
No data available

10.3 Possibility of hazardous reactions
No data available

10.4 Conditions to avoid
No data available

10.5 Incompatible materials
Strong oxidizing agents, acids, Amines, Bases

10.6 Hazardous decomposition products
Other decomposition products - No data available

11. TOXICOLOGICAL INFORMATION

11.1 Information on toxicological effects

Acute toxicity
LD50 Oral - Rat - 13.600 mg/kg
Remarks: Behavioral:Somnolence (general depressed activity). Lungs, Thorax, or Respiration:Dyspnea.
Nutritional and Gross Metabolic:Weight loss or decreased weight gain.

Skin corrosion/irritation
No data available

Serious eye damage/eye irritation
No data available

Respiratory or skin sensitisation
May cause sensitisation by skin contact.

Germ cell mutagenicity
No data available

Genotoxicity in vitro - Ames test - positive

Carcinogenicity

IARC: No component of this product present at levels greater than or equal to 0.1% is identified as probable, possible or confirmed human carcinogen by IARC.

Reproductive toxicity

No data available

Specific target organ toxicity - single exposure
No data available

Specific target organ toxicity - repeated exposure
No data available

Aspiration hazard
No data available

Potential health effects

Inhalation	May be harmful if inhaled. Causes respiratory tract irritation.
Ingestion	May be harmful if swallowed.
Skin	May be harmful if absorbed through skin. Causes skin irritation.
Eyes	Causes serious eye irritation.

Additional Information
RTECS: KC2100000

---

12. ECOLOGICAL INFORMATION

12.1 Ecotoxicity
No data available

12.2 Persistence and degradability
Biodegradability   Result: - According to the results of tests of biodegradability this product is not readily biodegradable.

Remarks: No data available

12.3 Bioaccumulative potential
No data available

12.4 Mobility in soil
No data available

12.5 Other adverse effects
Toxic to aquatic life with long lasting effects.
No data available

---

13. SECTION 13: Disposal information

13.1 Waste treatment methods

Product
Offer surplus and non-recyclable solutions to a licensed disposal company.

Contaminated packaging
Dispose of as unused product.

---

14. TRANSPORT INFORMATION

14.1 UN number

ADR/RID: 3082	IMDG: 3082	IATA-DGR: 3082

14.2 UN proper shipping name

ADR/RID:	ENVIRONMENTALLY HAZARDOUS SUBSTANCE, LIQUID, N.O.S. (Reaction product: bisphenol-A-(epichlorhydrin) and epoxy resin (number average molecular weight <= 700))
IMDG:	ENVIRONMENTALLY HAZARDOUS SUBSTANCE, LIQUID, N.O.S. (Reaction product: bisphenol-A-(epichlorhydrin) and epoxy resin (number average molecular weight <= 700))
IATA-DGR:	Environmentally hazardous substance, liquid, n.o.s. (Reaction product:

bisphenol-A-(epichlorhydrin) and epoxy resin (number average
molecular weight <= 700))

14.3   Transport hazard class(es)
ADR/RID: 9   IMDG: 9   IATA-DGR: 9

14.4   Packaging group
ADR/RID: III   IMDG: III   IATA-DGR: III

14.5   Environmental hazards
ADR/RID: yes   IMDG Marine pollutant: yes   IATA-DGR: yes

14.6   Transport in bulk according to Annex II of MARPOL 73/78 and the IBC Code
No data available

14.7   Special precautions for user

Further information

EHS-Mark required (ADR 2.2.9.1.10, IMDG code 2.10.3) for single packagings and combination packagings
containing inner packagings with Dangerous Goods > 5L for liquids or > 5kg for solids.

15.   REGULATORY INFORMATION

15.1   Safety, health and environmental regulations/legislation specific for the substance or mixture
No data available

16.   OTHER INFORMATION

Further information
Copyright 2015 Sigma-Aldrich Co. LLC. License granted to make unlimited paper copies for internal use
only.
The above information is believed to be correct but does not purport to be all inclusive and shall be used
only as a guide. The information in this document is based on the present state of our knowledge and is
applicable to the product with regard to appropriate safety precautions. It does not represent any
guarantee of the properties of the product. Sigma-Aldrich Corporation and its Affiliates shall not be held
liable for any damage resulting from handling or from contact with the above product. See www.sigma-
aldrich.com and/or the reverse side of invoice or packing slip for additional terms and conditions of sale.

Technical Bulletin

JEFFAMINE® D-230 Polyetheramine

JEFFAMINE D-230 polyetheramine is characterized by repeating oxypropylene units in the backbone. As shown by the representative structure, JEFFAMINE D-230 polyetheramine is a difunctional, primary amine with an average molecular weight of about 230. The primary amine groups are located on secondary carbon atoms at the end of the aliphatic polyether chain.
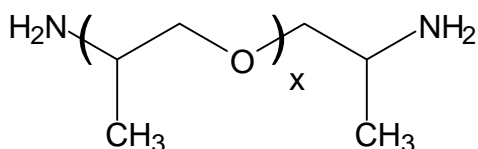
$x \approx 2.5$

APPLICATIONS
- Epoxy curing agent
- Reacts with carboxylic acids to form hot melt adhesives
- Reacts quickly with isocyanates
- Salts may be formed readily for surfactant use

BENEFITS
- Low viscosity, color and vapor pressure
- Completely miscible with a wide variety of solvents, including water
- Provides tough, clear, impact resistant coatings, castings, and adhesives
- Coatings are free of surface blush prevalent with many amine curing agents

SALES SPECIFICATIONS

Property	Specifications	Test Method*
Appearance	Colorless to pale yellow liquid with slight haze permitted	ST-30.1
Color, Pt-Co	25 max.	ST-30.12
Primary amine, % of total amine	97 min.	ST-5.34
Total acetylatables, meq/g	8.3 – 9.1	ST-31.39
Total amine, meq/g	8.1 – 8.7	ST-5.35
Total amine, % acetylatables	94.0 min.	Calculated
Water, wt%	0.20 max.	ST-31.53, 6

*Methods of Test are available from Huntsman Corporation upon request.

ADDITIONAL INFORMATION

Regulatory Information

DOT/TDG Classification	Amines, liquids, corrosive, N.O.S. (polyoxypropylenediamine)
HMIS Code	3-1-0
CAS Number	9046-10-0
US, TSCA	Listed
Canadian WHMIS Classification	E
Canada, DSL	Listed
European Union, EINECS/ELINCS	Polymer Exempt
Australia, AICS	Listed
Japan, ENCS	Contact Huntsman Regulatory
Korea, ECL	Listed
China, IECSC	Listed

Typical Properties

AHEW (Amine hydrogen equivalent wt.), g/eq	60
Equivalent wt. with isocyanates, g/eq	120
Viscosity, cSt, 25°C (77°F)	9.5
Density, g/ml (lb/gal), 25°C	0.948 (7.90)
Flash point, PMCC, °C (°F)	121 (250)
pH, 5% aqueous solution	11.7
Refractive index, n_D^{20}	1.4466
Vapor pressure, mm Hg/°C	1/100
	10/133

TOXICITY AND SAFETY

For additional information on the toxicity and safe handling of this product, consult the Material Safety Data Sheet (Safety Data Sheet in Europe) prior to use of this product.

HANDLING AND STORAGE

Materials of Construction

At temperatures of 75-100°F (34-38°C)

Tanks	Carbon steel
Lines, valves	Carbon steel
Pumps	Carbon steel
Heat exchange Surfaces	Stainless steel
Hoses	Stainless steel, polyethylene, polypropylene, and TEFLON®
Gaskets, packing	Polypropylene or TEFLON® (elastomers such as neoprene, Buna N, and VITON® should be avoided)
Atmosphere	Nitrogen or dry air

At temperatures above 100°F (38°C)

Tanks	Stainless steel or aluminum
Lines, Valves	Stainless steel
Pumps	Stainless steel or Carpenter 20 equivalent
Atmosphere	Nitrogen

[1]VITON® and TEFLON® are registered trademarks of Dupont.

JEFFAMINE® D-230 polyetheramine may be stored under air at ambient temperatures for extended periods. A nitrogen blanket is suggested for all storage, however, to reduce the effect of accidental exposure to high temperatures and to reduce the absorption of atmospheric moisture and carbon dioxide. It should be noted that pronounced discoloration is likely to occur at temperatures above 140°F (60°C), whatever the gaseous pad.

Cleanout of lines and equipment containing JEFFAMINE D-230 polyetheramine can be accomplished using warm water and steam. In the event of spillage of this product, the area may be flushed with water. The proper method for disposal of waste material is by incineration with strict observance of all federal, state, and local regulations.

AVAILABILITY

JEFFAMINE D-230 polyetheramine is available in tank cars, tank wagons, 55-gallon (208L) drums of 430 pounds (195kg) net weight, and 5-gallon (19L) cans. Samples are available in North America and Asia by contacting our sample department at 1-800-662-0924. Samples in other locations, including Europe, are available by contacting any Huntsman Corporation sales office.

Material Safety Data Sheet

acc. to OSHA and ANSI

Revision date: Oct. 29, 2014

1 Identification of substance:

- **Product details:**

- **Trade name:** Carbon nanotubes

- **Manufacturer/Supplier:**

  Nanostructured & Amorphous Materials, Inc.
  16840 Clay Road, Suite #113
  Houston, TX 77084, USA

2 Composition/Data on components:

- **Chemical characterization:**
  Description: (CAS#)
  Fullerene (CAS# 99685-96-8), 95%

3 Hazards identification

- **Hazard description:** Xi Irritant

- **Information pertaining to particular dangers for man and environment**
  R 36/37 Irritating to eyes and respiratory system.

4 First aid measures

- **After inhalation**
  Supply fresh air. If required, provide artificial respiration. Keep patient warm.
  Seek immediate medical advice.

- **After skin contact**
  Immediately wash with water and soap and rinse thoroughly.
  Seek immediate medical advice.

- **After eye contact**
  Rinse opened eye for several minutes under running water. Then consult a doctor.

- **After swallowing** Seek immediate medical advice.

5 Fire fighting measures

- **Suitable extinguishing agents**
  CO2, extinguishing powder or water spray. Fight larger fires with water spray.

- **Special hazards caused by the material, its products of combustion or resulting gases:**
  In case of fire, the following can be released:
  Carbon monoxide (CO)

- **Protective equipment:**
  Wear self-contained respirator.
  Wear fully protective impervious suit.

6 Accidental release measures

- **Person-related safety precautions:**
  Wear protective equipment. Keep unprotected persons away.
  Ensure adequate ventilation

- **Measures for environmental protection:**
  Do not allow material to be released to the environment without proper governmental permits.

- **Measures for cleaning/collecting:** Ensure adequate ventilation.

- **Additional information:**
  See Section 7 for information on safe handling
  See Section 8 for information on personal protection equipment.
  See Section 13 for disposal information.

7 Handling and storage

- **Handling**

- **Information for safe handling:**
  Keep container tightly sealed.
  Store in cool, dry place in tightly closed containers.
  Ensure good ventilation at the workplace.

- **Information about protection against explosions and fires:**
  No special measures required.

- **Storage**

- **Requirements to be met by storerooms and receptacles:**
  No special requirements.

- **Information about storage in one common storage facility:**
  Store away from oxidizing agents.

Store away from halogens.
Do not store together with acids.

- **Further information about storage conditions:**
  Keep container tightly sealed.
  Store in cool, dry conditions in well sealed containers.

8 Exposure controls and personal protection

- **Additional information about design of technical systems:**
  Properly operating chemical fume hood designed for hazardous chemicals
  and having an average face velocity of at least 100 feet per minute.

  Components with limit values that require monitoring at the workplace:

  Graphite

	mg/m^3
ACGIH TLV	2
Belgium TWA	2.5
Finland TWA	5
France VME	2
Germany MAK	6
Ireland TWA	5
Korea TLV	2
Netherlands MAC-TGG	2
Poland TWA	2
Sweden NGV	5 (dust)
Switzerland MAK-W	2.5
United Kingdom	5-LTEL
USA PEL	15 mppcf

- **Additional information:** No data

- **Personal protective equipment**

- **General protective and hygienic measures**
  The usual precautionary measures for handling chemicals should be
  followed.
  Keep away from foodstuffs, beverages and feed.
  Remove all soiled and contaminated clothing immediately.
  Wash hands before breaks and at the end of work.
  Avoid contact with the eyes.
  Avoid contact with the eyes and skin.

- **Breathing equipment:**
  Use suitable respirator when high concentrations are present.

- **Protection of hands:** Impervious gloves

- **Eye protection:** Safety glasses

- **Body protection:** Protective work clothing.

9 Physical and chemical properties:

- **General Information**

- **Form:** Powders

- **Color:** Black

- **Odor:** Odorless

-   **Value/Range   Unit   Method**

- **Change in condition**

- **Melting point/Melting range:**   3652-3697 ° C   (subl/vac)

- **Boiling point/Boiling range:**   Not determined

- **Sublimation temperature / start:**   Not determined

- **Flash point:**   Not applicable

- **Ignition temperature:**   Not determined

- **Decomposition temperature:**   Not determined

- **Danger of explosion:**
  Product does not present an explosion hazard.

- **Explosion limits:**

- **Lower:**   Not determined

- **Upper:**   Not determined

- **Vapor pressure:**   Not determined

- **Density:**   at   20 ° C   ~ 2.1 g/cm³

- **Solubility in / Miscibility with**

• **Water:**   Insoluble

10 Stability and reactivity

- **Thermal decomposition / conditions to be avoided:**
  Decomposition will not occur if used and stored according to
  specifications.

- **Materials to be avoided:**
  Oxidizing agents
  Acids
  Halogens
  Interhalogens
  Alkali metals

- **Dangerous reactions** No dangerous reactions known

- **Dangerous products of decomposition**: Carbon monoxide and carbon dioxide

11 Toxicological information

- **Acute toxicity:**

- **Primary irritant effect:**

- **on the skin**: Irritant to skin and mucous membranes.

- **on the eye**: Irritating effect.

- **Sensitization**: No sensitizing effects known.

- **Subacute to chronic toxicity:**
  The inhalation of graphite, both natural and synthetic, has caused
  pneumoconiosis in exposed workers. The pneumoconiosis found is similar
  to coal worker's pneumoconiosis.

- **Additional toxicological information:**
  To the best of our knowledge the acute and chronic toxicity of this
  substance is not fully known.
  No classification data on carcinogenic properties of this material is
  available from the EPA, IARC, NTP, OSHA or ACGIH.

12 Ecological information:

- **General notes:**
  Do not allow material to be released to the environment without proper
  governmental permits.

13 Disposal considerations

- **Product:**

- **Recommendation**
  Consult state, local or national regulations to ensure proper disposal.

- **Uncleaned packagings:**

- **Recommendation:**
  Disposal must be made according to official regulations.

14 Transport information

Not a hazardous material for transportation.

- **DOT regulations:**

- **Hazard class:**   None

- **Land transport ADR/RID   (cross-border)**

- **ADR/RID class:**   None

- **Maritime transport IMDG:**

- **IMDG Class:**   None

- **Air transport ICAO-TI and IATA-DGR:**

- **ICAO/IATA Class:**   None

- **Transport/Additional information:**
  Not dangerous according to the above specifications.

15 Regulations

- **Product related hazard informations:**

- **Hazard symbols:** Xi Irritant

- **Risk phrases:** 36/37 Irritating to eyes and respiratory system.

- **Safety phrases:**

26   In case of contact with eyes, rinse immediately with plenty of water and seek medical advice.

- **National regulations**
  All components of this product are listed in the U.S. Environmental Protection Agency Toxic Substances Control Act Chemical Substance Inventory.

- **Information about limitation of use:**
  For use only by technically qualified individuals.

16 Other information:

Employers should use this information only as a supplement to other information gathered by them, and should make independent judgement of suitability of this information to ensure proper use and protect the health and safety of employees. This information is furnished without warranty, and any use of the product not in conformance with this Material Safety Data Sheet, or in combination with any other product or process, is the responsibility of the user.